University of "Roma Tre"

Doctoral Thesis

Soft Computing techniques for diagnostics and optimisation of building energetic behavior

Author:
Fabio Moretti

Supervisor:
Stefano Panzieri

A dissertation submitted in partial fulfilment of the requirements for the degree of Doctor of Philosophy in Computer Science and Automation

at the

MCIP Lab
Computer Science and Automation Department

April 2015

"The noblest pleasure is the joy of understanding."

Leonardo da Vinci

University of "Roma Tre"

Abstract

Compuer Science Engineering
Computer Science and Automation Department

Doctor of Philosophy in Computer Science and Automation

Soft Computing techniques for diagnostics and optimisation of building energetic behavior

by Fabio Moretti

Understanding and controlling building dynamics is a major task and still an open issue for many researchers. In this work, the goal is to achieve energy efficiency improvement through application of soft computing techniques on real case applications. The pattern followed is based on Smart Cities paradigm, aiming to actively involve citizens increasing cities energy efficiency, their well-being and self-knowledge. Developing methodologies applied to real world problems is challenging, since in many cases the knowledge of the dynamics is incomplete, uncertainty is high and signals are noisy. Soft Computing techniques are well suited for coping those problems: as they are based on human mind pattern, they provide good generalisation, iterative learning and self adaptation. This dissertation focuses on diagnostics and optimisation issues applied mainly to buildings, a framework for high level building behavior is proposed based on fuzzy rules data fusion and multiobjective optimisation algorithm for fenestration design and thermal heating control are proposed. Some implementations of these techniques have been applied to "Smart Village" R.C. Casaccia test case, a small prototype of a Smart City.

Acknowledgements

My work, started in 2012 involved many people I want to thank for their kindness and support. First of all my Ph.D. advisor Stefano Panzieri for his advices and support, he has been a guide leading my work toward the right path. I want to thank also Mauro Annunziato and Stefano Pizzuti, who made possible the collaboration between ENEA and Roma Tre University, allowing me to work on my research in an enthusiastic and proper environment. I want of course thank my current and past ENEA colleagues: Fiorella Lauro, Sabrina Romano, Claudia Meloni, Francesco Pieroni, Francesco Romanello, Matteo De Felice, Francesco Marino, Marco Camponeschi, Paolo Cicolin, and the "czech guys" Martin Macas and Petr Kadera.. with you all I had a great time from working and personal points of view, friends, more than colleagues. Thanks also to Henrik Madsen, who made possible my visiting period at DTU and Peder Bacher, his help has been really awesome as well as his kindness and enthusiasm. Thanks to MCIP Lab colleagues too for the time spent together, in particular Chiara Foglietta, with whom I worked during my starting period. A special thank to my family for their continuous support and encouragement, they have been a referring point during these years. Finally, I want to thank Chiara for being close to me during good and, overall, bad periods of this difficult path, her help and support have been really important.

Contents

List of Figures

List of Tables

Acronyms

AHU Air Handling Unit

AI Artificial Intelligence

ANN Artificial Neural Network

BAGGING Bootstrap AGGregatING

BEM Basic Ensemble Method

BEMS Building Energy Management System

EC Evolutionary Computation

D-S Dempster-Shafer

FL Fuzzy Logic

FTP File Transfer Protocol

GEM Generalised Ensemble Method

HMI Human Machine Interface

HTTP HyperText Transfer Protocol

HVAC Heating Ventilation and Air Conditioning

HVACR Heating Ventilation Air Conditioning and Refrigeration

ICT Information and Communication Technlogy

JDL Joint Directors of Laboratories

MAE Mean Absolute Error

MAPE Mean Absolute Percentage Error

MIMO Multiple Input Multiple Output

MLP Multi Layer Perceptron

MOA Multi Objective Algorithm

MOGA Multi Objective Genetic Algorithm

MOOP Multi Objective Optimisation

MOP Multi Objective Problem

MPC Model Predictive Control

NDS Non-Dominated Set

NN Neural Network

NSGA Non-dominated Sorting Genetic Algorithm

NSGA-II Elitist Non-dominated Sorting Genetic Algorithm

ODBC Open DataBase Connectivity

ODE Ordinary Differential Equation

OR Operative Research

P Proportional

PAES Pareto Archived Evolutionary Strategy

PI Proportional Integral

PD Proportional Derivative

PID Proportional Integral Derivative

PLC Power Line Communication

PMV Predicted Mean Vote

PPD Percentage People Dissatisfied

PSC Preprocessing Situation Cause

PSO Particle Swarm Optimsation

RC Research Center

RBF Radial Basis Function

RTU remote terminal Unit

SBX Simulated Binary Crossover

SC Soft Computing

SCADA Supervisor Control And Data Acquisition

SDE Stochastic Differential Equation

SFTP Secure File Transfer Protocol

SISO Single Input Single Output

SOP Single Objective Problem

SOOP Single Objective Optimisation

SPEA Strenght Pareto Evolutionary Algorithm

STP Smart Town Platform

SVM Support Vector Machines

VAV Variable Air Volume

VEGA Vector Evaluated Genetic Algorithm

WSEA Weighted Sum Evolutionary Algorithm

WNM Wavelet Network Model

WS Web Service

XML eXtensible Markup Language

Introduction

Since the 60s, Artificial Intelligence (AI) has been increasingly used in many applications both in academic and industry fields. In particular, Operative Research (OR) applications for monitoring industrial processes. In 1980s, with the increasing of computational capacity, Neural Network (NN), Fuzzy Logic (FL) and Evolutionary Computation (EC) played a major role in many countries, dramatically increasing productivity. Nowadays these techniques, as well as Chaos Theory and Probabilistic reasoning are categorised as *Soft Computing (SC)* methodologies. Soft computing main concept was firstly introduced in 1965 [1] and [2] is based on paradigm of the human mind: inaccurate calculation, iterative learning, self adaptation, generalisation capability, and so on. Soft computing methodologies mimic consciousness and cognition in several many aspects: they can learn from experience, they can generalise into domains where direct experience is absent, they are robust to noise and lack of information, and they can perform mapping from inputs to the outputs faster than inherently serial analytical representations.

On the other hand, the so called *hard computing* techniques are based on accurate calculations, strict modelling and poor tolerance to any type of change of contour conditions. Of course there is not a best choice and in many real-world problems it must be found a balanced trade-off between accuracy, complexity, time and efficiency.

Soft computing methodologies are commonly used to enhance AI and incorporate human expert knowledge in computing processes. Their applications include the design of intelligent autonomous systems/controllers and handling of complex systems with unknown parameters.

Many control strategies methodologies over the past three decades relies on such modelling and model-based methods have found their way into practice and provided satisfactory solutions to the spectrum of complex systems under various uncertainties. However,

as Zadeh stated in 1962 [3]:

> *[...]often the solution of real life problems in system analysis and control has been subordinated to the development of mathematical theories that dealt with over-idealized problems bearing little relation to theory[...]*

In one of his latest articles [4] related to the historical perspective of system analysis and control, Zadeh has considered this decade as the era of intelligent systems and urges for some tuning:

> *[...]I believe the system analysis and controls should embrace soft computing and assign a higher priority to the development of methods that can cope with imprecision, uncertainties and partial truth.[...]*

Such modern relativism, as well as utilization of the human brain as a role model on the decision making processes, can be regarded as the foundation of intelligent systems design methodology. Nowadays, soft SC techniques are largely used on many application fields. In this dissertation we mainly focus on methodologies concerning Smart Cities main issues, in particular building and partly public lighting too. The proposed work's main goal is to try bridging the gap between Smart City concept and real cases applications, trying to develop and apply as much as possible such methodologies. Since 2012 R.C. ENEA Casaccia has been a test case for Smart City-oriented installations, such as sensorised building, outdoor cameras, parking lighting control, occupancy monitoring... For such reasons, it has been defined "Smart Village", a small prototype of a Smart City, and it has been the working test for some of the applications described in this work. Dissertation structure is divided in 7 chapters. In chapter 1 concepts of SC and Building Energy Management System (BEMS) are introduced, typical energy saving approaches are discussed, from the simpler to advanced ones. Moreover, an overview on typical control approaches is carried out. Chapter 2 describes the implementation of the Information and Communication Technlogy (ICT) platform, the logical division, Database structure, communication system and acquisition/actuation modules. Chapter 3 describes the building diagnostics framework. Firstly, the three-hierarchical levels (Preprocessing, Situations, Causes) structure is shown: the idea is to identify building malfunctions or bad behaviours through the progressive information aggregation.

Starting from data retrieved aggregated, namely Preprocessings, a data fusion process is performed in order to obtain Situations, an higher level of information that describes possible states of the building, the aggregation of situations lead to Causes, the origin of anomalous behaviour. Secondly, a test case applied on an actual building is performed. This work has been published in [5]. Chapter 4 focuses on multiobjective optimisation, a formal definition of the problems and the optimality condition is given, then some of Multi Objective Algorithm (MOA) are presented and implemented and finally a critical comparison has been carried out, based on evaluation metrics of Pareto fronts such as Dominance Ratio, Spacing and Hypervolume. Chapter 5 describes heating optimisation of F40 building, located in R.C. Casaccia. Firstly, a description of the building, thermal plant and distribution system is given, then optimisation results are shown. We used NSGA-II algorithm for minimising thermal consumptions while keeping thermal comfort on acceptance levels. As objective functions evaluator, F40 building simulator has been used. We investigate a seasonal and daily optimisation approach, reaching remarkable potential savings. A Grey Box modeling approach on the same building has been carried out for overcoming computational issues due to simulation time expense. In chapter 6 we propose a novel approach for optimal design of building fenestration: the main idea is to find out the most important shading devices features for optimising the trade-off between shading during summer and winter. Although this work is based on multiobjective optimisation, the main focus in this case is on post-Pareto processing. Input variables of optimal solutions set have been investigated for identifying which have the most importance during design phase. We used a NN Ensemble model for objective functions evaluations. Despite not related to building the work discussed in chapter 7 is interesting as application case of Smart Lighting based on SC techniques. An hybrid statistical-NN ensemble method is proposed for traffic flow forecasting. The main idea is to adapt public lighting according to traffic flow of $n-step-ahead$, adapting consumptions to actual users needs. Hybrid model shows a significant improvement to previous used black-box models. This work is going to appear on Neurocomputing Special Issue 2014.

Chapter 1

Overview on Soft Computing methodologies applied to building energy management systems

1.1 Building Energy Management System

The BEMS concept was introduced in the early 1970s during the world's first big energy crisis. The oil crisis was the driving force of the intelligent building. It was the first sign of the rising awareness that energy resources are exhaustible. The second driving force of intelligent building was the raising awareness of environmental pollution by inefficient consumption of energy in production lines as well as in buildings in the beginning of the 1980s. The expansion of computer technology in the early 1980s introduced a "smart" or "intelligent" building which was one step towards a new digital computer era. It provided energy efficiency as well as optimum environmental conditions. Managing the high-tech buildings in an energy efficient manner and to the occupants' satisfaction would have become an impossible task without intelligent control systems. On the other hand, an intelligent building is one that creates an environment that maximizes the efficiency of the occupants of the building while at the same time allowing effective management of energy resources with minimum costs. The intelligence of a building depends on the elements that go to make up its intelligence. There are at least three attributes that an intelligent building should possess:

- The building should know what is happening inside and immediately outside;
- The building should decide the most efficient way of providing a convenient comfortable and productive environment for the occupants;
- The building should response quickly to occupants' requests.

These attributes may be translated into a need for various technology and management systems. The successful integration of these systems will produce the intelligent building containing a building automation system in order to enable the building to respond to external climate factors and conditions. Simultaneous sensing, control, and monitoring of the internal environment and storage of the data generated as knowledge of the building performance in a central computer system, is an important feature of an intelligent building.

The thermodynamic processes involved either intend to ensure the well being of the occupants of the building or consist of ancillary production conditions of a physical nature. This should be controlled by means of a technical future-oriented automation system which is physically ideal, economical, cost effective and efficient in terms of energy consumption. An integrated building automation system should also include all other technical and administrative processes that may be automated for reasons of security and rationalization, in order to increase the productivity of the building. The assignment of the BEMS is to run the building in such a way that following requirements as the state of the art should be fulfilled:

- reducing the energy consumption and environmental pollution;
- security for man, machine, production and environment;
- improving the efficiency of the process and reducing processing time;
- improving transparency of the process features by useful instrumentation;
- operation-oriented maintenance management of technical installations in order to increase machine running time and reduce maintenance costs.

1.2 Building control techniques

Energy Efficiency can be achieved through BEMS in several ways [6]:

- *Energy Consumption Awareness.* First energy efficiency step in buildings is increasing awareness of users and involve them to actively partecipate to the common goal, as well as encouraging good habits. Many existing tools are available for increasing user awareness such as Smart Meters [7], Microsoft Hohm [8], Berkeley Energy Dashboard [9]. Those tools anyway are not sufficient to reach remarkable saving on the long term, because typically they do not provide detailed informations required for an in-depth analysis of the inefficiency causes. Thus, although user awareness is the basic approach to energy efficiency, its effectiveness is quite limited, as demonstrated by experimental studies [10, 11].

- Reducing Standby Consumptions. Another simple approach consists in eliminating or drastically reducing energy wastes due to electrical appliances left in standby mode. Despite its apparent simplicity, such an approach can produce significant energy savings. It has been estimated that most consumer electronics and office devices consume more energy in standbymode than in activemode, as they remain in standby for very long times [12]. The standby mode can be detected by monitoring the energy consumption of the specific device. This requires a metering infrastructure which, of course, should have a very low energy consumption [10]. Once the standby mode has been detected, the device can be switched off. To this end, different strategies can be used to trade off energy saving for user satisfaction. The easiest way is to let the user decide about when to switch off a device that entered the standby mode[13].

- *Activity Scheduling.* Scheduling is a robust, largely diffused control to reduce consumptions. Such static control is very effective in tertiary where activities are strongly dependent to time schedules. Even in residential building such control can be useful in particular situations, e.g. scheduling energy-consuming tasks not requiring user interaction if energy fares are a priori known. Such BEMSs approach is proposed in [13] and [14]

- *Advanced control.* A significant fraction of energy is wasted due to an expensive use of Heating Ventilation and Air Conditioning (HVAC) and artificial lighting

systems, thus advanced control on such systems is essential for effective energy management in buildings. The use of intelligent techniques for user-presence detection and prediction is advised to adaptively tune the activation time of electrical equipments, especially for those whose latency in bringing the environment into the desired conditions is non negligible. Techniques for learning user preferences may also be extremely useful for adaptively managing electrical appliances, as they help to avoid overestimating user needs and just take into account their actual requirements. An *Energy on demand* based approach is one of the most effective ways to increase efficiency.

The main focus is Advanced control, which enables the highest potential savings respect on former strategies, in particular on HVAC systems. Main control techniques can be categorised as:

- Classical control;
- Advanced control;
- Soft control;

1.2.1 Classical Control Techniques

Classical techniques are basically on/off and PID control, and despite their simple nature, they are widely used in commercial and residential buildings [15]. On/off control is one of the simplest techniques that is practised in buildings for the saving energy while keeping users comfort at acceptance level. Proportional Integral Derivative (PID) control is a feedback control that minimise the difference between measured and target value (in this case setpoint and temperature) controlling input signal properly. It based on three main components:

- proportional term, related to current offset;
- integral term depends on the accumulation of past errors;
- derivative term predicts the future offsets based on the current rate of change of the process.

The control signal is obtained through the contribute of these three actions. Sometimes neglecting one or more actions may increase the effectiveness. For instance, Proportional (P) control and Proportional Integral (PI) control are two mostly used control algorithms in thermostat control, as thermal dynamics in a building are usually slow. Classical control techniques have been applied on the dynamic control of cooling systems [16, 17], room temperature control [18, 19], heater control [18], supply air pressure control [20], Air Handling Unit (AHU) [21], Variable Air Volume (VAV) [22].

There are many disadvantages in using PID control though: they cannot handle multi-variable and noisy nature of real case buildings rooms, hence, large errors may occurr. Furthermore, they are inefficient in terms of consumption, therefore a large use may not be the best choice in long term [23]. Finally, it requires a time-consuming tuning of the parameters for each building zone after the installation.

1.2.2 Advanced control techniques

Classical control strategies are applied in building control in a limited range of cases due to their strict limitation. In fact, they cannot cope with non-linear and Multiple Input Multiple Output (MIMO) systems, such HVAC processes. Advanced Control techniques, instead, use a dynamic model of the process in order to control the target variables [24]. These techniques can be divided in

- predictive control;
- adaptive control;
- optimal control.

Model Predictive Control (MPC) is based on a predictive model and a cost function, the former provides the future state of the system based on past its informations, while the latter has to be minimised along the time prediction horizon. The cost function can be modelled as energy cost, consumption, error, user comfort or a weighted combination of multiple factors and is subject to constraints and internal and/or external disturbances. MPC has been largely used in building automation systems due to its robustness and computational efficiency. Furthermore, it can easily cope with many variables problems

and slow changing dynamics. Hence, a plenty of applications has been developed in residential and tertiary buildings. The most time-consuming task is the model design. For MPC, can be applied any of these categories: white box, black box or grey-box. White-box models are based on first principles and generally use on simulation tools, where a detailed description of the building is given, they are independent or low dependent on data and can predict accurately the state of the building. On the other hand, they require a big effort for design and implementation, they are computationally expensive and their scalability is very limited. Grey-Box models are generally analogous to electrical RC networks. They are dynamic first order models produced using lumped thermal capacitance and resistance of the building. Black-Box models are data driven: they fit linear and non-linear mathematical functions to the measured data of the building.

Adaptive control is a specific type of non-linear control system applicable to processes with changing dynamics in normal operating conditions subjected to stochastic disturbances. They control the processes in a closed loop and the information about the system characteristics are obtained on-line while the system is operating. When the parameters of the plant dynamic model are unknown and/or vary in time the adaptive control system still can obtain or sustain the desired level of control system performance. Conventional control systems use feedback to reject the effect of disturbances upon the controlled variables. Further, they do not determine the control system performance. Instead, adaptive control system measures a particular performance index of the control system using the inputs, the states, the outputs and the known disturbances. After analysing the measured performance index with the reference PI's, adaptation mechanism modifies the parameters of the adjustable controller in order to maintain the performance index of the control system. Hence the adaptive control system can be interpreted as a feedback system where the controlled variable is the performance index [25]. Wen et al. [26] present the use of feed forward adaptive control for a four room building and they have devised a model of the building relating lumped thermal capacitors and resistors. Neural networks can also be used to generate a model for adaptive control that has been illustrated in [27]. Extensive work has been done related to the application of adaptive control in building HVAC systems and they can be observed in [28–31].

The optimal control algorithm solves an optimization problem to minimize a certain cost function. The objectives of optimization in HVAC systems are generally minimization of energy consumption and control effort and maximization of thermal comfort. Examples

of optimal control design include active thermal storage control [32], passive thermal storage control [33], energy optimisation of HVAC system [34, 35], VAV system control [36], and building heating and cooling control [37, 38]

1.2.3 Soft control methods

Soft control methods are based on techniques capable to work under uncertainty, vague informations and poor knowledge of the systems and can be categorised as:

- Artificial Neural Network (ANN);
- FL;
- EC;
- Chaos Theory;
- Support Vector Machines (SVM).

Fist studies have been carried out in 60s by Hu [39], results were limited for lacking of learning phase, that was firstly introduced in 1974 [40]. In 1987 ANN has been used for time series prediction [41]. Since late 80s and early 90s ANNs have been largely used in many application fields. ANN replicates human brain NN both in structure and working process. In fact, is based on a set of neurons interconnected structured in (fig. inputs (biological dendrites), activation function (cell body), output (axon) and interconnection with other neurons (synapses). Its similarity is depicted in figure 1.1. In order perform an input-output mapping NN, as biological one, must be trained through an algorithms that according to a learning dataset tunes weights properly to fit that particular relationship.

Thus, given an input vector $\mathbf{x} \in \Re^n$, and weights w_i, value incoming to neuron is (1.1):

$$net = \sum_{i=i}^{n} x_i w_i \tag{1.1}$$

Such relationship can be expressed also in the form (1.2)

$$net = \prod_{i=1}^{n} x_i^{wi} \tag{1.2}$$

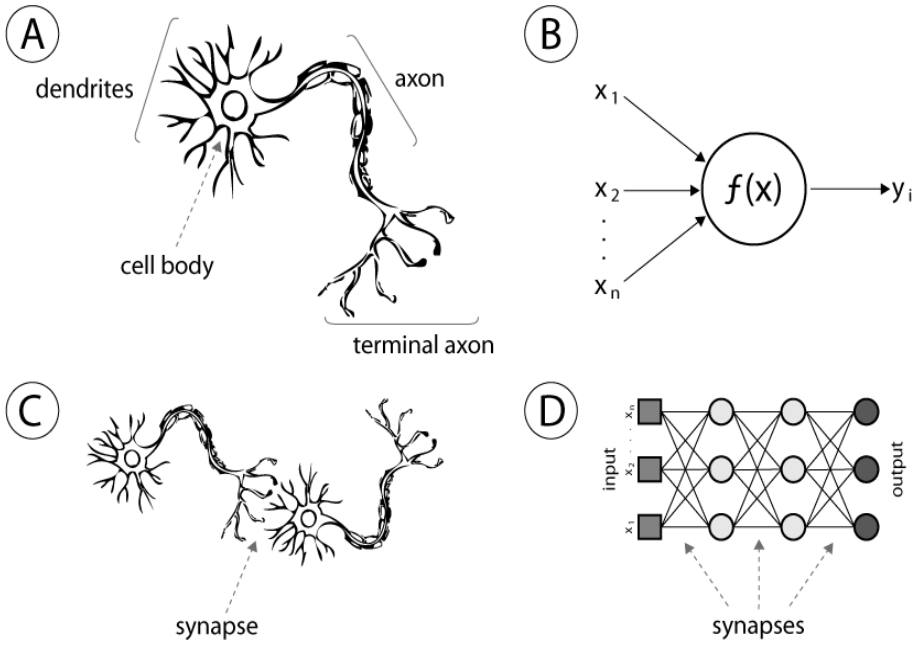

FIGURE 1.1: Struttura neuronale

Obtained value, plus a *bias* is used by activation function which give the neuron output. Activation functions usually are monotonic increasing with a co-domain in $[-1, 1]$ or $[0, 1]$. Their output can be boolean or continuous, although the latter is preferable. NN have been widely used in building control, such as Predicted Mean Vote (PMV)-based thermal comfort controller for zone temperature control [42], optimization of air conditioning setback time based on outdoor temperature [43], and fan control of an air cooled chiller [44]. Among most recent applications, Zhang [45] used an Radial Basis Function (RBF) based NN optimised through Particle Swarm Optimsation (PSO) algorithm for energy consumptions prediction , Lee [46] developed an on-line kernel-based unsupervised learning for cooling prediction, Melo [47] used a NN based model surrogate to replace Energy Plus for building shell labelling, while Asadi for building retrofit optimisation [48], other applications can be found in [49–51]. Although industry is sometimes reluctant to use black-box modelling, its effectiveness and suitability on real applications is evident.

FL replace classic Aristotelic true/false logic introducing grey shades over the black and white assumptions. Controllers based on FL rely on if-then-else rules (cf. § 3 for more detailed description of FL). Fuzzy systems are able to map the non-linear model characteristics of the system and logic controllers using the rule base would allow the application of a multi-criteria control strategy incorporating an expert system. In

buildings control, FL has been applied for a thermal comfort control based on PMV [52, 53], which controls temperature, humidity, and air velocity in an AHU. In [54] FL has been used for a three-level supervisory control of the water and air supply distribution systems, Guillemin [55] for controlling artificial and natural light through shading devices and Eftekhari [56] for natural ventilation control.

Chapter 2

Integrated ICT Platform for data acquisition and control

This chapter describes the ICT framework developed for enabling diagnostic and optimisation activities. Firstly, a context about the R.C. ENEA Casaccia is given, describing technologies installed and main purposes of the application fields macro area: Building, Lighting and Mobility. Successively, a description of logical structure of the platform is given, as well as of Database entities and communication system. Finally, an implemented automatic control for thermostat is described.

2.1 Research Center ENEA Casaccia "Smart Village"

Research Center (RC) ENEA Casaccia is located in Cesano di Roma about 30 km in north of Rome, its extension is $140000m^2$. Since 2012, a small prototype of a Smart City, called **Smart Village** has been developed inside the RC. The main purpose of the Smart Village is integrating different technologies into a centralised control center in order to apply advanced methodologies for improving energy efficiency and social interactions. Application areas regards mainly Lighting, Building Networks and Mobility. The common goal for all the areas is the *Energy on Demand* approach, such that energy is provided only when actually needed. The connection among these entities is the ICT Platform. Once technologies and methodologies robustness has been verified, this demo

case can be used as a baseline comparison for furthers implementation of a Smart City in real cases.

Figure 2.1 depicts installations carried out. F40 building has been largely sensorised in order to apply control logics at room level, while in F64 and 8 building cluster (highlighted in red) sensors installation has been less diffuse. In particular, in the cluster the idea is to develop a distributed higher level control approach, in order to replicate building network behaviour. Smart lighting application is focused on the equipment of two IP Cameras on lighting towers located in the parking lot and Power Line Communication (PLC) modules on towers lamps. The idea is to adaptively dimmer the light according to traffic flow obtained through image analysis. Mobility application's main idea is to elaborate presence data retrieved trough employees badge, estimate pedestrian flow inside the R.C. and showing estimations on a oriented graph. These control logics are managed through Smart Town Platform (STP).

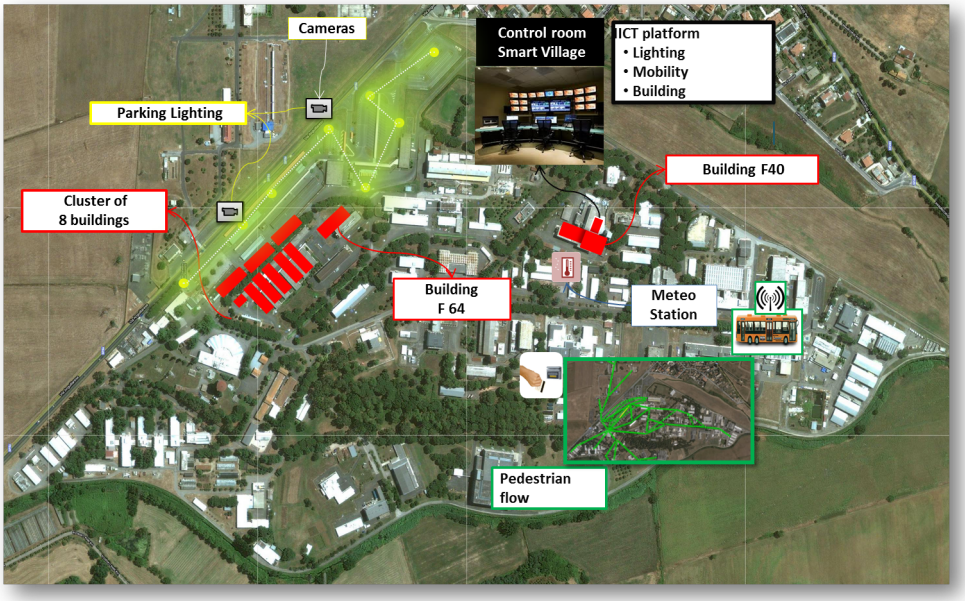

FIGURE 2.1: R.C. Casaccia

2.2 Platform description

The proposed platform is the communication node among several facilities in the Smart City. The platform must be independent from infrastructures present as the lower level, but must allow the data acquisition in a centralized way in order to analyse them and

then eventually control infrastructures. Therefore, the main utility of this platform is the integration of data from several sensors. Each facility can be seen as a vertical structure, since data coming from sensors are acquired and analysed in order to implement control procedure of the system, without analysing data generated from other systems. Instead, the platform is a horizontal structure allowing communication among vertical systems, so as to improve efficiency of the systems under energetic, monetary and citizens welfare point of view. Platform is able to redistribute to researchers and operators data it has collected, and aggregated data, as indexes of interest and analysis of probable diagnosis, after fault occurrence. Currently, platform has been designed to capture data from three facilities: the public lighting, the building network and the mobility infrastructure. Platform has been realized more generic as possible, such that code refactoring in case of addition of other infrastructure is limited. This platform was inspired by the structure of existing Supervisor Control And Data Acquisition (SCADA) systems. A SCADA is a system largely diffuse in industrial control for retrieving and on-line data analysis. It also manage failures, alarms and provides a Human Machine Interface (HMI) for visualization. It is mainly composed by a Database, remote terminal Unit (RTU), a communication system and eventually many other modules. Analogously, the platform consists of a central Database, several modules, which perform functions such as data acquisition, actuation, alarms management, and a web interface that allows authorized users to have services, as consultation of sensors data, visualization of time series, graphs and histograms. The platform has been designed to acquire and process heterogeneous types of sensors, whereby Databases and tables are characterized by a generalized structure, in order to extend the platform to future upgrade. Heterogeneity of the monitored data has suggested additional functionality to the system: the ability to execute data fusion algorithms in order to carry out a situation assessment. This module is a process that extracts high-level information on the system state thanks to aggregation of low-level data. In order to maintain the platform robust to malfunction, acquisition and actuation modules are independent from other modules. Alarm monitoring is handled by a dedicated module, which checks periodically if the sensor values are within the thresholds.

2.3 Structure

At implementation level, the platform is divided into two sections: one purely devoted to reporting data and monitoring alarms, other purely dedicated to web interfacing and to web services. At logic level, the platform is divided into four layers: presentation, application, data and sensor layer as shown in figure 2.2.

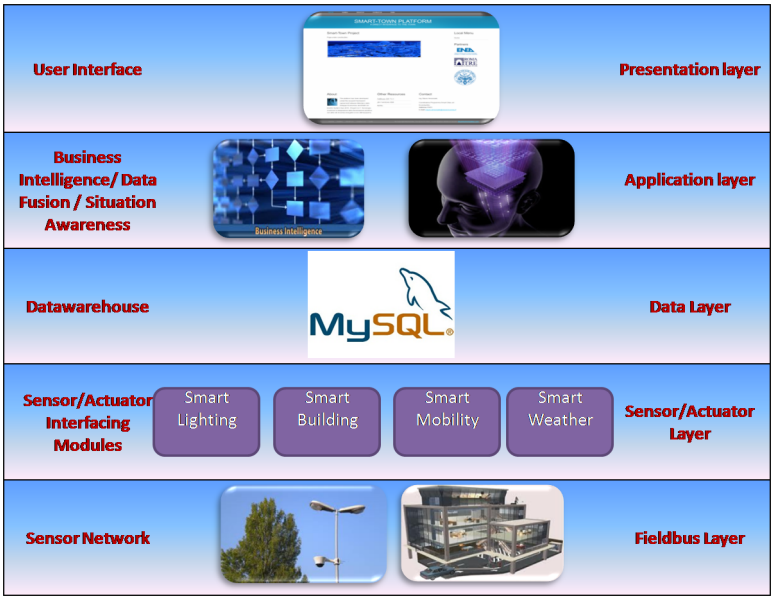

FIGURE 2.2: ICT platform levels structure

- *Presentation Layer.* User interface web application (servlet, html, jsp).
- *Application Layer.* In this layer, business intelligence activities are processed. In particular, building diagnostics and optimisation processes, data fusion, control logics and anomalies handling.
- *Data Layer.* Datawarehouse layer where heterogeneous data is stored.
- *Sensor/Actuator Layer.* In this layer, modules interfacing Database with sensor are developed. Each module is independent and dedicated to a particular sensor category.

At implementation level, the platform is divided into 5 projects:

- *Communication.* Java Application. Handle connection between DB and sensor interfacing modules layer, error logs and shared variables.

- *DataAcquisition*. Java Application. Manage data retrieving from multiple local or remote BEMSs and DB insert.
- *BuildingDiagnostics*. Java Application. Processes data fusion for building diagnostics evaluations.
- *BuildingControl*. Java Application. Dedicated to control logics and actuations.
- *ServerSmartTown*. Java Web Application. Web interface for data retrieving and visualization.

2.3.1 Database

Figure 2.3 shows MySQL DB developed in the Smart Town Platform. The detailed description of tables is out of the scope of the dissertation, but it is worth to distinguish principal sections characterizing relationship schemas.

- *Diagnostics*. Is the major frame of the DB. The main tables are preprocessing, processing, situation and causes, correlated by junction tables. Such structure reflects diagnostics process designed (cf. § 3.3), each phase has a dedicated historical table. Preprocessing table is used for preparing data before diagnostics process (e.g. normalisation, discretisation...).
- *Actuation* contains tables for actuation logics such as thresholds, comparing rules, scheduling. Moreover a historical table has been introduced for both high level and low level controls
- *KPI* tables report global analysis about performance of the assets monitored by STP
- *Alarms* tables provides failures and alarms management.

2.3.2 Communication System

This subsection describes interfacing modules developed in R.C. ENEA Casaccia for data acquisition and actuation.

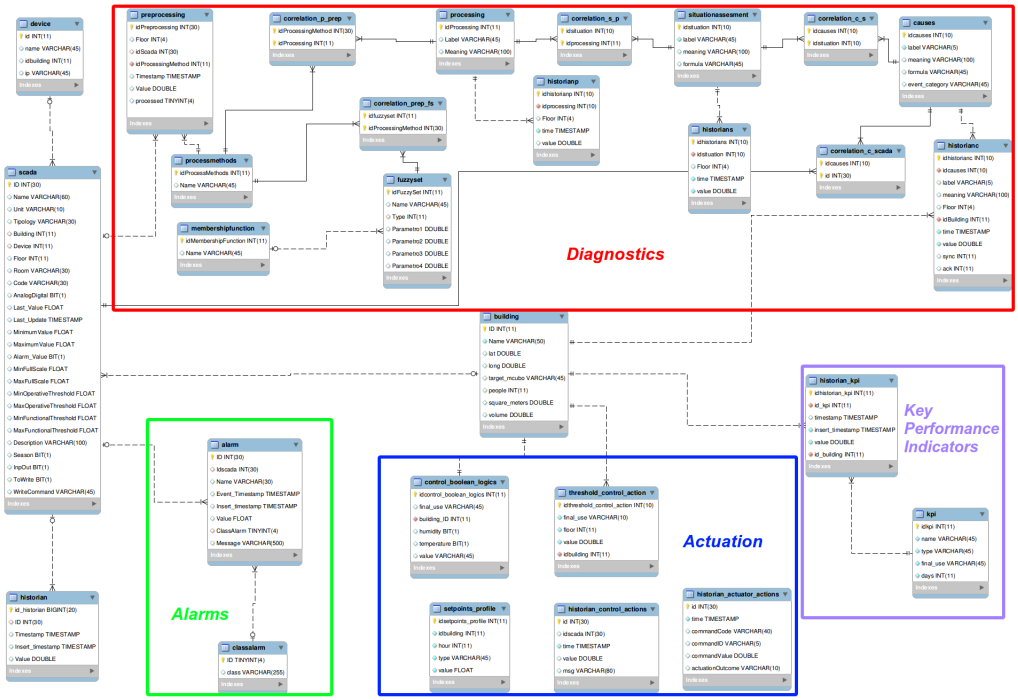

FIGURE 2.3: Database structure

2.3.2.1 Smart Building Module

Smart Building Module interfaces field sensor installed on buildings to Database. In particular it interfaces with two proprietary BEMS, in one case, through parsing an eXtensible Markup Language (XML) retrieved through HyperText Transfer Protocol (HTTP) request, in the other one, directly through Open DataBase Connectivity (ODBC) connection. Actuation in carried out through a cycling thread reading desired actuation on DB and then forwarding packages to BEMS through Web Service (WS).

2.3.2.2 Smart Lighting Module

Smart Lighting module structure is similar to Smart Building, it interface to a BEMS dedicated to lamps dimming and consumption retrieving. Data are retrieved through an Secure File Transfer Protocol (SFTP) Push XML parsing. As in the building module, actuation are processed through WS. Through this module we can measure electric total consumption and dim lamps of the parking lot.

2.3.2.3 Smart Mobility Module

Smart Mobility module is dedicated to employees badges information retrieving, the module simply interfaces to R.C. main employee database and trough ODBC connection acquire data. Since each employee is linked to a working room, data elaboration provides information about estimated occupancy on the buildings, moreover pedestrian flow in the R.C. can be estimated through a connected oriented graph connecting each building and main paths.

2.3.2.4 Smart Weather Module

Smart Weather module acquires weather data from Meteo Station through HTML parsing, retrieved through File Transfer Protocol (FTP) connection to Meteo Station data logger. Measures retrieved are:

- External temperature;
- External humidity;
- Pressure;
- Wind speed and direction;
- Rain level;
- Global solar radiation.

Communication system is summarised in figure 2.4

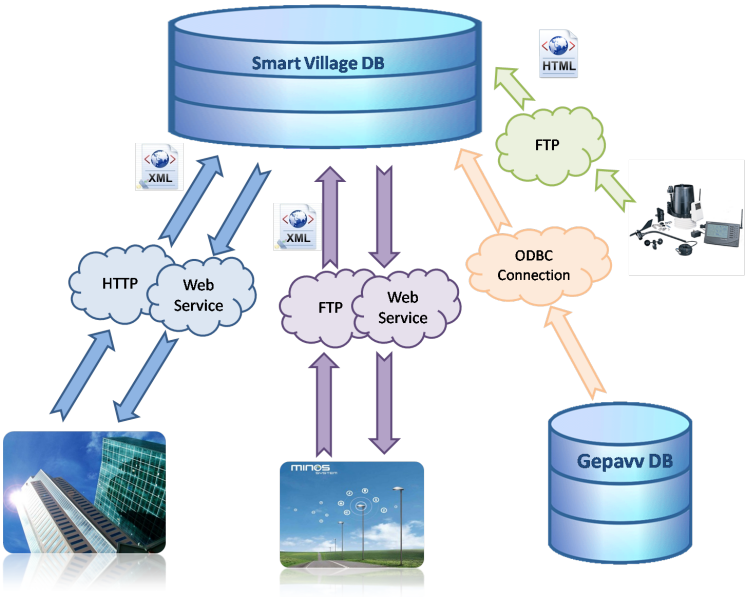

FIGURE 2.4: Communication System

2.4 Thermostat Control

Thermostat adaptive control is an application aimed to dynamic controlling thermostat setting in the F40 building rooms. The main purpose is to provide a simple interface between optimisation methodologies and building actuations. Optimisation outputs are stored in database and subsequently a cycling Java Thread applied on-line such setting through WS. Moreover, a control system has been integrated into this applications, which takes in account occupancy and weather data for defining a hourly setting curve for thermostats of each room. Thus, according to occupancy, rooms are divided into active (at least one employee associated to that room has badged), a nd inactive. While active rooms are regulated according to a static 24 hour profile if in normal weather conditions, and a dynamic profile if in particular conditions, inactive rooms setpoints are always set to a lower/higher value depending on summer/winter seasons in order to keep fans turned off. Figure 2.5 shows the process described.

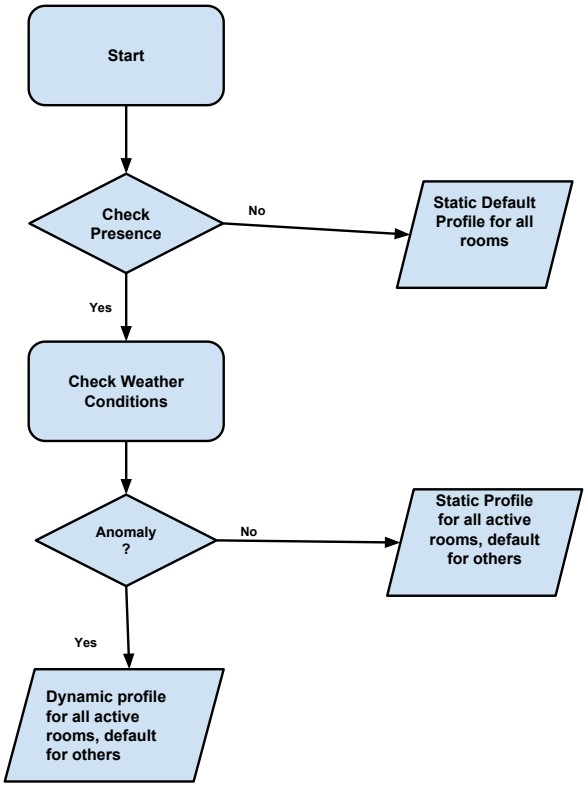

FIGURE 2.5: Thermostat control process

Chapter 3

Diagnostics of building energetic behavior

Energy efficient management of building systems is a crucial issue in order to minimize energy consumption and costs. In particular, consumptions related to residential and commercial sectors in developed regions are estimated to 40% or more of final energy use annually [57]. Furthermore, heating, ventilation and air conditioning (HVAC) system consumes 30% of the primary energy in Europe [58], 14% of the primary energy in the U.S., and about 32% of the electricity generated in the U.S. [59]. Building energy system and the monitoring of its energy and environmental performance has been the subject of great interest in recent years. In Europe, member states have set an energy savings target of 20% by 2020, mainly through energy efficiency measures. Controlling and understanding buildings energetic behaviour is a crucial first step to take in account when tackling maintenance, diagnostics and energy efficiency improvement tasks. Nowadays, sensors are largely diffused in modern buildings, and the cheaper cost may lead to economical beneficial installing also in existing non sensorised buildings. In such context, exploiting properly heterogeneous information sources, performing data fusion processes, is fundamental in order to achieve a further step to energy saving goals. Data fusion techniques combine data from multiple sensors, and related information from associated databases, to achieve improved accuracies and more specific inferences than could be achieved by the use of a single sensor alone [60–63]. While fusion process is an everyday natural task for humans and animals as merging multiple senses stimulus, many studies have been carried out on automated data fusion tasks over the past years.

The major part of the applications over the last decades mainly focuses on military issues as threat or target recognition [64], intruders detection[65] and target tracking [66]. Non military applications were increasingly developed, mainly in industrial processes [67], robotics [68], pattern recognition, [69, 70], environment [71] and medical fields [72–74]. In principle, fusion of multi-sensor data provides significant advantages over single source data. For instance, multiple sources of the same data can improve reliability of the information, merging properly multiple observations the measure, while a set of heterogeneous data can lead to an higher level of information, improving the assessment on the behaviour of processes or phenomena. According to Joint Directors of Laboratories (JDL) data fusion is a *multi-level, multifaceted process handling the automatic detection, association, correlation, estimation, and combination of data and information from several sources.* The most fundamental characterization of data fusion involves a transformation of the observed variables (provided by multiple sources) and a decision or inference system (produced by fusion estimation and/or inference processes) providing a higher level information about the state of the process or system. According to [75] data-related fusion process must cope with 4 big categories of problems:

- Imperfection
- Correlation
- Inconsistency
- Disparateness

3.1 Data Fusion algorithms overview

- Probabilistic
- Evidence
- Fuzzy

Probabilistic data fusion process is based on Bayes estimator computing probability distribution of the state x_k given a set of observations $Z_k = z_1, z_2, \cdots, z_k$ as in 3.1

$$p(x_k|Z^k) = \frac{p(z_k|x_k)p(x_k|Z^{k-1})}{p(Z^k|Z^{k-1})} \tag{3.1}$$

where $p(Z_k|x_k$ represents likelihood function and $p(x_k|Z^{k-1}$ prior distribution. Denominator is a normalising term.

Evidence theory, proposed by Dempster [76] and formalised by Shafer [77], is based on *Belief* and *plausibility* functions and can be somehow considered as an extension of Bayesian theory. The main idea is, given a set X of states of the system called *frame of discernment*, and their set of combinations, namely the power set, $P = 2^X$, to assign to each element E of the power set a belief mass function m. Belief mass function has two main properties:

$$m(\phi) = 0 \tag{3.2}$$

$$\sum_{E \in P} m(E) = 1 \tag{3.3}$$

Such as the belief mass of an empty set is always zero while the sum of beliefs of the entire power set is one. Belief of an element E quantifies the evidence supporting such element and is defined as

$$bel(E) = \sum_{B \subseteq E} m(B) \tag{3.4}$$

Plausibility of E measures evidences not rejecting E and it defined in (3.5)

$$pl(E) = \sum_{B \cap E \neq \phi} m(B) \tag{3.5}$$

Probability interval is given by:

$$bel(E) \leq P(E) \leq pl(E) \tag{3.6}$$

Dempster-Shafer (D-S) theory is easier to be applied compared to Bayesian theory because a priori probabilities distribution assignment is not required. Instead, uncertainty can be expressed assigning mass totally to entire frame of discernment $m(E = X) = 1$, and then masses can be progressively assigned when supporting data is available. A drawback of such approach is mainly the lack of applicability in complex problems, as power set exponentially grows.

Fuzzy modelling was originally proposed by [1] and has been further developed by several authors, including [78]. Fuzzy theory relaxes the axioms of classical Aristotelian logic based on true/false (crisp) values. Rules are of the form: *"IF X is A THEN Y is B"*, where A is a fuzzy set over the input domain X and B a fuzzy set over the output domain Y. If X is a collection of objects denoted generically by x, then a fuzzy set A in X is a set of ordered pairs:

$$A = (x, \mu_A(x)|x \in X) \tag{3.7}$$

$\mu_A(x)$ is called membership function (generalized characteristic function), which maps X to the membership space M. Its range is the subset of non-negative real numbers whose bounds are finite. For $sup(\mu_A(x)) = 1$ we have normalised fuzzy set, which are those commonly used. Therefore, in fuzzy sets the key task is the definition of the membership function (fuzzyfication). This can be any kind of analytical function whose parameters have to be properly tuned according to the meaning of the fuzzy set itself. A fuzzy set operation is an operation on fuzzy sets. These operations are generalisation of crisp set operations. There is more than one possible generalization. The most widely used operations are called standard fuzzy set operations. There are three operations: fuzzy complements, fuzzy intersections, and fuzzy unions. The membership function of the intersection (logical and) of two fuzzy sets A and B is defined as:

$$\mu_{A\cup B}(X) = Min(\mu_A(X), \mu_B(X))\forall x \in X \tag{3.8}$$

The Intersection operation in Fuzzy set theory is the equivalent of the AND operation in Boolean algebra. The membership function of the union (exclusive or) is defined as:

$$\mu_{A\cap B}(X) = Max(\mu_A(X), \mu_B(X))\forall x \in X \tag{3.9}$$

The Union operation in Fuzzy set theory is the equivalent of the OR operation in Boolean algebra. The membership function of the complement (negation) is defined as:

$$\mu_{\neg A}(X) = 1 - \mu_A(X)\forall x \in X \tag{3.10}$$

The complement operation in fuzzy set theory is the equivalent of the NOT operation in Boolean algebra.

The vague nature of fuzzy logic make this approach suitable for problems where information about modelled entity is not well defined. Moreover this representation is particularly useful when integrated with human experts knowledge. Applications of fuzzy logic to data fusion can be found in [79], [80].

To sum up, probabilistic approach is well-known and reliable but requires a deep knowledge of modelled aspects of the system or process and an accurate tuning. D-S provides uncertainty modelling and ambiguous data, moreover rule combination is a powerful technique for representing multiple sources fusion, although its applicability in large sets decrease. Fuzzy theory, based on membership function, is a very intuitive approach for handling human experts knowledge and uncertainty of informations.

3.2 Building Diagnostics through fuzzy logic

Building diagnostics research begun relatively earlier respect of other diagnostics applications such as aerospace, nuclear or military fields. First works were carried out in late 80s [81, 82]. In 90s, several applications for building systems were developed and tested in laboratories. The major part of works proposed focused on AHU and HVAC systems. In the early 1990s, the International Energy Agency (IEA) commissioned the Annex 25 collaborative research project on real-time simulation of HVAC&R systems for building diagnostics and optimisation. In that work, a wide variety of detection and diagnosis methods were investigated. Typically, two approaches can be used for building diagnostics processes: a top-down approach, where the process starts from high level information knowledge or aggregated building level measurements (e.g. general electric consumption, floor lighting consumptions, daily thermal energy...) and then progressively drills down to lower levels causes affecting the abnormal behaviour of higher level measurements or performances. Bottom-up approach starts from low level measures for isolating the problem and then climb up the hierarchy propagating the problem in order to find out how it affects building performances.

3.3 PSC model for building diagnostics

Preprocessing Situation Cause (PSC) model is a three-hierarchical levels rule based framework aimed to identify high level anomalies on the building. In our work a two phases process has been carried out: design phase of building malfunction events was based on a top-down approach: firstly, typical building abnormal events were classified, then, a set of possible situations related to each cause were identified and, finally a set of aggregated measures have been correlated to each situation. Such structures is divided into three levels of information and partially reflects JDL data fusion model.

- *Causes.* Reasons of the anomalous status of the building, typical causes involves occupants behaviour, systems malfunction, structural design errors or exceptional events.
- *Situations.* Anomalous situations of the building, they include assumptions regarding abnormal behaviour of energy vectors related to working schedules, occupancy, weather or structural characteristics.
- *Preprocessing.* Sensor data eventually statistically aggregated, typical preprocessings are trends, outliers and mean values.

The second phase is based on a bottom-up approach: starting from sensors data collected, information is increasingly aggregated to higher levels such that starting from locally failure detected, original, high level causes are guessed. Table 3.2 enumerates the list of preprocessings identified, table 3.3 situations and table 3.4 the causes. It is worth to underline that although such framework is designed to be as more general and scalable, it depends obviously to building characteristics and monitoring system installed, hence, such lists are not, and not intended to be, an exhaustive set of possible anomalies. However, this framework can be continuously updated according to different data, systems and experts assumptions. Table 3.2 groups preprocessings according to data source typologies, for readability reasons, such typologies have been shortened, table 3.1 shows complete meanings. The structure of Preprocessing table regarding consumptions is logically divided into final uses and energy vectors:

- Electric consumption

  - Lighting
  - Emergency
  - Fancoil
  - E.M.F.
- Thermal heating consumption
- Thermal cooling consumption

Furthermore, preprocessing related to occupancy, weather, calendar, working schedule are listed. Situations table 3.3 reflects preprocessing division, therefore is divided into final uses and energy vectors as well.

Acronym	Meaning
LEC	Lighting Electric Consumption
EEC	Emergency Electric Consumption
EMFC	Electro Motive Force Consumption
CEC	Chiller Electric Consumption
CTC	Chiller Thermal Consumption
FCCE	Fancoil Electric Consumption
TFF	thermal Fluid Flow
HTC	Heater Thermal Consumption
IT	Indoor Temperature
IH	Indoor Humidity
EA	Equipment Availability
OB	Occupancy Badge
OS	Occupancy Sensor
WS	Working Schedule
WD	Weather Data

TABLE 3.1: Preprocessings acronym legenda

Measure		Preprocessing
LEC	P_1	Outlier electric consumption
	P_2	Anomalous trend electric consumption
	P_3	Change of mean value of power absorbed
	P_4	Cumulated consumption normalised
	P_5	No consumption
EEC	P_6	Outlier electric consumption
	P_7	Anomalous trend electric consumption
	P_8	Change of mean value of power absorbed
	P_9	Cumulated consumption normalised
	P_{10}	No consumption
EMFC	P_{11}	Outlier electric consumption
	P_{12}	Anomalous trend electric consumption
	P_{13}	Change of mean value of power absorbed
	P_{14}	Cumulated consumption normalised
	P_{15}	No consumption
CEC	P_{16}	Anomalous trend electric consumption
	P_{17}	Anomalous difference between electric and thermal energy
	P_{18}	Cooling Efficiency Anomalous
	P_{19}	Change of mean value of power absorbed compared to nominal
	P_{20}	Cumulated consumption normalised
	P_{21}	No consumption
FCEE	P_{22}	Outlier electric consumption
	P_{23}	Anomalous trend electric consumption
	P_{24}	Change of mean value of power absorbed
	P_{25}	Cumulated consumption normalised
	P_{26}	No consumption
CTC	P_{27}	Outlier thermal energy consumption
	P_{28}	Anomalous difference between electric and thermal energy
	P_{29}	Cooling Efficiency Anomalous
	P_{30}	Change of mean value of power absorbed compared to nominal
	P_{31}	Cumulated consumption normalised
	P_{32}	No consumption
GEC	P_{33}	Cumulated consumption normalised
TFF	P_{34}	Anomalous trend thermal fluid flow
HTC	P_{35}	Outlier thermal energy consumption
	P_{36}	Anomalous difference between electric and thermal energy
	P_{37}	Cooling Efficiency Anomalous
	P_{38}	Change of mean value of power absorbed compared to nominal
	P_{39}	Cumulated consumption normalised
	P_{40}	No consumption
IT	P_{41}	Outlier indoor temperature
	P_{42}	Indoor and outdoor temperature similar
	P_{43}	Anomalous trend indoor temperature
	P_{44}	Setpoint change frequency high
	P_{45}	Thermostat value variance high
	P_{46}	Setpoint mean value

Measure		Preprocessing
IH	P_{47}	Outlier indoor humidity
	P_{48}	Indoor and outdoor humidity similar
	P_{49}	Anomalous trend indoor humidity
EA	P_{50}	Communication interruption
OB	P_{51}	Occupancy Room Percentage
	P_{52}	Probability current room occupancy
	P_{53}	Occupancy building level
OS	P_{54}	Instantaneous room occupancy
WS	P_{55}	Working schedule
WD	P_{56}	Outdoor temperature
	P_{57}	Outdoor humidity
	P_{58}	Pressure level
	P_{59}	Wind Speed
	P_{60}	Wind Direction
	P_{61}	Rain Level
	P_{62}	Solar radiation Level

Table 3.2: Preprocessings

	Situations
S_1	Anomalous consumption on electric devices (lighting)
S_2	Anomalous thermal consumptions on heating equipment (electric)
S_3	Anomalous consumption on electric devices (e.m.f.)
S_4	Uncontrolled external air incoming
S_5	Local thermostat setpoint anomalous
S_6	Anomalous thermal consumptions on cooling equipment (electric)
S_7	Local electric consumption outside working schedule (e.m.f.)
S_8	Lighting equipment turned on outside working schedule
S_9	Thermal losses on distribution system
S_{10}	Places illuminated without presence
S_{11}	Energy consuming auxiliary devices turned on
S_{12}	Insufficient thermal power of heating plant
S_{13}	Insufficient thermal power of cooling plant
S_{14}	Shading devices position modified
S_{15}	Unexpected Emergency lighting turned on
S_{16}	Electric devices turned on without presence (e.m.f)
S_{17}	Electric circuits malfunction
S_{18}	Electric energy supply interrupted
S_{19}	Anomalous number of electric devices turned on (e.m.f)
S_{20}	Unbalanced number of occupancy level compared to working schedule

Table 3.3: Situations

	Causes
C_1	Insufficient Lighting equipment installed power
C_2	Malfunction of scheduled control in thermal plant
C_3	Malfunction on heating plant pumps
C_4	Malfunction on thermal plant AHU
C_5	Malfunction on thermal plant chiller
C_6	Thermostat control failure (heating)
C_7	Thermostat control failure (cooling)
C_8	Distribution system overload or maintenance
C_9	Occupants open windows
C_{10}	Occupants changes setpoint
C_{11}	Occupants leave electric equipment turned on (lighting)
C_{12}	Occupants leave electric equipment turned on (e.m.f.)
C_{13}	Occupants leave electric equipment turned on (heating)
C_{14}	Occupants leave electric equipment turned on (cooling)
C_{15}	Insufficient insulation on thermal distribution system (heating)
C_{16}	Insufficient insulation on thermal distribution system (cooling)
C_{17}	Regulation system failure (heating)
C_{18}	Regulation system failure (cooling)
C_{19}	Thermal plant sizing wrong (heating)
C_{20}	Thermal plant sizing wrong (cooling)
C_{21}	Thermal plant degradation (heating)
C_{22}	Thermal plant degradation (cooling)
C_{23}	Insufficient light level in rooms
C_{24}	Occupants dazzling sunlight
C_{25}	Holiday

TABLE 3.4: Causes

3.4 Application case: F40 diagnostics

In this section, application of heating energy consumption diagnostics through fuzzy logic in F40 building is presented. Such office building, located at R.C. ENEA Casaccia cf. § 2.1 and is composed of three floors and is equipped with an advanced monitoring system aimed at collecting energy consumption (electrical and thermal) and the environmental conditions. For a more detailed description of the building cf. § 5.1. Fan coil electric maximum power consumption of the building second floor was analysed and considered in this experimentation with a 10 minutes time step. Furthermore, people presence and time of the day were recorded with a 10 minutes time step. On the second floor of the building F40 there are 20 fancoil units, characterized by an electrical power of $22W$, $28W$, $40W$ corresponding to the three possible speeds. At the time of testing, the switching on and off of fan coil units were fully manual. Thus, in this study the diagnostics analysis of fan coil units results in a occupant behaviour diagnosis. A dataset of about one day (22 December 2013 - 23 December 2013) was considered. In order to verify the reliability and the effectiveness of the proposed FDD approach, an "artificial" fault was created in the afternoon of Monday 23 December. In that day, between 14:00 and 14:40, with a low people presence, all the fan coil units of the second floor were switched on creating an anomalous peak of energy demand. In order to preprocess electric consumption outliers, statistical peak detection [83] and dbscan [84] methods are used.

Time	Power(kW)	S function	Mzscore
22/12/2013 19:10	0.10	0.10	2.63
23/12/2013 01:30	0.12	0.12	3.30
23/12/201 07:30	0.17	0.17	4.96
23/12/2013 14:10	0.22	0.20	6.63
23/12/2013 14:20	0.21	0.20	6.30

TABLE 3.5: Fault detection results with Peak Detection Method. Parameters values used: $k = 4$, $h = 1$.

Finally, the experimentation concerned the application of the fault diagnosis method on the selected testing day is proposed. The fault diagnosis system is based on fuzzy sets and fuzzy logic. A fuzzyfication of low level signals and a fuzzy sets composition providing a real value, in the lattice [0,1], capable of indicating the seriousness or the alarm degree (1 maximum alarm degree, 0 no alarm degree) of the detected fault with the cause under examination. Thus, in order to characterize the diagnostics index for

Time	Presence	Power(kW)	zPresence	zPower
23/12/2013 07:30	10	0.17	1.78	3.06
23/12/2013 12:00	5	0.03	0.61	0.01
23/12/2013 13:50	3	0.15	0.15	2.62
23/12/2013 14:00	2	0.22	-0.08	4.15
23/12/2013 14:10	2	0.22	-0.08	4.15
23/12/2013 14:20	2	0.21	-0.08	3.93
23/12/2013 14:30	2	0.15	-0.08	2.62
23/12/2013 14:40	2	0.17	-0.08	3.06

TABLE 3.6: Fault detection results with DBSCAN Method. Parameters values used: $\epsilon = 0.5$, $minPts = 5$.

an anomalous fan coil electric consumption out of the working hours for the three floors of the building, the main criterion and process variables for the alarm degree of the detected fault have been defined. The main criterion is: *"IF a fault in fan coil electric consumption occurs AND people presence in the floor is low AND NOT in working hours THEN the diagnostics index is high"*. In order to avoid fake faults, anomaly has to be detected by S-function, Mzscore and DBSCAN simultaneously. In terms of fuzzy sets the diagnostic index can be translated in one of the two ways:

$$C_{13}a = min(S_2, 1 - S_{20}) \tag{3.11}$$

$$C_{13}b = w \cdot S_1 + (1 - w) \cdot S_2 \tag{3.12}$$

where w is a real number in $[0, 1]$ (in the experimentation $w = 0.7$). Following situations have been considered:

- S_2: Anomalous thermal consumptions on heating equipment (electric)
- S_{20}: Unbalanced number of occupancy level compared to working schedule

They are defined as:

$$S_2 = F_1 \wedge F_2 \wedge F_3 \tag{3.13}$$

$$S_{20} = F_4 \wedge F_5 \tag{3.14}$$

Preprocessing P_{22} is obtained through three fuzzy functions intersection, while P_{53} and P_{55} fuzzyfying one sole function, see table 3.7

$$P_{22} = F_1 \wedge F_2 \wedge F_3 \tag{3.15}$$

$$P_{53} = F_4 \tag{3.16}$$

$$P_{54} = F_5 \tag{3.17}$$

Fuzzy set	Linguistic Meaning	μ_{F_i}	Parameters
F_1	*"S function of peak detection is high"*	Sigmoid	$c = 0.05; t = 0.01$
F_2	*"Mzscore of peak detection is high"*	Sigmoid	$c = 2; t = 1$
F_3	*"Dbscan value is high"*	Sigmoid	$c = 1.5; t = 0.5$
F_4	*"not working hours"*	Gaussian	$m = 12; s = 4$
F_5	*"people presence"*	$y = x/p$	$p = 18$

TABLE 3.7: Fault detection results with DBSCAN Method. Parameters values used: $\epsilon = 0.5$, $minPts = 5$.

where p is the floor maximum presence (in particular $p = 18$ for the second floor of the building) and:

$$Sigmoid = \frac{1}{1 + e^{\frac{c-x}{t}}} \tag{3.18}$$

$$Gaussian = e^{-\frac{(x-m)^2}{2s^2}} \tag{3.19}$$

In table 3.8, the fault detection and diagnosis results on the testing day are reported. It can be observed that definition $C_{13}a$ (3.11) performs much better than $C_{13}b$ (3.12) since provides higher alarm values (0.89) in situations where power was too high with respect to the hour of the day. Figure shows the diagnostics index behaviour $C13a$ (the red smooth line) with respect to the normalized power consumption and the normalized people presence, over the testing day.

Time	Power	Presence	F_1	F_2	F_3	F_4	F_5	S_2	S_{20}	$C_{13}a$	$C_{13}b$
22/12 19:10	0.10	0	0.99	0.65	0.52	0.80	0	0.52	0	0.52	0.36
23/12 01:30	0.12	0	1	0.79	0.72	0.97	0	0.72	0	0.72	0.50
23/12 07:30	0.17	10	1	0.95	0.96	0.47	0.56	0.95	0.47	0.53	0.81
23/12 14:10	0.22	2	1	0.99	0.99	0.14	0.11	0.99	0.11	0.89	0.73
23/12 14:20	0.21	2	1	0.99	0.99	0.15	0.11	0.99	0.11	0.89	0.72

TABLE 3.8: Diagnostics results on tested day

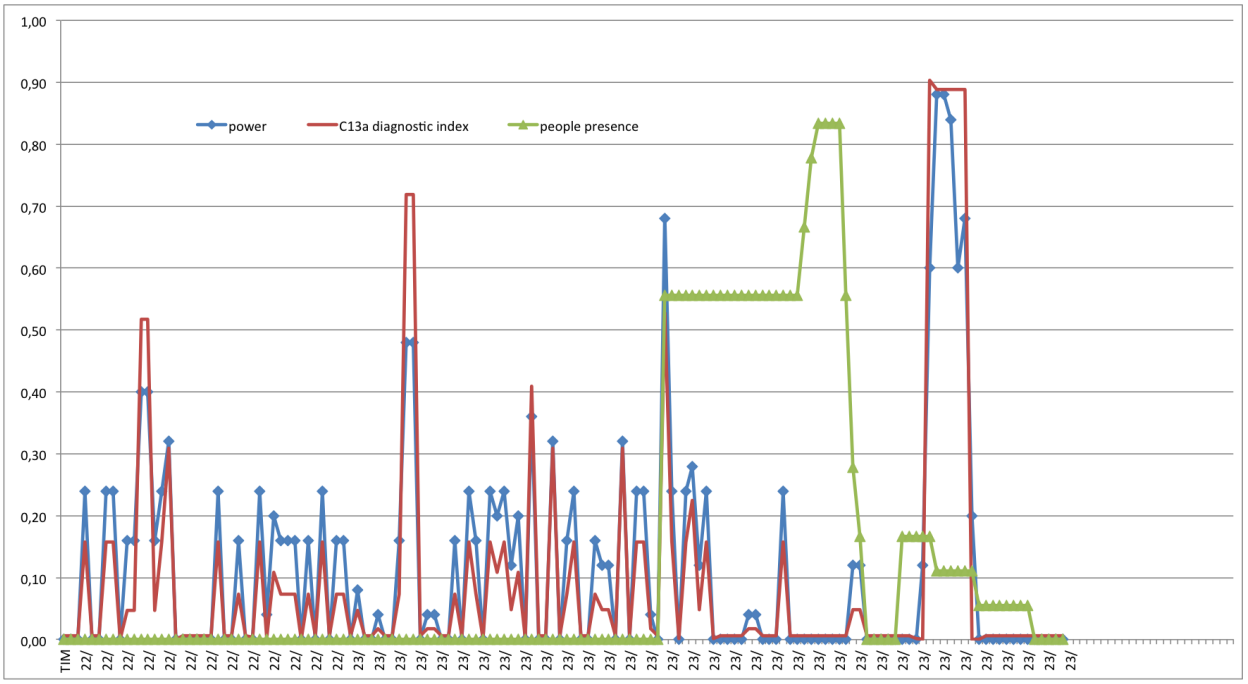

FIGURE 3.1: Thermal Plant Schema

3.5 Conclusion

In this chapter firstly a brief overview on data fusion methodologies and design pattern is given, then the diagnostics process idea is proposed, included the framework implementation. Then finally, rule-based approach in order to diagnostic abnormal electric consumptions of fan coils caused by improper use by the employees is presented. The use of fuzzy rules allows exploitation of a-priori knowledge about the diagnosis going to be analysed and enable to model easily input variables and to combine them together. Furthermore, aggregation of multiple fault detection techniques allowed a robust analysis, reducing fake faults risks. In the experimentation, two relationship rules for evaluation of the cause taken into account were compared. In the present work people presence data, time and electric power were considered.

Chapter 4

Multiobjective Evolutionary Optimisation

4.1 Multiobjective problem

Multi Objective Optimisation (MOOP) is a process aiming to optimise a set of objective functions, many applications has been carried on, due to the multi-objective nature of the majority of the problems we face everyday. The major difference between Single Objective Optimisation (SOOP) and MOOP is not, despite the evidence, just on the number of the objectives to be optimised, instead, it requires a substantially different approach. In MOOP the research space is multidimensional, depending on the objective functions number and the relationship between decision space and research space is often non-linear. Hence, it can be difficult mapping decision variables and research spaces. Furthermore, coping with a Multi Objective Problem (MOP) generally implies handling conflicting objectives, thus a trade-off between the objective is required.

There are two main approaches for coping MOOPs:

- Preference-based approach
- Ideal approach

Preference-based approach exploits previous knowledge of the problem, as preference order of the objectives, to weight the importance of each objective function, turning the

MOP into a Single Objective Problem (SOP). This approach is strongly dependent on the weights and the impact they have on the outcome of the optimisation.

Ideal approach aim to find a set of solution and then, eventually, assign preferences. For this reason, it is crucial to find a wide range of different solutions. In fact a well distributed set of solutions in the research space give relevance to each objective function. Figure 4.1 shows an example of non uniform distribution: in this case the relevance of the first objective function is very low.

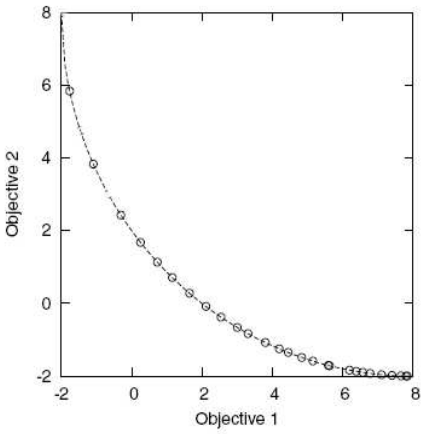

FIGURE 4.1: Non-uniform distribution of the solutions

Equation 4.1

$$\begin{cases} Min/Max & f_m(x) & m = 1, 2, ..., M \\ subject \quad to & g_j(x) \geq 0 & j = 1, 2, ..., J \\ & h_k(x) = 0 & k = 1, 2, ..., K \\ & x_i^{(L)} \leq x_i \leq x_i^{(U)} & i = 1, 2, ..., n \end{cases} \tag{4.1}$$

Where:

- M objectives number;
- J inequality constraints;
- K equality constraints;
- n decision variables number;
- $x_i^{(L)}$ $x_i^{(U)}$ upper and lower bounds of decision variables.

Hence, research space is N-Dimensional and objectives space is M-dimensional. MOP main properties are:

- Linearity
- Convexity

Definition 4.1.1 (Linearity). MOP is linear if each objective and constraint is linear.

Convexity definition is given in 4.1.2

Definition 4.1.2 (Convexity). A function $f : \Re^n \to \Re$ is convex if $\forall x^{(1)}, x^{(2)} \in \Re^n$,

$$f(\lambda x^{(1)} + (1-\lambda)x^{(2)}) \leq \lambda f(x^{(1)}) + (1-\lambda) f(x^{(2)})$$

$\forall\, 0 \leq \lambda \leq 1$

Thus,

Definition 4.1.3. MOP is convex if each objective and constraint is convex.

4.1.1 Optimality Condition in MOPs

Optimality condition is based on dominance criterion:

Definition 4.1.4 (Dominance). A solution $x^{(1)}$ dominates another solution $x^{(2)}$ ($x^{(1)} \preceq x^{(2)}$) if, given M objectives:

1. $f_i(x^{(1)}) \not\trianglerighteq f_i(x^{(2)})\ \forall i = 1...M$
2. $\exists\, i \mid f_i(x^{(1)}) \trianglelefteq f_i(x^{(2)})$ per $i = 1...M$

Definition 4.1.5 (Strict Dominance). A solution $x^{(1)}$ dominates another solution $x^{(2)}$ ($x^{(1)} \prec x^{(2)}$) if, given M objectives::

$$f_i(x^{(1)}) \trianglelefteq f_i(x^{(2)})\ \forall i \in M$$

Where dominance symbol is $\preceq$, strict dominance $\prec$, a worst solution $\triangleright$ and a better solution $\triangleleft$. Dominance criterion is based on following properties:

- Asymmetry. If a solution $x^{(1)}$ does not dominate $x^{(2)}$, it is not implied that $x^{(2)}$ dominates $x^{(1)}$.
- Not-Reflexivity. A solution cannot dominate itself.
- Transitivity. If $x^{(1)} \preceq x^{(2)}$ and $x^{(2)} \preceq x^{(3)}$, hence $x^{(1)} \preceq x^{(3)}$

Figure 4.2 shows an example of dominance criterion: 5 solutions and 2 objective functions are represented. Solution 2 is dominated by every other, 3 and 5 are the non dominated ones, which belong to Non-Dominated Set (NDS) defined as *Pareto Front*.

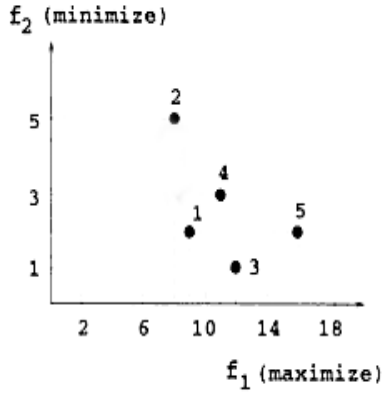

FIGURE 4.2: Popolazione di 5 soluzioni

Definitions 4.1.6 and 4.1.7 define the Pareto Optimal conditions.

Definition 4.1.6 (Pareto Optimal Set). Given a solutions set S, optimal Pareto is the set of non-dominated solutions.

Definition 4.1.7 (Local Pareto Optimal Set). Given a set of solutions S, the solution set $\underline{P}$ is a Pareto Local Optimum if:

$$\nexists\, y \; suchthat \; \|y - x\|_\infty \leq \epsilon \qquad \forall x \in \underline{P}$$

with $\epsilon > 0$

4.1.2 Pareto front search algorithms

In this section we present some algorithms commonly used for identifying the set of non-dominated solutions, hence, they are implemented in almost every MOA. The *Simply*

Pareto Front Algorithm (Algorithm 1), is easy to implement and largely diffused, its complexity is $O(MN^2)$.

Algorithm 1 Simply Pareto Front Algorithm

Require: P {Initial Population}
1: $i \leftarrow 1 \quad j \leftarrow 1$ {Initialising indexes}
2: $P' = \{\emptyset\}$ {Initialising solutions set}
3: **for all** $j \in P(i \neq j)$ **do**
4: **if** $P(j) \preceq P(i)$ **then**
5: **go to** *step* 12
6: **else if** $j \leq |P|$ **then**
7: $j \leftarrow j + 1$
8: **else**
9: $P' = P' \cup \{i\}$
10: **end if**
11: **end for**
12: $i \leftarrow i + 1$
13: **if** $i \leq |P|$ **then**
14: **go to** *step* 3
15: **end if**
16: **return** P'

Kung's Algorithm is a more efficient algorithm and is based on *Divide et Impera*. Solutions set is divided recursively into Top and Bottom, once the set are ordered, they are merged again (Algorithm 2). Its complexity is

$$\begin{cases} O(N \log N) & M = 2, M = 3 \\ O(N(\log N)^{M-2}) & M \geq 4 \end{cases}$$

Third algorithm presented (Algorithm 3) assigns a dominance rank to each solution and is based on previous algorithms (1) o (2).

Figure 4.3 shows an example of ranked solutions.

4.2 Multiobjective Algorithms

MOA are classified into two main categories: "classic" and multiobjective. Classic ones are based on the preference approach previously described, while multiobjective ones are based on ideal approach. Firsts approach was proposed by Box in 1957 [85], and was based on the assignment of a preference to each objective, Naimes [86] proposed the ϵ-Constraint method, where all the objectives but one are turned into constraints.

Algorithm 2 Kung's Algorithm

Require: P {Initial Solutions Set}
1: $P \leftarrow PopulationSorting(P)$ {Descending order sorting according to first objective}
2: **Front(P)** {Recursive Function}
3: **if** $|P| = 1$ **then**
4: **return** P
5: **else**
6: $T = Front\left(P^{(1)} - P^{(|P|/2)}\right)$
7: $B = Front\left(P^{(|P|/2+1)} - P^{(|P|)}\right)$
8: $M \leftarrow T$ {Initialising Merged Set}
9: **for all** $j \in B$ **do**
10: **if** $P(j) \not\succeq P(i)\ \forall\ i \in T$ **then**
11: $M \leftarrow M \cup \{j\}$
12: **end if**
13: **end for**
14: **return** M
15: **end if**

Algorithm 3 Non-Dominated Sorting

Require: P {Initial Population}
1: $j \leftarrow 1$
2: **while** $P \neq \emptyset$ **do**
3: $P_i \leftarrow Kung's Algorithm(P)$
4: $P \leftarrow P \backslash P_i$
5: $j \leftarrow j + 1$
6: **end while**
7: **return** $P_i\ \forall\ i = 1, ..., j$

Shaffer [87] firstly used ideal approach based algorithm called Vector Evaluated Genetic Algorithm (VEGA), Fonseca and Fleming proposed Multi Objective Genetic Algorithm (MOGA) in 1993 [88], Srinivas [89] in 1994 idealised Non-dominated Sorting Genetic Algorithm (NSGA) and successively improved by Deb [90] into Elitist Non-dominated Sorting Genetic Algorithm (NSGA-II) in 2000. Strenght Pareto Evolutionary Algorithm (SPEA) was proposed by Zitzler [91], Pareto Archived Evolutionary Strategy (PAES) by Knowles in 1999 [92]. A more detailed survay of the methods can be found in [93]. In this section, some of the well-known optimisation algorithms are presented.

4.2.1 Weighted Sum Evolutionary Algorithm

Weighted Sum Evolutionary Algorithm (WSEA) is the first and simplest MOA, formally described in (4.2):

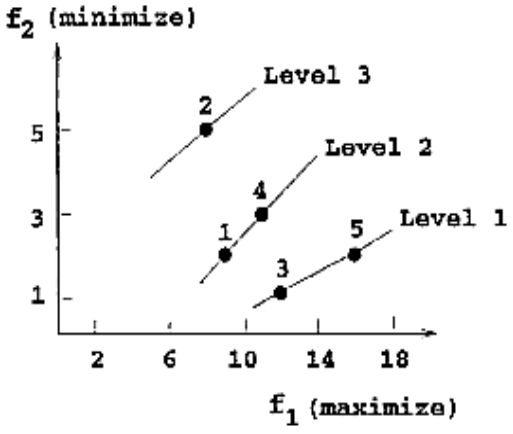

FIGURE 4.3: Non-Dominance levels

$$\begin{cases} Min/Max & F(x) = \sum_{m=1}^{M} w_m f_m(x) & m = 1, 2, ..., M \\ & g_j(x) \geq 0 & j = 1, 2, ..., J \\ & h_k(x) = 0 & k = 1, 2, ..., K \\ & x_i^{(L)} \leq x_i \leq x_i^{(U)} & i = 1, 2, ..., n \end{cases} \tag{4.2}$$

Such approach, as demonstrated in [94], poorly cope non-convex problems, moreover, it requires normalisation of the objective functions and strongly depends on the choice of weights vector.

4.2.2 Epsilon-Constraint Method

ϵ-Constraint method, proposed by Haimes [86], partially overcomes the difficulties on non-convex problems, and is based on the idea of turning every objective but one into constraint with user specified bounds.

$$\begin{cases} Min/Max & f_\mu(x) & \\ subject \quad to & f_m(x) \leq \epsilon_m & m = 1, 2, ..., M \; m \neq \mu \\ & g_j(x) \geq 0 & j = 1, 2, ..., J \\ & h_k(x) = 0 & k = 1, 2, ..., K \\ & x_i^{(L)} \leq x_i \leq x_i^{(U)} & i = 1, 2, ..., n \end{cases} \tag{4.3}$$

ϵ_m represents the upper bound of the function f_m Figure 4.4 shows how the choice of the two-objective problem affects the result of the optimisation.

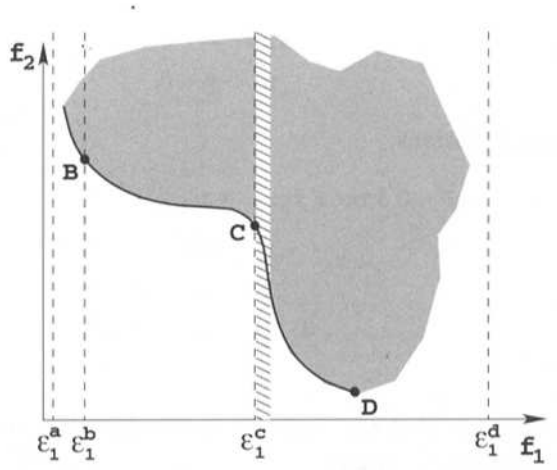

FIGURE 4.4: ϵ-Constraint method example

4.2.3 Vector Evaluated Genetic Algorithm

VEGA split population into M smaller groups, where M is the number of the objectives. Each subset is evaluated according to one objective independently in order to avoid scaling problems. Ordered population subsets are then merged together. Figure 4.5 shows an example of the optimisation process.

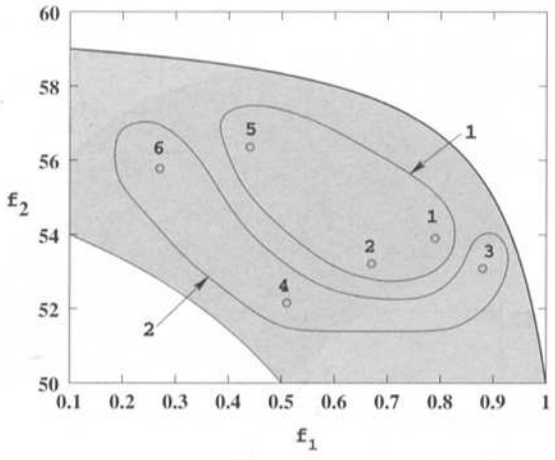

FIGURE 4.5: VEGA example

The main drawback of VEGA is the extreme priority given to "champion" solutions, namely the best in one objective and usually the worst in another one. Such approach, thus, may hamper the spreading of the optimal solutions set.

4.2.4 Multiple Objective GA

MOGA was the first algorithm based on dominance ranking process [88]. Thus, the rank of i_{th} solution of a population is given by (4.4)

$$r_i = 1 + n_i \tag{4.4}$$

Where n_i is the number of solutions dominating i, thus, non-dominated solutions have rank 1. Figure 4.6 shows an example of ranking process. Once rank is assigned, a raw fitness function is given to each solution. The value of the raw fitness is higher for the best solutions and lower for the worst, the mapping function used for intermediate solutions is usually linear.

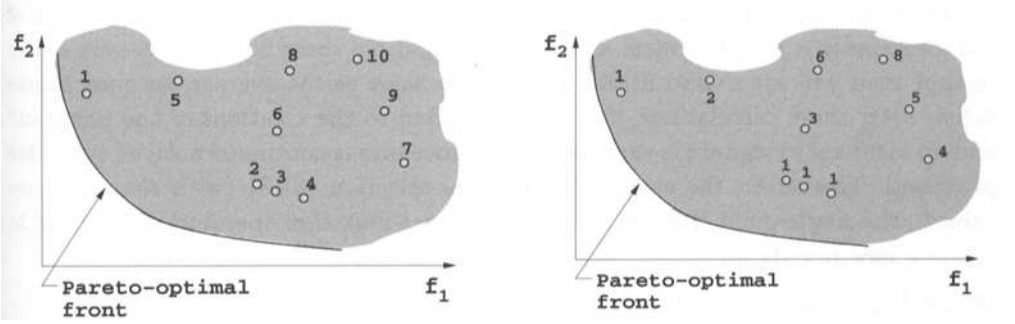

FIGURE 4.6: Ranking in MOGA

In order to maintain diversity among non-dominated solution, the concept of sharing function has been introduced [95]. The sharing function Sh(d) is given by (4.5)

$$Sh(d) = \begin{cases} 1 - \left(\frac{d}{\sigma_{share}}\right)^{\alpha} & se\ d \leq \sigma_{share} \\ 0 & altrimenti \end{cases} \tag{4.5}$$

Where d is the distance between two solutions, σ_{share} is a value depending on the crowding of the solution.

The *niche count* given to each solution is given by (4.6)

$$nc_i = \sum_{j=1}^{N} Sh(d_{ij}) \tag{4.6}$$

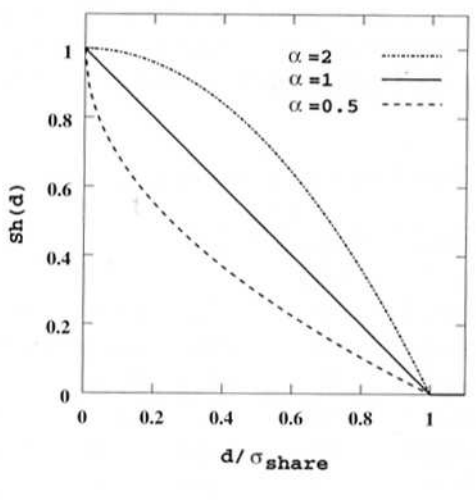

FIGURE 4.7: α values comparison

In MOGA, the distance between two solutions, given M objectives, is determined by (4.7):

$$d_{ij} = \sqrt{\sum_{k=1}^{M} \left(\frac{f_k^{(i)} - f_k^{(j)}}{f_k^{max} - f_k^{min}} \right)} \tag{4.7}$$

Niche count is given by (4.8)

$$nc_i = \sum_{j=1}^{|r_i|} Sh(d_{ij}) \tag{4.8}$$

Where $|r_i|$ is the number of solution having the same rank of i_{th} solution. The final fitness is given by the relationship between raw fitness and niche count. Progressive assignment of raw fitness can mislead the optimal solutions set because may happen that non-dominated solutions has different raw fitness. Moreover, the sharing factor can advantage a dominated isolated solution over a non-dominated crowded solution. This problem can be avoided using levelled ranking sorting, as in NSGA-II.

4.2.5 NSGA-II

NSGA-II proposed by Deb in 2000 [90], is based on levelled ranking described in Algorithm 3. as shown in figure 4.8.

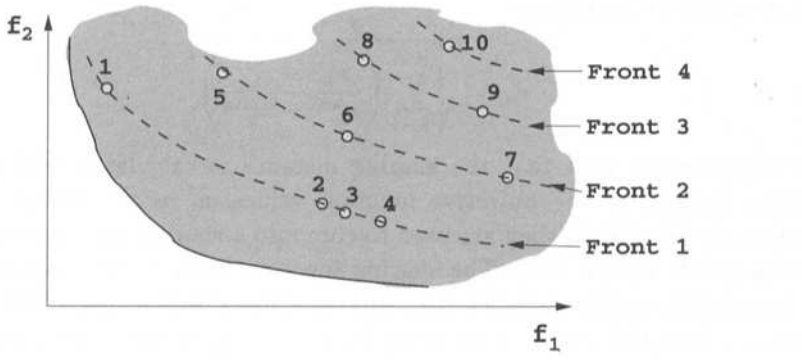

FIGURE 4.8: Levelled Ranking of 10 solutions

In order to maintain diversity among non-dominated solution, *crowding distance* is used. For each ranked level, an infinite crowding distance factor is given to extreme solutions, to the others, a value proportional to the distance to the others, as shown in figure 4.9.

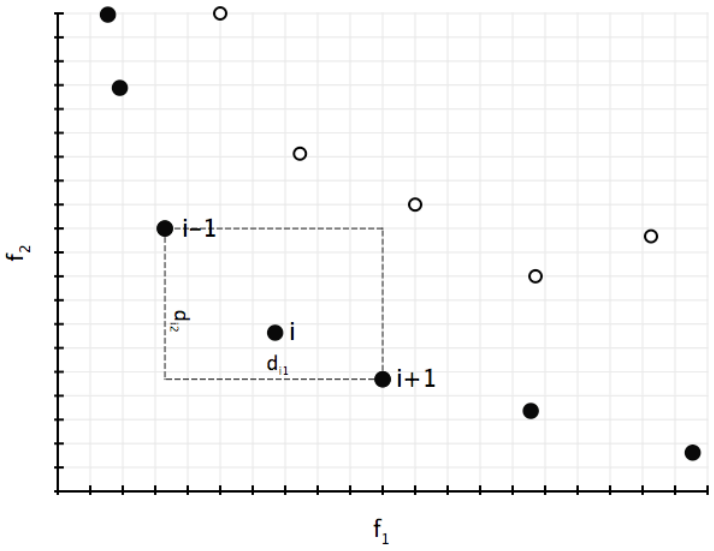

FIGURE 4.9: Crowding distance assignment example

During solutions comparison, if the ranking level is the same, crowding distance is taken into account. Pseudocode of ranking level sorting (4), crowding distance sorting (5) and NSGA-II (6) are presented:

Elitism process enable to maintain best solutions of the previous generations during optimisation process, such that converging process in accelerated and the risk of decreasing the current optimal state is prevented. NSGA-II is a very efficient MOA, does not require initial parameters to be set, maintain the spreading of the Pareto Set wide.

Algorithm 4 Ranking Level Sorting

Require: P {Initial Population}
1: $j \leftarrow 1$
2: **while** $P \neq \emptyset$ **do**
3: $P_i \leftarrow NonDominatedSorting(P)$ {Returns all non dominated individuals}
4: $P \leftarrow P \backslash P_i$
5: $j \leftarrow j + 1$
6: **end while**
7: $P \leftarrow P \cup P_i \; \forall \, i = 1, ..., j$
8: **return** P {Population ordered by rank level}

Algorithm 5 Crowding Distance Sorting

Require: P {Population belonging to the same rank level}
Require: M {Cardinality of objectives}
1: **for** $1 \leq i \leq |P|$ **do**
2: $d_i \leftarrow 0$ {Initialization of Crowding Distances}
3: **end for**
4: **for** $1 \leq m \leq M$ **do**
5: AscendingOrderSort(P,f_m) {Population sorted respect to f_m values}
6: $d_{(1,m)} \leftarrow d_{(|P|,m)} \leftarrow \infty$
7: **for** $2 \leq j \leq |P| - 1$ **do**
8: $d_{(j,m)} \leftarrow d_{(j,m)} + \frac{f_{(j+1,m)} - f_{(j-1,m)}}{f_m^{max} - f_m^{min}}$
9: **end for**
10: **end for**
11: **return** P {Population with crowding distance value assigned}

Algorithm 6 NSGA-II

Require: N {PopulationSize}
1: $P \leftarrow InitalizePopulation(N)$
2: $P \leftarrow RankingLevelSorting(P)$
3: **for all** rank levels **do**
4: $P_i \leftarrow CrowdingDistanceSorting(P_i)$
5: $P \leftarrow P \cup P_i$
6: **end for**
7: **while** *notStopCondition* **do**
8: $P_{selected} \leftarrow Selection(P)$ {Based on rank and crowding distance}
9: $P_{offspring} \leftarrow Crossover(P_{selected})$
10: $P_{mutated} \leftarrow Mutation(P_{offspring})$
11: $P \leftarrow P \cup P_{mutated}$ {Applying Elitism}
12: $P \leftarrow RankingLevelSorting(P)$
13: **for all** rank levels **do**
14: $P_i \leftarrow CrowdingDistanceSorting(P_i)$
15: $P \leftarrow P \cup P_i$
16: **end for**
17: $ReplacePopulation(P, N)$ {Takes the best N individuals of P}
18: **end while**
19: **return** P_1 {Returns individuals belonging to the first rank}

4.3 Comparative study

In this dissertation work, NSGA-II has been largely applied. The implementation of the algorithm was adapted to the requirement of managing both discrete and continuous variables in the same problem. In order to evaluate the quality of the algorithm, it has been firstly compared to

1. RAND: A random search algorithm
2. WSGA: Weighted-Sum Genetic Algorithm
3. NSGA-II: Non-Dominated Sorting Genetic Algorithm

The RAND algorithm is a trivial random search in the input space, with the same number of overall fitness evaluations of the other algorithms. At the end of this sampling, all the non-dominated solutions are considered inside the Pareto Front.

4.3.1 Benchmark Problems

In order to test algorithms performance, ZDT1 (4.9), ZDT2 (4.10) and ZDT3 (4.11) were used [96].

$$ZDT1: \begin{cases} g(x) &= 1 + \frac{9}{n-1}\sum_{i=2}^{n} x_i \\ h(f_1, g) &= 1 - \sqrt{\frac{f_1}{g}} \\ min\ f_1(x) &= x_1 \\ min\ f_2(x) &= g(x)h(f_1, g(x)) \\ 0 \leq x_i \leq 1 & \quad \forall\ i = 1, \cdots, n \end{cases} \tag{4.9}$$

$$ZDT2: \begin{cases} g(x) &= 1 + \frac{9}{n-1}\sum_{i=2}^{n} x_i \\ h(f_1, g) &= 1 - (\frac{f_1}{g})^2 \\ min\ f_1(x) &= x_1 \\ min\ f_2(x) &= g(x)h(f_1, g(x)) \\ 0 \leq x_i \leq 1 & \quad \forall\ i = 1, \cdots, n \end{cases} \tag{4.10}$$

$$ZDT3: \begin{cases} g(x) & = & 1 + \frac{9}{n-1}\sum_{i=2}^{n} x_i \\ h(f_1, g) & = & 1 - \sqrt{\frac{f_1}{g}} - (\frac{f_1}{g})sin(10\pi f_1) \\ min\ f_1(x) & = & x_1 \\ min\ f_2(x) & = & g(x)h(f_1, g(x)) \\ 0 \leq x_i \leq 1 & & \forall\ i = 1, \cdots, n \end{cases} \tag{4.11}$$

4.3.2 Metrics

Dominance Ratio metric was suggested by Zitzler in 1999 [97]. It compares two fronts and returns the percentage of solutions of the first one dominated by the second one, with respect to all the solutions of the first front.

So given fronts F1 and F2,

$$\mathrm{DR} = \frac{\sum_{i=1}^{|F1|} d_i}{|F1|} \qquad d_i = \begin{cases} 1 & \text{if } \exists\ j \mid F1_i \succeq F2_j \\ 0 & otherwise \end{cases} \tag{4.12}$$

Therefore, the smaller the value the better the first front respect to the second is and a value of one implies that the first front is completely dominated by the second. Since dominance operator is not symmetric, DR(F1, F2) is not always equal to 1−DR(F2, F1). Moreover, since the evaluation of dominance ratio regards only dominance, it doesn't consider spreading of solutions.

Spacing metric, proposed by Schott in 1995 [98], evaluates relative distance between consecutive solutions belonging to non-dominated set. It is related to the spread of each non-dominated set independently. The lower spacing value is the more uniform the distribution of solutions is.

Hypervolume metric was proposed by Zitzler and Thiele in 1999 [96]. It evaluates both dominance and spreading of solutions. This metric calculates the area covered by the hypervolume whose vertices are the solutions set and a reference point, a vector of worst values each objective function can assume. Since no scaling is used, a good spread of high magnitude solutions in an objective implies a better performance value with respect to a good spread of low magnitude solutions in another objective. In order to reduce the computational load of such metric we used a Monte Carlo estimation of the hypervolume,

considering the percentage of random points which are dominated by the Pareto front we are measuring. As reference point, was considered the worst values among all the solutions of the Pareto fronts considered.

4.3.3 Results

Table 4.1 shows optimisation parameters used in the test both for NSGA-II and WSGA. The number of performances request is 14000, NSGA-II and WSEA were executed 10 times.

Population	70
Generations	20
Selection	Binary Tournament
Crossover	SBX
Crossover Probability	0.8
Mutation	Polynomial
Mutation Probability	1/30
Elitism	Generational
Population Type	Real parameters

TABLE 4.1: Multiobjective algorithms parameters

Figures 4.10, 4.11, 4.12 shows that NSGA-II outperforms other algorithms in continuous convex problems, non-convex and discrete.

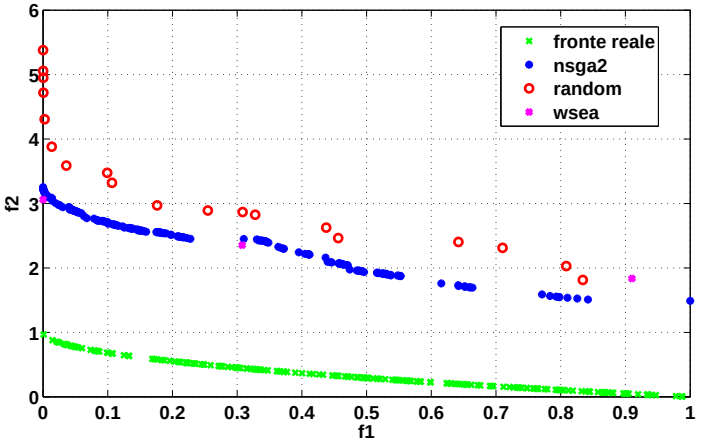

FIGURE 4.10: Pareto fronts on ZDT1

Table 4.2 sum up dominance ratio values of the Pareto fronts obtained. As we can see NSGA-II Pareto front is almost non-dominated by any other front.

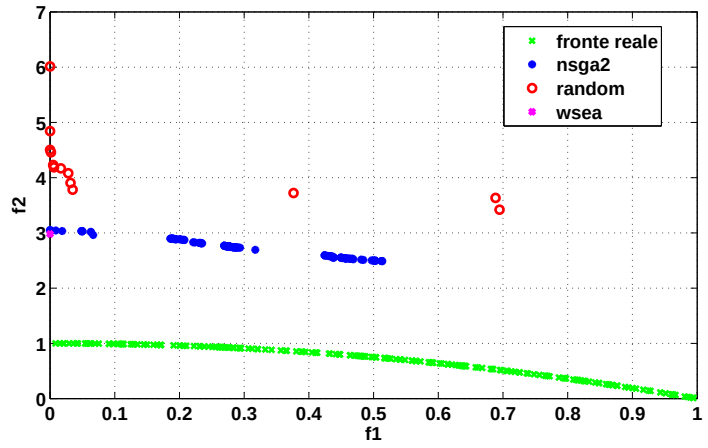

FIGURE 4.11: Pareto fronts on ZDT2

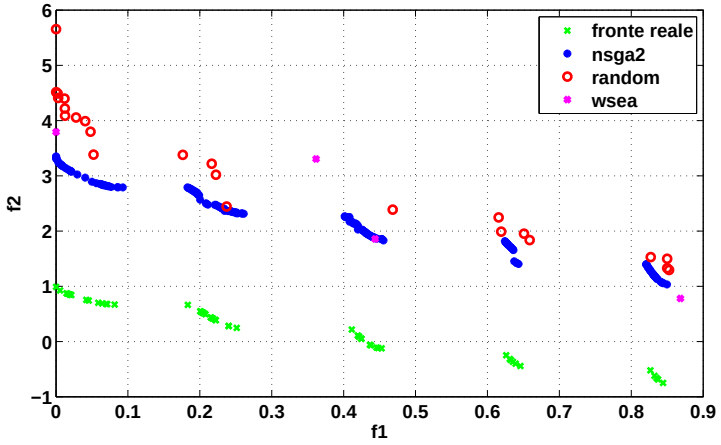

FIGURE 4.12: Pareto fronts on ZDT3

(F1/F2)	NSGA-II			RAND			WSGA		
	zdt1	zdt2	zdt3	zdt1	zdt2	zdt3	zdt1	zdt2	zdt3
NSGA-II	-	-	-	0	0	0	0.17	0.11	0.01
RAND	1	1	1	-	-	-	0.73	1	0.58
WSGA	0.33	0	0.5	0.33	0	0.25	-	-	-

TABLE 4.2: Dominance Ratio on benchmark functions

Table 4.3 shows that NSGA-II presents the lowest spacing values and the highest hypervolume values (4.4)

(F1/F2)	NSGA-II			RAND			WSGA		
	zdt1	zdt2	zdt3	zdt1	zdt2	zdt3	zdt1	zdt2	zdt3
Spacing	0.01	0.12	0.01	0.09	0.28	0.22	0.05	0.19	0.32

TABLE 4.3: Spacing on benchmark functions

(F1/F2)	NSGA-II			RAND			WSGA		
	zdt1	zdt2	zdt3	zdt1	zdt2	zdt3	zdt1	zdt2	zdt3
Hypervolume	0.61	0.58	0.64	0.51	0.49	0.54	0.53	0.5	0.51

TABLE 4.4: Hypervolume on benchmark functions

4.4 Conclusions

This chapter is focused on the definition of MOPs and optimality condition, introducing the concept of Pareto front. Then describes some of the most known MOA, such as VEGA,NSGA-II. In order to compare performance, an implementation and testing has been carried out using well-known benchmark test suite functions. Performance are evaluated trough Dominance Ratio, Spacing and Hypervolume, showing the best performances of NSGA-II. This comparison was not intended to involve a critical up-to-date literature comparison, instead to test effectiveness and proper implementation of the algorithms, as NSGA-II was applied in other optimisation works.

Chapter 5

F40 optimisation

5.1 Building Description

F40 is a three storey building and a basement for thermal plant, and is connected on the east façade on another minor building, not included in monitoring campaign. It was built in 1982, the envelope is composed by a single layer of concrete, and windows and doors shutters are of the same type all over the building. It is a tertiary of building, with an area extension of $2287m^2$ and a volume of $8032m^3$, mainly composed by offices, EDP and Labs. Table 5.1 describes different typologies of the rooms, an average area and the estimated number of occupants associated to.

TABLE 5.1: Rooms description

Final Use	Number	Area	Occupants
Office	41	$15m^2$	$[1, 2]$
Laboratories	4	$32m^2$	$[0, 1]$
EDP	2	$20m^2$	$[3, 4]$
Meeting Room	1	$25m^2$	max 12
Confrence Room	1	$81, 2m^2$	max 50
WC	9	$15m^2$	–

Figure 5.1 shows the schema of the thermal plant. The heating system is centralised on the Research Center, while a chiller producing 180000 frig/hour is installed on the plant. $P_1 - P_5$ represent energy vector providing hot water to fancoils (P_1), radiators and AHU (P_2), cold water to fancoils (P_3) and AHU (P_4) and finally circuit for cooling towers (P_5). As shown, AHU provides air to building rooms, basement and a hall, belonging to the other building.

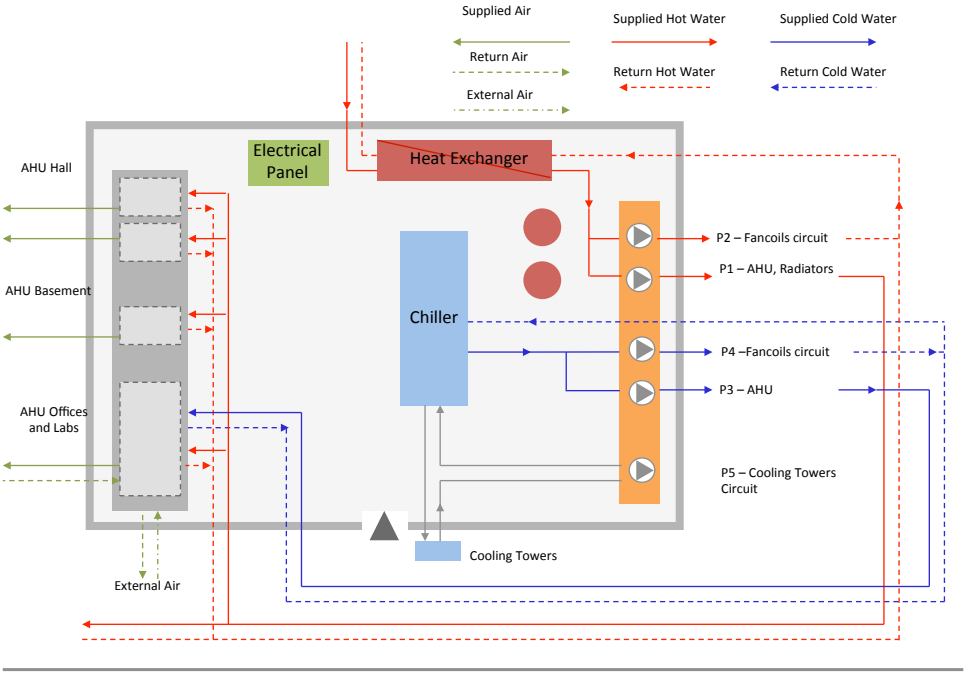

FIGURE 5.1: Thermal Plant Schema

Figure 5.2 shows the planimetry of the building, highlighting different uses of each space.

5.2 White Box Approach

White Box approach is based on a simulator modelling F40 building energy behaviour. The simulator is developed in MATLAB Simulink by "UniversitÃ Politecnica delle Marche" and is based on HAMBASE model ([99], [100]). Simulator required a considerable effort in tuning and design and is capable to model thermal and electrical consumptions, based on presence and meteorological data. Table 5.2 describes which inputs can be handled and table 5.3 the outputs simulator retrieves.

In order to test the reliability of the simulator, it has been compared to measured thermal energy consumption. On a test case of two months (January-March 2014) daily Mean Absolute Percentage Error (MAPE) is 9.36%, while hourly MAPE is 17.93%. Figures 5.3 and 5.4 shows the comparison.

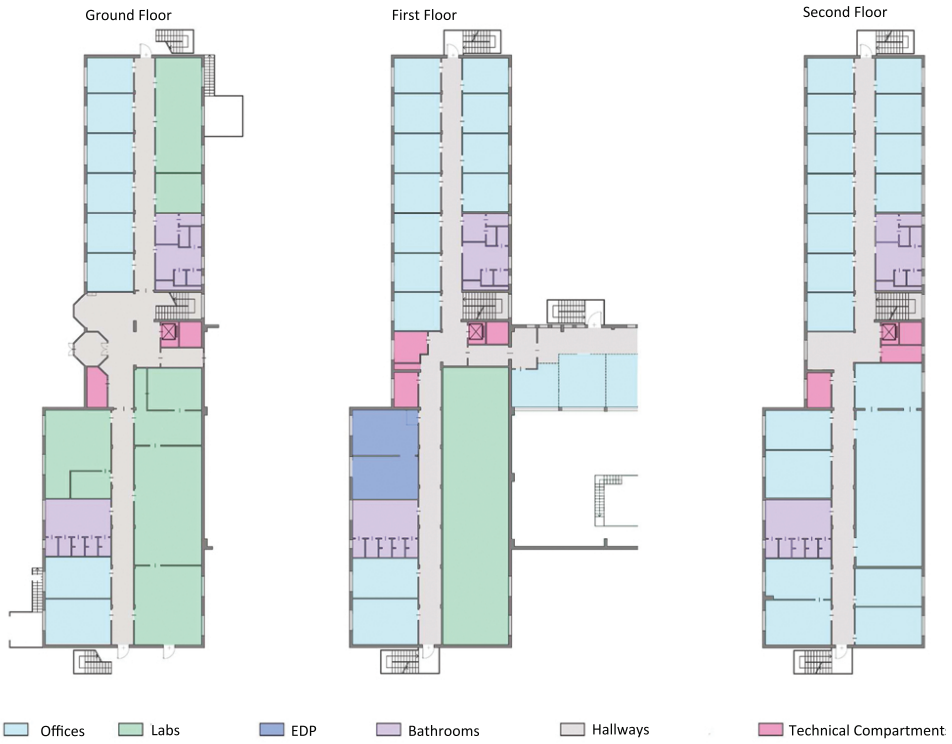

FIGURE 5.2: F40 planimetry

5.2.1 Problem Definition

The goal of the optimisation is to find optimal set points of indoor rooms and thermal plant supply water in order to minimise thermal consumptions and maximise users comfort. Comfort is expressed in terms of Percentage People Dissatisfied (PPD) a function of PMV. PMV is a comfort index introduced by Fanger [101] and is based on variables depending on environment and user subjective factors:

Variable	Meaning	Unit
s_air	Air temperature set point in zones	[]
s_water	Supply water temperature set point	[]
s_flow	Supply water flow	$[kg/h]$
R_diff	Diffuse solar radiation	$[Wm^{-2}]$
Te	Exterior air temperature	[]
Rdir	Direct solar radiation	$[Wm^{-2}]$
C_c	Cloud cover(1...8)	
Rh_e	Relative humidity outside	[%]
Ws	Wind velocity	$[ms^{-1}]$
Wdir	Wind direction	[degrees from north]
P_p	People Presence	

TABLE 5.2: Simulator Input

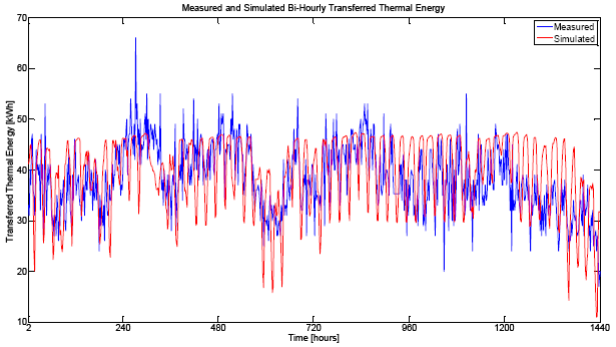

FIGURE 5.3: Hourly Thermal Heating Comparison

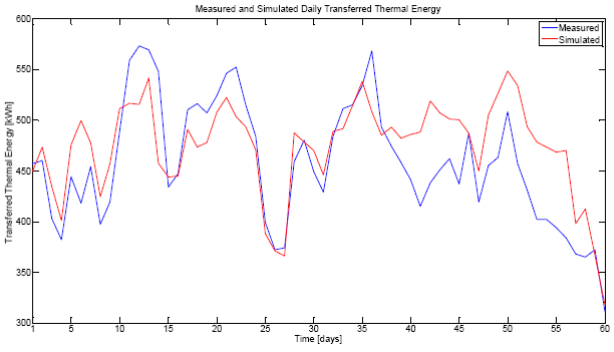

FIGURE 5.4: Daily thermal heating comparison

- functions of clothing:
  - Clothing insulation in clothes
  - Ratio of clothed/nude surface area
- functions of activity:
  - Metabolic heat production (w/m^2)

Variable	Meaning	Unit	Range
Ta	indoor temperatures	$[C]$	
Ts	radiant temperatures	$[C]$	
Rh	indoor relative humidities	$[0, 1]$	
Td	Indoor and Outdoor difference	$[C]$	
Te	external temperature	$[C]$	
Rhe	outdoor relative humidities	%	$[0, 1]$
Q	Thermal Power per zone	$[W]$	
Q_e_fan	Fan Electric loads	$[W]$	
T_out	Fancoil output air temperatures	$[C]$	
flow_r	heating plant return water flow	$[kg/h]$	
T_r	heating plant return water temperature	$[C]$	
flow_r_zone	return water flow per zone	$[kg/h]$	
T_r_zone	return water temperature per zone	$[C]$	
flow_d_zone	discharge water flow per zone	$[kg/h]$	
T_d_zone	discharge water temperature per zone	$[C]$	
c_airflow	airflow control per fancoil	Int	$[0, 3]$
E	Thermal Energy per zone	$[kWh]$	
E_tot	Overall Thermal Energy	$[kWh]$	
PMV	Predicted Mean Vote per zone	Int	$[-3, 3]$
PPD	Percentage of Person Dissatisfied per zone	%	$[5, 100]$
PMV_mean	mean Predicted Mean Vote	%	$[5 - 100]$
E_u	heating plant useful energy	$[kWh]$	
used_ch4	used natural gas	$[m^3]$	
E_e	heating plant electric energy	$[kWh]$	
kWh_to_CO2eq	heating plant equivalent Co2 (summer)	$[Co2eq]$	
NG_to_CO2eq	heating plant equivalent Co2 (winter)	$[Co2eq]$	
flow_d	heating plant discharge water flow	$[kg/h]$	
T_d	heating plant discharge water temperature	$[C]$	
Q_u	heating plant useful power	$[W]$	
flow_ch4	natural gas flow	$[m^3/h]$	
Q_e	heating plant electric power	$[W]$	
eta	heating plant efficiency	%	$[0, 1]$
eer	Chiller Energy Efficiency Ratio	%	$[0, 1]$

Table 5.3: Simulator Output

  - Metabolic free energy production (external work)(w/m^2)

- Environmental variables:

  - Air temperature (Â°C)
  - Mean radiant temperature (Â°C)
  - Relative air speed (m/s)
  - Vapor pressure of water vapour (mb)

Table 5.4 describes the different levels of comfort PMV takes into account.

Value	Sensation
3	Hot
2	Warm
1	Slightly Warm
0	Neutral
-1	Slightly Cool
-2	Cool
-3	Cold

TABLE 5.4: PMV comfort levels

PPD evaluates the percentage of dissatisfied people based on PMV values according to

$$PPD = 100 - 95e^{-(0.03353 \cdot PMV^4 + 0.2179 \cdot PMV^2)} \tag{5.1}$$

As baseline, we considered actual setting of F40 before remote control installation.

- Supplied Water Temperature: Â°65.
- Supplied Water Flow: $42000 kg/h$
- Indoor Air Temperature: Â°21

Since an application of an online daily optimisation in a continuous research space based on a simulator would be unlikely to be applied, and a too small change on thermostats setpoint would not affect actuators, we limited the research space, discretising design variables according to table 5.5.

Variable	Lower Bound	Upper Bound	Step
S_air	17.5	22.5	0.5
S_water	30	80	1

TABLE 5.5: Design Variables Discretisation

5.2.2 Results

As a first step, we performed an exhaustive research on the entire space and then compared Pareto front obtained to baseline. As testing period, we considered 3 months (16 November 2013 - 12 February 2014). Figure 5.5 shows comparison between Pareto

fronts obtained with and without fancoil control. Pareto fronts are obtained seasonal, thus a constant S_air and S_water for the whole 89 days has been set. As we can see, the baseline solution is dominated in both Pareto fronts, and 7% energy saving can be obtained without affecting comfort level.

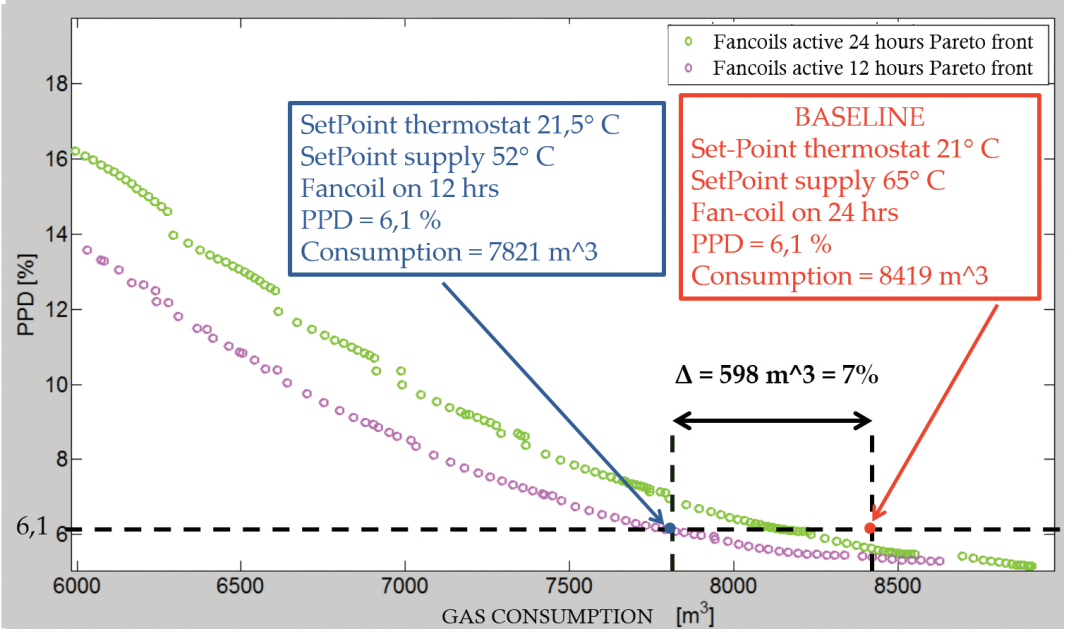

FIGURE 5.5: Exhaustive Search compared to baseline

Successively, we performed an optimisation based on NSGA-II algorithm in MATLAB environment. Since the total solution number of the dataset is 612, we considered a limited number of fitness evaluation for the optimisation, $\approx 1/4$. In order to investigate overall benefits of applying a daily approach over a seasonal approach, we performed both tests using the same number of fitness performance evaluations. Population individuals were binary coded in a 10 bit string according to (5.2). Table 5.6 recap parameters used. As we used a uniform mutation, which means during new offsprings generation a child solution bit may be randomly changed, before applying mutation we performed a Grey encoding, in order to avoid big changes on the real solutions. Without the encoding, in fact, a change on the most significative bit drastically change the real value, while the concept of genetic algorithm is to apply small changes in order to avoid local sub-optimal solutions.

$$\log_2 612 = \lceil 9.25 \rceil = 10 \tag{5.2}$$

Parameter	Value
Optimisation Type	Binary
Population	10
Generations	4
Runs	3
Selection	Tournament
Crossover	Single Point
Crossover factor	0.8
Mutation	Uniform
Mutation factor	0.001

TABLE 5.6: Optimisation parameters

Figure 5.5 shows front obtained trough optimisation and best pareto, namely the non dominated set obtained over all 612 combinations. As trade-off between energy consumption savings and thermal comfort, we chose a PPD threshold of 10% compliant to UNI EN ISO 7330 requirements. The closest value obtained is 9.1%, which led to 18.7% total saving. This approach, thought, cannot prevent the comfort to be over the threshold, since hourly/daily changing factors such meteorological conditions and occupancy are not handled. In fact, in 73% of the cases, PPD is exceed maximum the minimal law requirements. Daily optimisation approach recursively checks the maximum comfort level and adapts S_air and S_flow according to contour conditions. In such case threshold is never exceeded and the final savings compared to baseline are 19.2%.

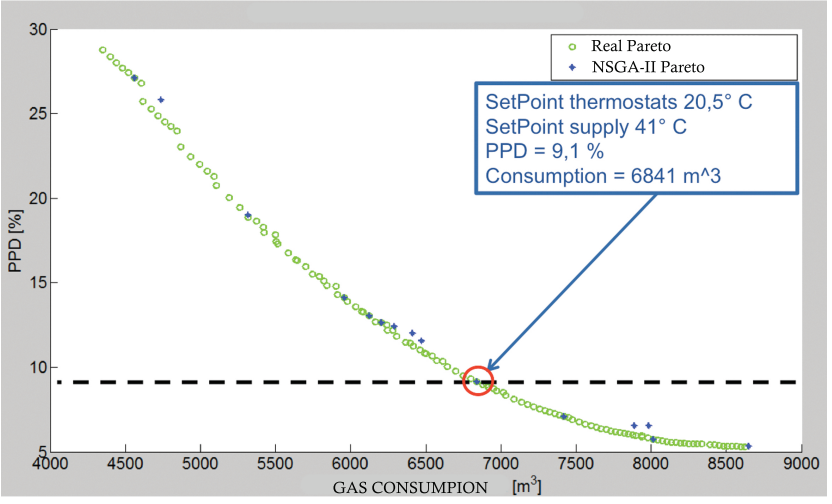

FIGURE 5.6: Seasonal optimisation

Table 5.7 recap results obtained with approaches described. As expected, best results are obtained optimising setpoints on a daily basis. Such approach not only lead to best results, but also avoids to exceed minimum comfort levels.

	Baseline	Exh.Search	Seasonal Opt.	Daily Opt.
Active Fancoils	24 hours	7.00-19.00	7.00-19.00	7.00-19.00
SetPoint Supplied Water [Â°C]	65 (fixed)	52 (fixed)	41 (fixed)	Daily changing
SetPoint Thermostats [Â°C]	21 (fixed)	21.5 (fixed)	21.5 (fixed)	Daily changing
Season PPD [%]	6.1	6.1	9.1	max 8.9
Season Gas Consumption $[m^3]$	8419	7821	6841	6801
Saving $[m^3]$	-	598	1578	1618
Saving [%]	-	7	18.7	19.2
CO_2 saved $[kg]$	-	1136	2998	3074

TABLE 5.7: Optimisation summary

5.3 Grey Box Modeling

Grey box modeling approach is based on the combination of the physical a priori knowledge of the building dynamics, typically white box models, and data driven measures, namely black box models. Such models combine the benefits of the former ones, including data driven parameters estimation into a set of differential equations whose paramaters are uncertain. Hence, physical dynamics are descibed by a set of Stochastic Differential Equation (SDE) in continuous time. The main difference between SDE and Ordinary Differential Equation (ODE) is the uncertainty on parameters introduced by the former, respect of the deterministic nature of the latter. Formally, an ODE is described by 5.3

$$dX_t = f(X_t, u_t, t)dt \quad t > 0 \tag{5.3}$$

where f is a deterministic function of the time t and the state X. In such cases, the solution is deterministic, therefore, future states of the system can be predicted without any error. On the other hand, SDE is described by:

$$dX = AXdt + BUdt + dw(t) \tag{5.4}$$

where $w(t)$ is a stochastic process, introduced for tackling lack of model informations (e.g. some physical dynamics are not modeled by the differential equations), unrecognized inputs affecting the system and noise or errors on the measurements. Therefore, future states predictions are subject to uncertainty, so proper statistical methods for model performance evaluation must be carried out.

Given a Stochastic Linear time-invariant model

$$dx_t = (A(\theta)x_t + B(\theta)u_t)dt + \sigma(\theta)dw_t \tag{5.5}$$

$$y_k = C(\theta)x_k + D(\theta)u_k + e_k \tag{5.6}$$

where t is time, x_t is a state vector, u_t is an input vector, y_k is an output vector, θ is a vector of parameters, A, B, σ, C and D are nonlinear functions, w_t is a standard Wiener process and e_k is a white noise process. Estimation of parameters θ is carried out through maximum likelihood. Given a sequence of measurements $Y_k = [y_k, y_{k-1}, \cdots, y_1, y_0]$ the combinations of paramters θ maximising the likelihood function is found [102–104]. Likelihood function is the joint probability density:

$$L(\theta; Y_n) = p(Y_n|\theta) \tag{5.7}$$

5.3.1 Building Thermal Measures and Actuations

By the thermal consumptions point of view, following measures are available:

- Thermal Plant
  - Thermal Energy $[kWh]$
  - Supplied water flow volume $[m^3]$
  - Supplied water temperature $[^\circ C]$
  - Return water temperature $[^\circ C]$
  - Valve opening percentage $[\%]$
- Rooms
  - Indoor air temperature $[^\circ C]$
  - Status fancoil $[0, 1]$
- Weather
  - Outdoor temperature $[^\circ C]$
  - Outdoor humidity $[\%]$
  - Pressure $[mb]$

- Wind Speed $[m/s]$
- Wind Direction $[°]$
- Rain Level $[mm]$
- Global Solar Radiation $[w/m^2]$

Actuations possible are:

- Supplied water temperature of the thermal plant $[°C]$. The regulation is processed through a three-way thermovalve that partializes flow incoming from central heater and the flow returning from the building circuit.
- Air temperature setpoint of each room $[°C]$. Regulation through fancoils on/off.
- On/Off fancoil of each room.

5.3.2 Building behaviour analysis

First part of the work is focused on design of specific actuation strategies in order to highlight building reaction, to verify if and how reactions suit physical dynamics and for checking accuracy of measured data. as shown in table 5.8.

5.3.2.1 Indoor Temperatures

We analyzed for each sensorised room whether the temperature reacts to setpoint change or not. Since some of the rooms are closed or just locally controlled, in order to evaluate average building temperature we considered only a part of the rooms. Figure 5.7 shows different behavior of the rooms, in 5.7a a correctly responding room temperature, corrsponging to just 51% of the rooms (see table 5.9). Some of the rooms reacts but cannot reach desired setpoint, showing somehow and under reaction to input 5.7b, corresponding to 22% of the rooms. Other unexpected behavior are outscale, outlier (even if in limited number), constant values and no reaction at all. Hence, as averaged building temperature, we considered only rooms correctly responding to the input.

Starting	Ending	SP_rooms	Sp_TP
19-01-2014-18:30:00	19-01-2014-23:00:00	19.5	65
19-01-2014-23:00:00	20-01-2014-01:00:00	30	65
20-01-2014-19:30:00	21-01-2014-00:15:00	30	65
22-01-2014-19:00:00	23-01-2014-00:15:00	12	5
23-01-2014-19:00:00	24-01-2014-02:00:00	30	90
24-01-2014-02:00:00	24-01-2014-09:30:00	30	65
24-01-2014-09:30:00	24-01-2014-16:10:00	12	65
24-01-2014-16:10:00	24-01-2014-22:00:00	12	65
8-02-2014-12:00:00	8-02-2014-15:00:00	20.5	50
8-02-2014-15:00:00	8-02-2014-18:00:00	20.5	45
8-02-2014-18:00:00	8-02-2014-21:00:00	20.5	40
8-02-2014-21:00:00	9-02-2014-00:00:00	20.5	35
9-02-2014-17:30:00	9-02-2014-21:00:00	20.5	50
9-02-2014-21:00:00	10-02-2014-10:00:00	20.5	40
13-02-2014-16:30:00	13-02-2014-21:30:00	25	55
13-02-2014-21:30:00	14-02-2014-01:30:00	12	55
14-02-2014-01:30:00	14-02-2014-10:00:00	25	55
14-02-2014-10:00:00	14-02-2014-13:30:00	25	50
14-02-2014-13:30:00	14-02-2014-18:00:00	18	50
14-02-2014-18:00:00	14-02-2014-23:00:00	25	50
14-02-2014-23:00:00	15-02-2014-02:00:00	25	45
15-02-2014-02:00:00	15-02-2014-10:00:00	18	45
15-02-2014-10:00:00	15-02-2014-16:15:00	25	45
15-02-2014-16:15:00	15-02-2014-19:45:00	25	40
15-02-2014-19:45:00	15-02-2014-22:30:00	18	40
15-02-2014-22:30:00	16-02-2014-01:15:00	25	40

Table 5.8: Actuation History

Input reaction	Rooms	Number	%
Correct	003,008,103,105,106,107,109, 111,112,201,202,203,204,205,207, 208,209,210,216,CR,MR	21	51%
Underreaction	007,011,104,108,110,113,114 213,215	9	22%
Outilier	101,102	2	5%
Outscale	006	1	2.50%
No reaction	004,005,200,206,211,212, 214	7	17%
Constant	100	1	2.50%

Table 5.9: Rooms temperature reaction

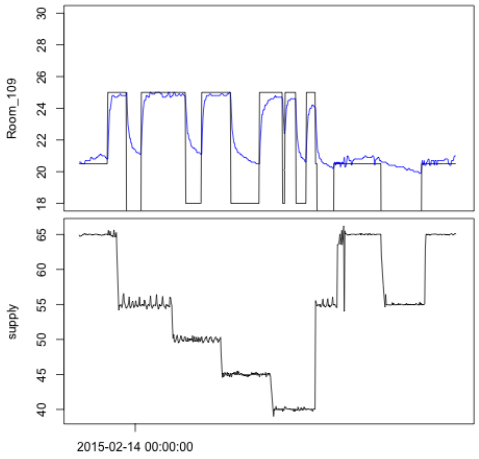

(A) Correct Reaction

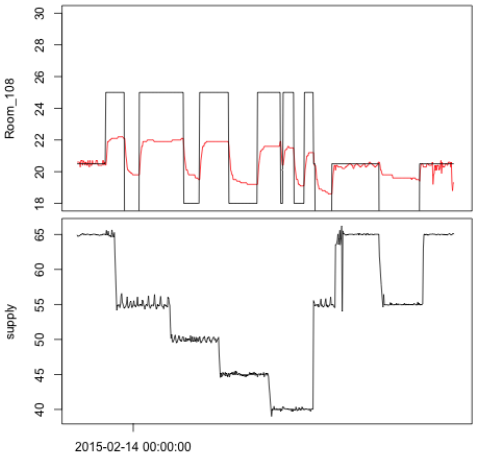

(B) Under Reaction

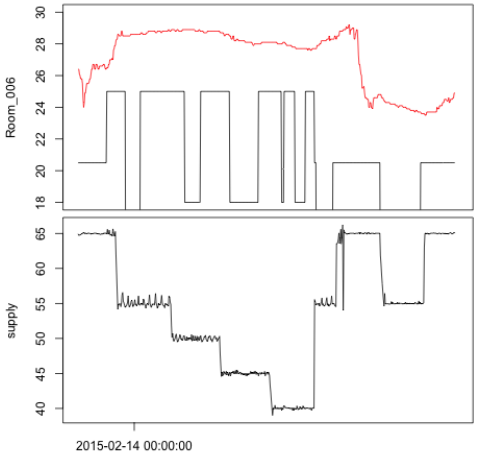

(C) Outscale

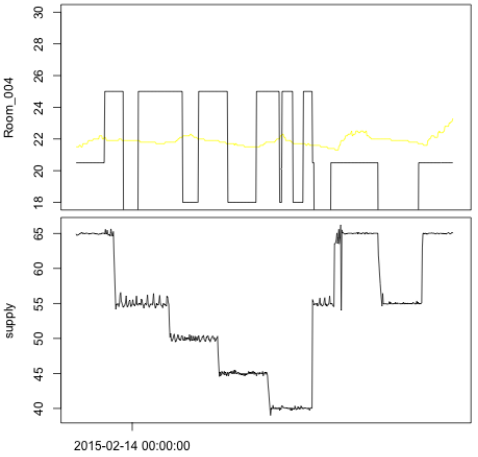

(D) No Reaction

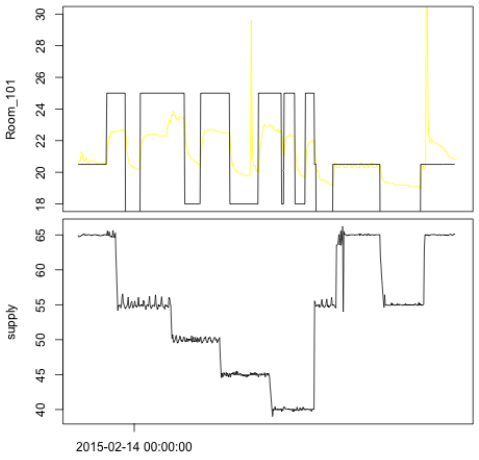

(E) Outliers

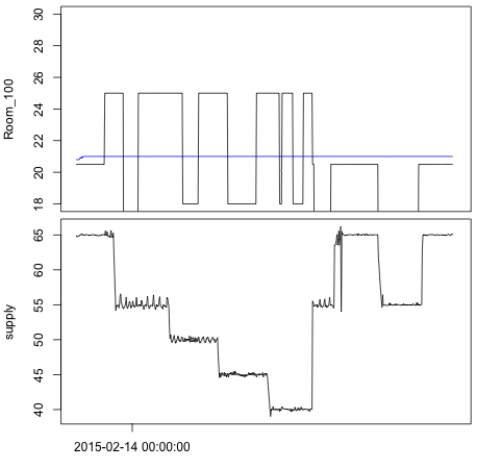

(F) Constant

FIGURE 5.7: Different indoor temperature reaction on setpoints changes

5.3.2.2 Thermal Plant

Thermal plant reaction followed by actuations on supplied water has been analysed. Figure 5.8 shows:

- Thermal energy consumer (kWh)
- Indoor temperature average and rooms set point ($°C$)
- Thermal plant supplied water temperature and setpoint ($°C$)
- Supplied water flow (m^3/h)

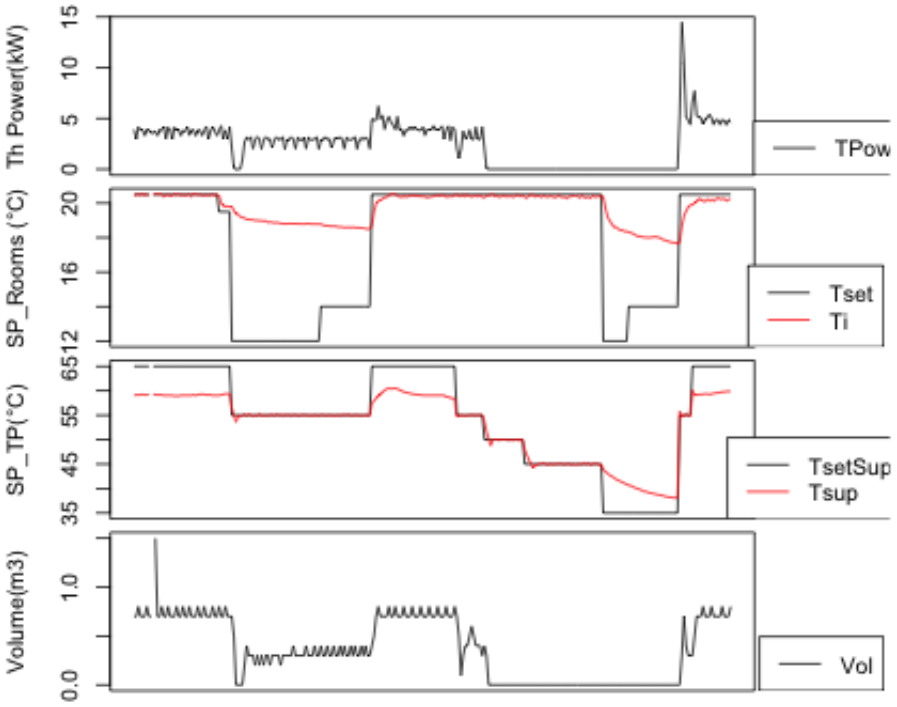

FIGURE 5.8: Thermal Plant Reaction with radiators/AHU circuit open

During the night between 8 and 9 February, supplied water was been gradually decreased, as a result, flow and consequently also thermal energy suddenly fall to zero. Such behaviour has been subsequently explained by the difference of flow rate of the two thermal circuits (radiators/AHU and fancoils, see figure 5.1): when supplied water setpoint decrease, thermovalve closes flow incoming from heat exchanger, as a result, flow balance changes, and since radiators/AHU circuit is bigger, its return flow overwhelms

the other one, causing the heat meter to read negative values for the flow running in the opposite way.

Second test session has been carried out with radiator circuit closed: as we can see, as the supplied water setpoint decreases, measured flow decreases as well, going to zero during step transitions. Since heatmeter is placed after the radiators return circuit, internal recirculation flow of the fancoil circuit is not measured. Thus, when flow measured is zero, the valve is partializing 100% internal circuit flow. Thermal behaviour is consistent, although expected decrease is supposed to be higher.

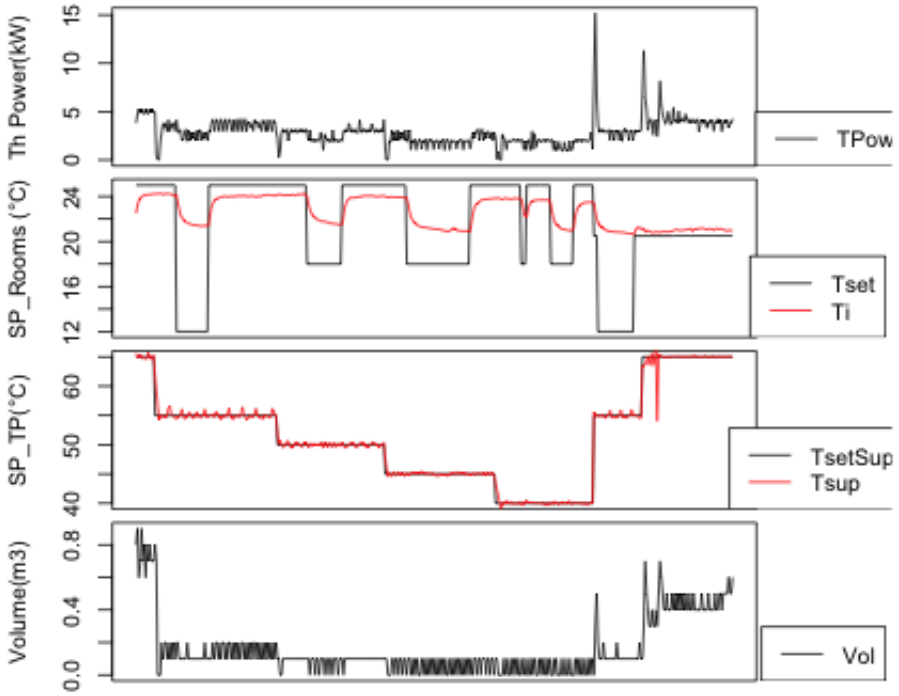

FIGURE 5.9: Thermal Plant Reaction with radiators/AHU circuit closed

5.4 Models design

During the first phase we identified building characteristics needed for starting physical modeling. Table 5.10 shows dimensional information of the building, including glazing area of the windows and walls transmittance. The approach idea is starting with an easy low parametrized model and then gradually increasing complexity in order to identify a reasonable trade-off between complexity and reliability.

TABLE 5.10: Building Characteristics

Characteristic	Value	Unit
Gross Surface	3210	$[m^2]$
Surface	2287	$[m^2]$
Gross Volume	8032	$[m^3]$
Volume	6024	$[m^3]$
Glazing area	148.18	$[m^2]$
Ceiling Transmittance per m^2	0.229	$[\frac{W}{m^2K}]$
Surface Transmittance per m^2	0.426	$[\frac{W}{m^2K}]$
Total Ceiling Transmittance	175.18	$[\frac{W}{m^2K}]$
Total Surface Transmittance	1367.46	$[\frac{W}{m^2K}]$

5.4.1 TiTreturn

First model is based on two states (T_i and T_{return}) and two inputs (T_e and T_{set}), while the output is the thermal energy of the heating system Phi_h. Table 5.11 recaps all the variables taken into account. The Stochastic Differential Equation (SDE) describing the heat balance of the system are (5.8) and (5.9).

TABLE 5.11: Model Variables

Variable	Meaning	Unit
T_i	Internal temperature	$[^\circ C]$
T_e	External temperature	$[^\circ C]$
T_{return}	Return water temperature	$[^\circ C]$
C_i	Internal heat capacity	$[\frac{J}{kg^\circ K}]$
C_h	Heat capacity of the heater	$[\frac{J}{kg^\circ K}]$
R_{ih}	Thermal resistance between internal and heater	$[\frac{m^2{}^\circ K}{W}]$
R_{ie}	Thermal resistance between internal and external	$[\frac{m^2{}^\circ K}{W}]$
R_{he}	Thermal resistance between heater and external	$[\frac{m^2{}^\circ K}{W}]$
Phi_h	Thermal energy of the heating system	$[wH]$

Equation (5.8) describes the state of $T_i(t+1)$ as a function of $T_i(t)$ plus a heat gain/loss proportional to the differences between external and supplied water temperatures. The function f_1 (5.10) is an average of the current supplied water temperature in the distribution system while f_2 (5.11) is a sigmoidal activation threshold of the rooms fancoils.

$$dT_i = \left(\frac{1}{C_i R_{ih}} \cdot (f_1 - T_i) f_2 + \frac{1}{C_i R_{ie}} \cdot (T_e - T_i)\right) dt + e^{P_{11}} dw_1 \tag{5.8}$$

$$dT_{return} = \left(\frac{1}{C_h R_{ih}} (T_i - f_1) f_2 + \frac{1}{C_h R_{he}} (T_e - f_1) + \frac{1}{C_h (T_{sup} - T_{ret}) \cdot fl \cdot cw}\right) dt + e^{p22} dw_2 \tag{5.9}$$

where

$$f_1 = \frac{T_{sup} - T_{ret}}{2} \tag{5.10}$$

$$f_2 = \frac{1}{1 + e^{-10(T_{set} - T_i)}} \tag{5.11}$$

Figure 5.10 shows RC circuit representation of the lumped model. We identified four primary layers, interior, in this case the whole building, the heating plant, the envelope,

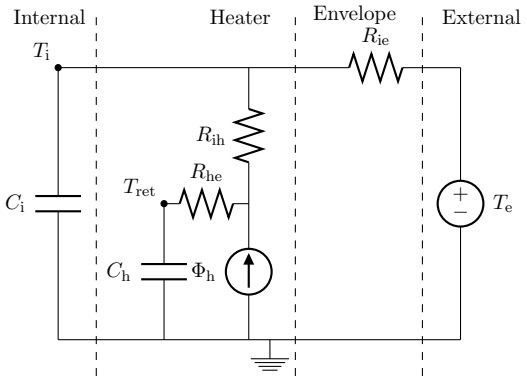

FIGURE 5.10: TiTreturn RC model

introduced for modeling the heat exchange resistance with the external, and the external. Internal layer is modeled with an internal heat capacity, while heater layer describes heat exhanges between internal and distribution system and the heat capacity of the heater. Envelope and external correlates internal/external heat exchanges and external temperature influence.

Figure 5.11 shows a qualitative analysis of the model response. In the top, indoor average temperature T_i and its estimation T_iHat are shown, as well as thermostat setpoint. In the middle, supplied water set point, temperature and return temperature estimation T_r are reported. Finally, the lower one compares heat energy consumed and its estimation. T_iHat is not affected by setpoints change and therefore is not capable to follow properly the real internal temperature. Moreover, thermal energy is overestimated.

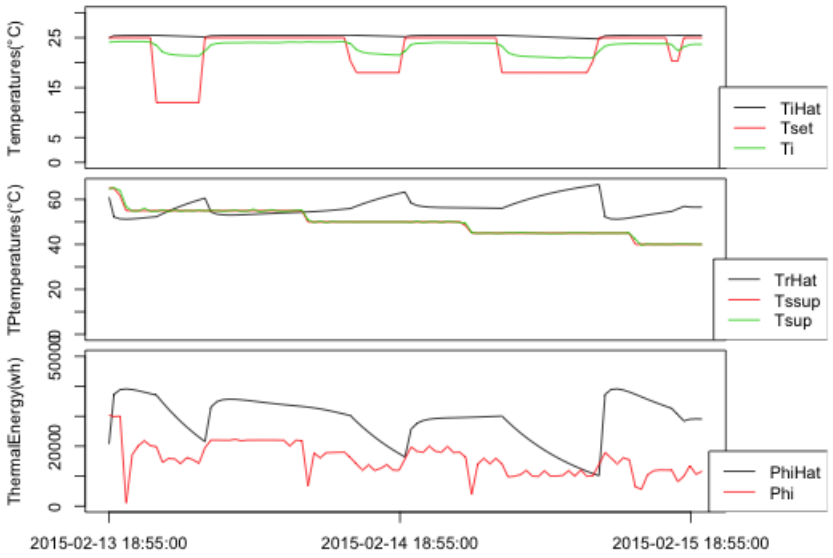

FIGURE 5.11: TiTreturn

5.4.2 TiTwTreturn

This version of the model introduces a third state T_w, representing the temperature of the walls of the building. Thus, in this model C_i represents just the internal heat capacity of the building, not including walls. T_i equation models the behaviour of internal building averaged temperature, that is affected by thermal plant heating and walls temperature gains. T_{return} is the same as the previous model. Table 5.12 summarize parameters used.

$$dT_i = \left(\frac{1}{C_i R_{ih}} \cdot (f_1 - T_i) f_2 + \frac{1}{C_i R_{iw}} \cdot (T_w - T_i) \right) dt + e^{P_{11}} dw_1 \tag{5.12}$$

$$dT_w = \left(\frac{1}{C_w R_{iw}} \cdot (T_i - T_w) + \frac{1}{C_w R_{we}} \cdot (T_e - T_w) \right) dt + e^{P_{22}} dw_2 \tag{5.13}$$

$$dT_{return} = \left(\frac{1}{C_h R_{ih}} (T_i - f_1) f_2 + \frac{1}{C_h R_{he}} (T_e - f_1) + \frac{1}{C_h (T_{sup} - T_{ret}) \cdot fl \cdot cw} \right) dt + e^{p33} dw_3 \tag{5.14}$$

TABLE 5.12: Model Variables

Variable	Meaning	Unit
T_i	Internal temperature	$[^\circ C]$
T_e	External temperature	$[^\circ C]$
T_w	Walls temperature	$[^\circ C]$
T_{return}	Return water temperature	$[^\circ C]$
C_i	Internal heat capacity	$[\frac{J}{kg^\circ K}]$
C_h	Heat capacity of the heater	$[\frac{J}{kg^\circ K}]$
C_w	Heat capacity of the walls	$[\frac{J}{kg^\circ K}]$
R_{ih}	Thermal resistance between internal and heater	$[\frac{m^2 {}^\circ K}{W}]$
R_{iw}	Thermal resistance between internal and walls	$[\frac{m^2 {}^\circ K}{W}]$
R_{we}	Thermal resistance between walls and external	$[\frac{m^2 {}^\circ K}{W}]$
R_{he}	Thermal resistance between heater and external	$[\frac{m^2 {}^\circ K}{W}]$

Figure 5.12 shows the RC circuit of the model. In this case, Envelope has its own heat capacity C_w, and three new heat resistance are introduced: R_{iw} and R_{we} describe the heat transfer between internal wall and external, while R_{he} is introduced for modeling heat losses in the pipes.

As we can see in figure 5.13, in this case $T_i Hat$ has a faster dynamics, reacting after a setpoint decrease, although the target indoor temperature T_i maintains an higher level

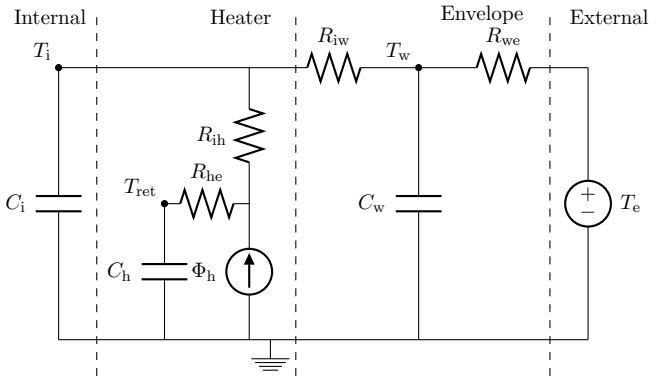

FIGURE 5.12: TiTwTreturn RC model

of lower bound temperature. Since the model is not considering rooms not controlled, a setpoint decrease causes a consistent internal temperature drop of T_iHat. This problem can be avoided introducing two different behaviours of the indoor temperature depending whether are controlled or not.

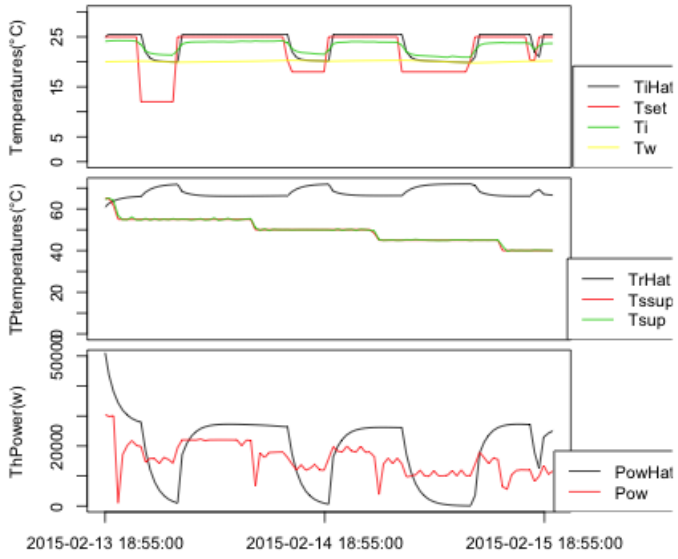

FIGURE 5.13: TiTwTreturn

5.4.3 TiTwTreturnTinc

In this model we introduced a new input on the system, T_{inc} which is an average of internal temperature of non controlled rooms. Such input is used in the equation (5.15) for modeling the heat gain of controlled rooms affected by the uncontrolled rooms overheat. R_{ir} describes the heat resistance between internal and non controlled rooms, table 5.13 describes all the parameters of this model.

$$dT_i = \left(\frac{1}{C_i R_{ih}} \cdot (f_1 - T_i) f_2 + \frac{1}{C_i R_{ie}} \cdot (T_w - T_i) + \frac{1}{(C_i R_{ir})} \cdot (T_{inc} - T_i) \right) dt + e^{P_{11}} dw_1 \tag{5.15}$$

$$dT_w = \left(\frac{1}{C_w R_{iw}} \cdot (T_i - T_w) + \frac{1}{C_w R_{we}} \cdot (T_e - T_w) \right) dt + e^{P_{22}} dw_2 \tag{5.16}$$

$$dT_{return} = \left(\frac{1}{C_h R_{ih}} (T_i - f_1) f_2 + \frac{1}{C_h R_{he}} (T_e - f_1) + \frac{1}{C_h (T_{sup} - T_{ret}) \cdot fl \cdot cw} \right) dt + e^{p33} dw_3 \tag{5.17}$$

TABLE 5.13: Model Variables

Variable	Meaning	Unit
T_i	Internal temperature	$[^\circ C]$
T_{inc}	Internal temperature of non controlled rooms	$[^\circ C]$
T_e	External temperature	$[^\circ C]$
T_w	Walls temperature	$[^\circ C]$
T_{return}	Return water temperature	$[^\circ C]$
C_i	Internal heat capacity	$[\frac{J}{kg^\circ K}]$
C_h	Heat capacity of the heater	$[\frac{J}{kg^\circ K}]$
C_w	Heat capacity of the walls	$[\frac{J}{kg^\circ K}]$
R_{ih}	Thermal resistance between internal and heater	$[\frac{m^2 {}^\circ K}{W}]$
R_{ir}	Thermal resistance between internal and non controlled rooms	$[\frac{m^2 {}^\circ K}{W}]$
R_{iw}	Thermal resistance between internal and walls	$[\frac{m^2 {}^\circ K}{W}]$
R_{we}	Thermal resistance between walls and external	$[\frac{m^2 {}^\circ K}{W}]$
R_{he}	Thermal resistance between heater and external	$[\frac{m^2 {}^\circ K}{W}]$

Figure 5.14 depicts RC model. The main difference is in the internal layer, the internal temperature T_i is affected by the new input T_{inc} according to thermal resistance R_{ir}.

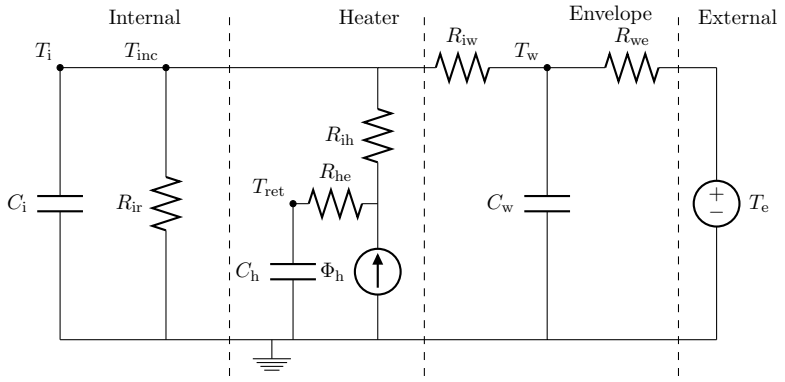

FIGURE 5.14: TiTwTreturnTinc RC model

As we can see in figure 5.15, T_iHat now follows properly the behaviour of T_i, as non controlled rooms contribute to keep temperature level higher then expected when thermostats are turned off. The heating plant dynamics however still does not replicates original behaviour.

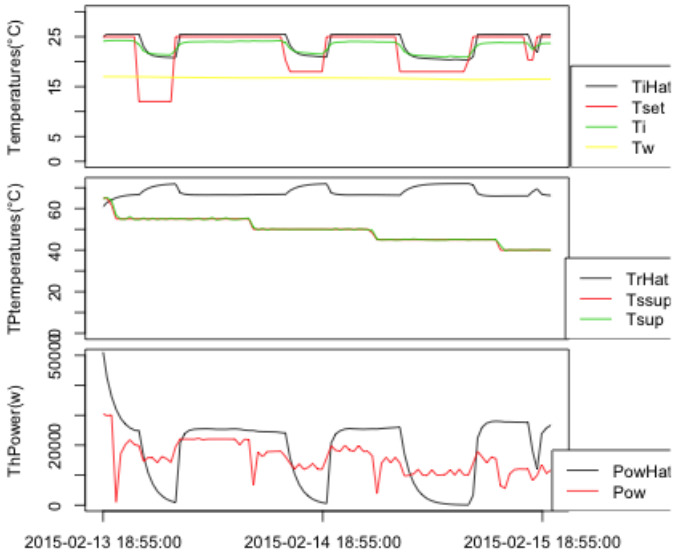

FIGURE 5.15: TiTwTreturnTinc

5.4.4 TiZTwTreturnTinc

In this version of the model we divided the building into 4 thermal zones, according to the pipes loop. The idea is to explicit the dynamics of the distribution system affecting different zones with a delay interval. Moreover, although the complexity is increased, zone division reflects more precisely the real structure of the building.

$$dT_{iZ1} = \left(\frac{1}{C_i R_{ih}} \cdot (f_1 - T_{iZ1}) f_2 + \frac{1}{C_i R_{ie}} \cdot (T_w - T_{iZ1}) + \frac{1}{(C_i R_{ir})} \cdot (T_{incZ1} - T_{iZ1})\right) dt + e^{P_{11}} dw_1 \tag{5.18}$$

$$dT_{iZ2} = \left(\frac{1}{C_i R_{ih}} \cdot (f_1 - T_{iZ2}) f_2 + \frac{1}{C_i R_{ie}} \cdot (T_w - T_{iZ2}) + \frac{1}{(C_i R_{ir})} \cdot (T_{incZ2} - T_{iZ2})\right) dt + e^{P_{12}} dw_1 \tag{5.19}$$

$$dT_{iZ3} = \left(\frac{1}{C_i R_{ih}} \cdot (f_1 - T_{iZ3}) f_2 + \frac{1}{C_i R_{ie}} \cdot (T_w - T_{iZ3}) + \frac{1}{(C_i R_{ir})} \cdot (T_{incZ3} - T_{iZ3})\right) dt + e^{P_{13}} dw_1 \tag{5.20}$$

$$dT_{iZ4} = \left(\frac{1}{C_i R_{ih}} \cdot (f_1 - T_{iZ4}) f_2 + \frac{1}{C_i R_{ie}} \cdot (T_w - T_{iZ4}) + \frac{1}{(C_i R_{ir})} \cdot (T_{incZ4} - T_{iZ4})\right) dt + e^{P_{14}} dw_1 \tag{5.21}$$

$$dT_w = \left(\frac{1}{C_w R_{iw}} \cdot (T_i - T_w) + \frac{1}{C_w R_{we}} \cdot (T_e - T_w)\right) dt + e^{P_{22}} dw_2 \tag{5.22}$$

$$dT_{return} = \left(\frac{1}{C_h R_{ih}} (T_i - f_1) f_2 + \frac{1}{C_h R_{he}} (T_e - f_1) + \frac{1}{C_h (T_{sup} - T_{ret}) \cdot fl \cdot cw}\right) dt + e^{p33} dw_3 \tag{5.23}$$

Table 5.14 summarize parameters used. For simplicity, we supposed the same thermal resistance and heat capacity among different zones.

TABLE 5.14: Model Variables

Variable	Meaning	Unit
T_{iZ_n}	Internal temperature in the zone	$[^\circ C]$
$T_{iZ_n nc}$	Internal temperature of non controlled rooms in the zone	$[^\circ C]$
T_e	External temperature	$[^\circ C]$
T_w	Walls temperature	$[^\circ C]$
T_{return}	Return water temperature	$[^\circ C]$
C_i	Internal heat capacity	$[\frac{J}{kg^\circ K}]$
C_h	Heat capacity of the heater	$[\frac{J}{kg^\circ K}]$
C_w	Heat capacity of the walls	$[\frac{J}{kg^\circ K}]$
R_{ih}	Thermal resistance between internal and heater	$[\frac{m^2 {}^\circ K}{W}]$
R_{ir}	Thermal resistance between internal and non controlled rooms	$[\frac{m^2 {}^\circ K}{W}]$
R_{iw}	Thermal resistance between internal and walls	$[\frac{m^2 {}^\circ K}{W}]$
R_{we}	Thermal resistance between walls and external	$[\frac{m^2 {}^\circ K}{W}]$
R_{he}	Thermal resistance between heater and external	$[\frac{m^2 {}^\circ K}{W}]$

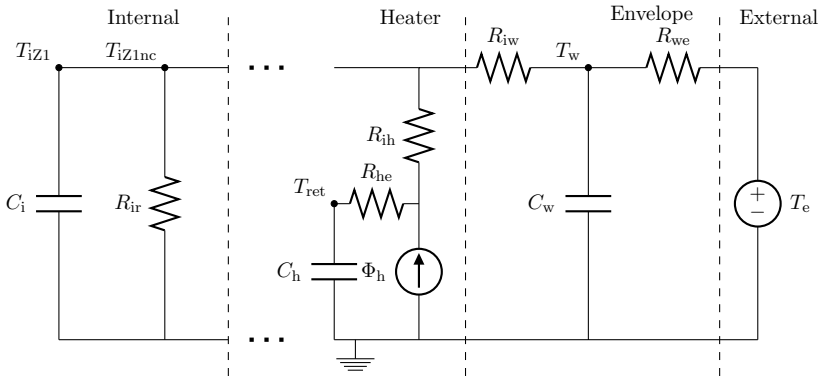

FIGURE 5.16: TiZTwTreturnTinc RC model

The RC model (figure 5.16) is structured as the previous, except for the internal, divided into 4 sub circuits affected by different average temperature zones.

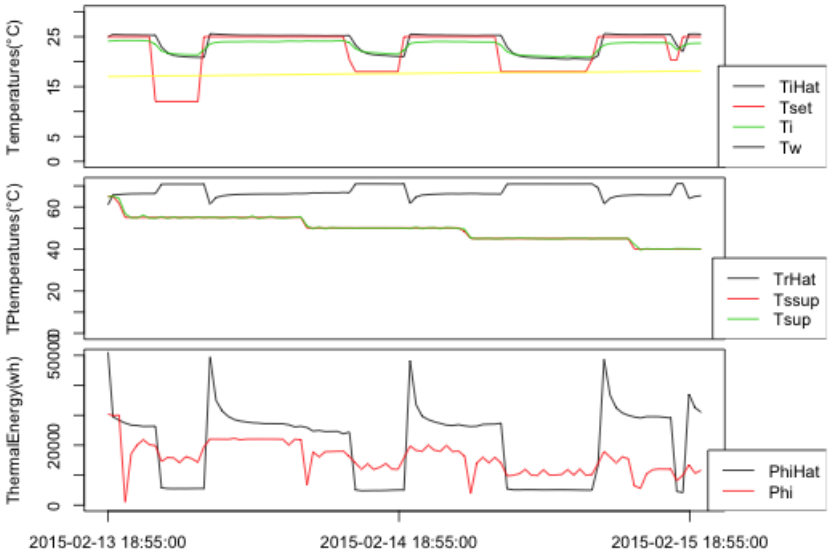

FIGURE 5.17: TiZTwTreturnTinc

5.4.5 TiZTwTreturnTincFlow

In the last model developed we introduced the measured flow as an input of the model, as the RC circuit and parameters are the same, they are not presented again.

$$dT_{iZ1} = \left(\frac{1}{C_i R_{ih}} \cdot (f_1 - T_{iZ_1}) f_2 + \frac{1}{C_i R_{ie}} \cdot (T_w - T_{iZ_1}) + \frac{1}{(C_i R_{ir})} \cdot (T_{incZ_1} - T_{iZ_1})\right) dt + e^{P_{11}} dw_1 \tag{5.24}$$

$$dT_{iZ2} = \left(\frac{1}{C_i R_{ih}} \cdot (f_1 - T_{iZ_2}) f_2 + \frac{1}{C_i R_{ie}} \cdot (T_w - T_{iZ_2}) + \frac{1}{(C_i R_{ir})} \cdot (T_{incZ_2} - T_{iZ_2})\right) dt + e^{P_{12}} dw_1 \tag{5.25}$$

$$dT_{iZ3} = \left(\frac{1}{C_i R_{ih}} \cdot (f_1 - T_{iZ_3}) f_2 + \frac{1}{C_i R_{ie}} \cdot (T_w - T_{iZ_3}) + \frac{1}{(C_i R_{ir})} \cdot (T_{incZ_3} - T_{iZ_3})\right) dt + e^{P_{13}} dw_1 \tag{5.26}$$

$$dT_{iZ4} = \left(\frac{1}{C_i R_{ih}} \cdot (f_1 - T_{iZ_4}) f_2 + \frac{1}{C_i R_{ie}} \cdot (T_w - T_{iZ_4}) + \frac{1}{(C_i R_{ir})} \cdot (T_{incZ_4} - T_{iZ_4})\right) dt + e^{P_{14}} dw_1 \tag{5.27}$$

$$dT_w = \left(\frac{1}{C_w R_{iw}} \cdot (T_i - T_w) + \frac{1}{C_w R_{we}} \cdot (T_e - T_w)\right) dt + e^{P_{22}} dw_2 \tag{5.28}$$

$$dT_{return} = \left(\frac{1}{C_h R_{ih}} (T_i - f_1) f_2 + \frac{1}{C_h R_{he}} (T_e - f_1) + \frac{1}{C_h (T_{sup} - T_{ret}) \cdot fl \cdot cw}\right) dt + e^{p33} dw_3 \tag{5.29}$$

Figure 5.18 shows a significant improvement on the heating and temperature estimation. The estimation $T_i Hat$ follows properly T_i and also $T_r Hat$ reflects accordingly the behaviour of the supplied water temperature. We tested the model in another period and in both cases the response is quite satisfactory, the error in the test showed in figure 5.19 amounts to $2\% \pm 0.23\%$ for the internal temperature estimation and $11.2\% \pm 2.4\%$ for thermal energy.

5.5 Conclusions

In this chapter we described a real case application on an actual building of the white and grey box approach for thermal optimisation. White box approach has been combined with NSGA-II optimisation algorithm and two different approaches has been tested: seasonal and daily control. Even if a white box approach is suitable in applications where a complete understanding of physical behavior of building dynamics is available,

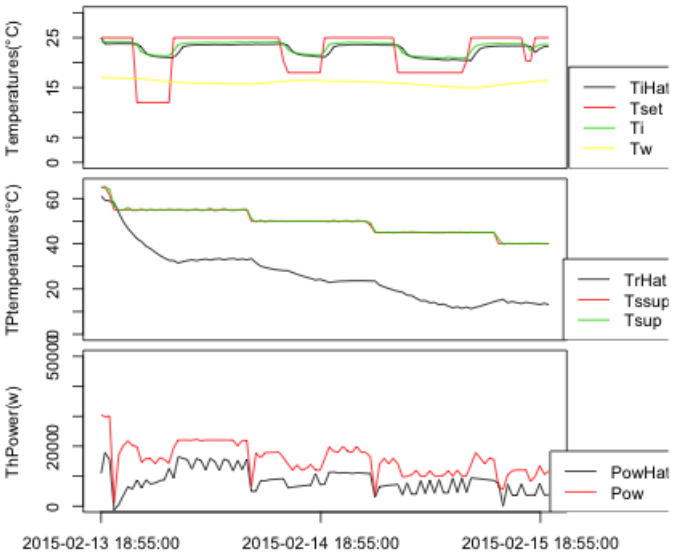

FIGURE 5.18: TiZTwTreturnTincFlow

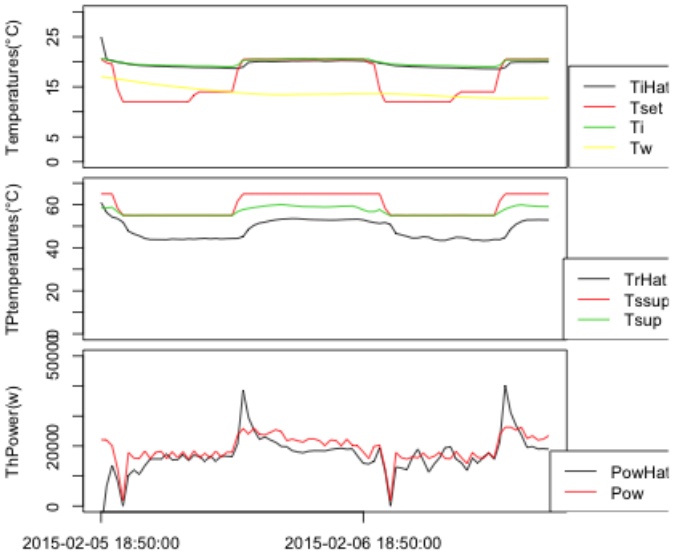

FIGURE 5.19: TiZTwTreturnTincFlow

we believe a grey box approach can be more scalable and less expensive from a computational point of view. Results on F40 building are promising, and a model based predictive control will be tested in order to evaluate actual effectiveness.

Chapter 6

Multiobjective optimisation of building fenestration design

In the majority of countries around the world buildings require large amounts of energy both for heating and cooling. Cooling loads due to solar gains represent about half of the global cooling loads for residential and non-residential buildings [105]. In addition, the ratio of glazed area on the total area of a building's façade represents one of the most important variables influencing the energy need for heating and cooling. Thus, identifying design parameters of shading devices could considerably increase thermal energy performance of the building.

In order to find out optimal parameters for design efficient building many studies has been carried out over the last decade: Radford et al. [106] applied dynamic programming for multi-criteria design optimisation of 4 parameters: thermal load, daylight availability, construction cost and usable area, Huang [107] used adaptive learning based on Genetic Algorithm (GA) for optimal tuning of PID controller of the HVAC system, Hauglustaine et al. [108] developed an interactive tool for optimizing building envelope parameters using GA, Wright [109] using multiobjective genetic algorithm for energy consumption and occupant thermal comfort optimisation, in particular on a mechanical system design point of view, Rolfman [110] studied the influence of extra insulation, new types of window and the introduction of a heat pump on CO_2 emissions. More recently, Wang et al. [111] applied a multiobjective optimisation for optimal design in green building, taking into account also the life-cycle of parameters (e.g. building orientation,

wall, roof and windows types, wall and roof layers..), that is the sum of consumptions and waste emissions associated to primary resources, processes and activities related to parameters choice. Life-cycle based evaluation was proposed also by Hasan [112], he used a combination of simulator and optimisation in order to find out the best design parameters (insulation thickness of wall, root and floor, U-Value of windows and type of heat recovery), Capozzoli et al. [113] proposed the use of the ANOVA approach for sensitive building energy design.

Moreover, many studies take in account also shading devices for building design optimisation: Tzempelikos [114] studied the impact of the use of motorized shading devices and lighting ignition control on buildings for cooling and lighting demand optimisation, Franzetti et al. [115] identified 14 parameters concerning the relationship between daylight and thermal loads, Ho et al. [116] investigated the best geometric configuration of shading devices for daylight exploitation, Li [117] studied daylight provided to an high populated residential building in Hong Kong, taking into account six parameters: building orientation and area, window area, glazing type, shading and colour of external surface. Manzan [118] proposed a study in which took in account both thermal and lighting consumptions in order find out the best geometrical and structural parameters of a shading panel through genetic optimisation on RADIANCE simulations. Subsequently, he improved his work [119] replacing RADIANCE with DAYSIM, which allows on-line evaluation of daylight coefficient and incorporates also behaviour control model Lightswitch.

TABLE 6.1: Design Variables

Variable Description	Boundaries	Unit	Distribution	Var.Name
Window aspect ratio	[1/2:2]	-	uniform	WH
Depth of reveal	[0:0.25]	m	uniform	s
Overhang depth	[0:2]	m	uniform	W_o
Overhang distance:				D_o
no storey above the window	[0:0.85]	m	uniform	
three storeys above the window	[0:4]	m	uniform	
six storeys above the window	[0:4]	m	uniform	
Overhang extension ratio	[0:3]	-	uniform	DW
Fin depth	[0:2]	m	uniform	W_f
Fin distance	[0:4]	m	uniform	D_f
Fin height:				H_f
no storey above the window	[0:2]	m	uniform	
three storeys above the window	[0:11]	m	uniform	
six storeys above the window	[0:20]	m	uniform	
Fin position	[right, left]	-	uniform	p

To sum up, many studies and applications have been carried on identification of optimal building design, in particular of HVAC systems, glazed areas and shading devices. A common requirement for this issue is the massive use of simulator tools (e.g. MATLAB, GBtool, TRNSYS, Simlab, BDA...) in order to find out the quality of design variables according to chosen criteria (e.g. consumption, welfare, economics or environment point of view). Since building dynamics are often highly non-linear, gradient-based optimisation algorithms are not well-suited in such cases [120], while Evolutionary based algorithms are less likely to get stuck in local optimum and less dependent to starting point. Moreover, since multiobjective optimisation is generally based on a set of optimal solutions, called Pareto front, instead of a single one, population based algorithms are an appropriate choice. In fact, many of previous works are based on such techniques. However, since Evolutionary optimisation algorithms are stochastic based, an high number of objective functions (or fitness) must be evaluated in order to obtain a wide range of optimal solutions. Besides, simulations are in most cases computationally expensive and time consuming, therefore is a common approach to implement a surrogate model approximating the real one. Plenty of applications have been carried out on several fields: recently was applied in pharmaceutical manufacturing [121], transportation network [122] and inverse heat conduction [123]. As the correlation between input forcing variables and output depending variables is generally non-linear, multi-linear regression models are usually not the best choice. To cope non-linearity nature of many real problems, Neural Network based models has been carried on. These types of models compute output variables from input by a composition of basic function and connections. During neural network learning phase a mapping between input-ouput is processed. Supervised learning maps minimizing error of training data, unsupervised learning attempt to find an underlying structure of data. Particularly interesting the work of Magnier [124]: he developed a Response Surface Approximation (RSA) model based on Neural Networks (NN) for mimic the behavior of TRNSYS simulation of building. On surrogate model, he applied multiobjective optimisation of total consumption and thermal comfort according to building design parameters (five windows dimension and concrete thickness) and HVAC system control parameters (temperature and humidity set points, thermostat delays, supply air flow rates). However, is difficult to generalize many real-world mechanics due to an high number of influencing factors. Since ensembling technique exploit diversity of the output of multiple models, is possible to achieve a more generalized prediction and therefore overcome the problem. First ensembling technique proposed was

Basic Ensemble Method (BEM) [125], the simplest way to combine M neural networks as an arithmetic mean of their outputs. A direct BEM extension is the Generalised Ensemble Method (GEM) in which the outputs of the single models are combined in a weighted average where the weights have to be properly set. In order to obtain diversity among different models of the ensemble Breiman [126] introduced the Bootstrap Aggregating technique: replacing training data set of each learner with a random combination of training data itself.

TABLE 6.2: Cross Correlation of design Variables

	Wf	*Hf*	*p*	*Wo*	*DW*	*WH*	*Df*	*Do*
s	-0.16	0.01	0.23	-0.27	0.1	-0.09	-0.05	-0.13
Wf		0.02	0.024	0.09	-0.03	0.38	-0.26	-0.15
Hf			-0.001	-0.18	0.05	0.14	0.19	0.21
P				-0.25	-0.15	0.12	-0.006	-0.11
Wo					0.11	-0.08	-0.008	0.34
DW						-0.13	-0.07	0.28
WH							0.3	-0.26
Df								0.16

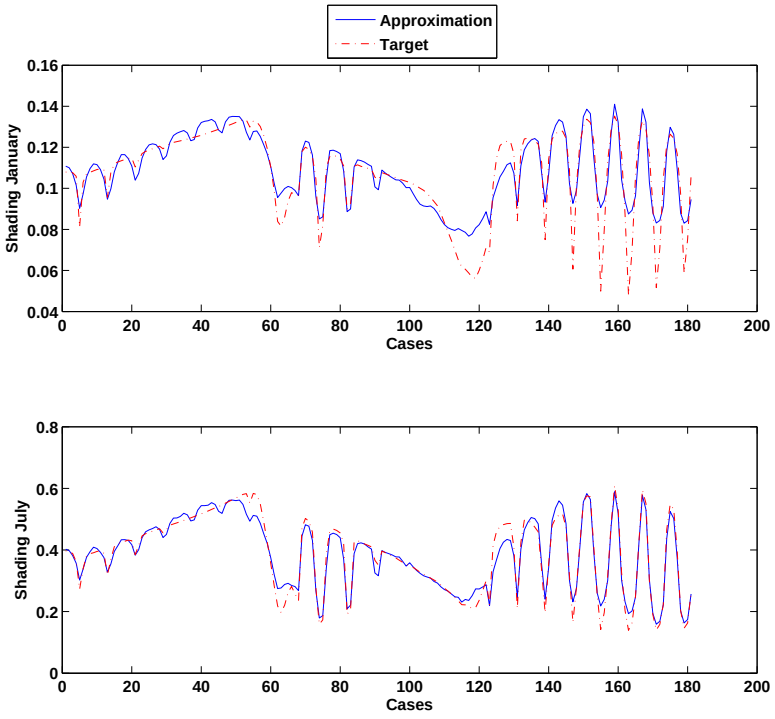

FIGURE 6.1: Surrogate Model

NSGA-II, proposed by Deb [90], is one of the most efficient MOEA [96], applies genetic algorithm principles of selection, crossover and mutation to each individual, fitness evaluation is based on dominance as first criterion and then on crowding distance, which

supports isolated solutions such that spreading is encouraged. It differs from NSGA [89] for the introduction of the elitism, a technique inspired by evolutionary theory, stating that best individual always survives over generations. Thus, in order to keep best individuals over the next generation, evolutionary principles are applied to generation n and $n+1$. As GA, also NSGA-II can be based on binary coded parameters or real parameters according to the nature of the problem (discrete or continuous). In our work we tackle both discrete and continuous variables, so we modified the code in order to handle both type of variables simultaneously.

6.1 Problem definition

The problem we deal with is to find out configurations of building shadow-casting objects such that shading factor on winter season is maximized and minimized during summer season. It is clearly a two conflicting objective optimisation. Table 6.1 shows design variables taken into account. They are all related to dimension and position of objects influencing the way shadow is cast. The following list describes the meaning of each variable:

- Variable 1: window aspect ratio, W/H, which is the ratio of the width of the window on its height. The area of the window was set to a constant value of 1.45 m^2 which, according to the fixed geometry assumptions, led to the maximum allowable height of the window with the lowest W/H.
- Variable 2: depth of the reveal, s, which represents the distance between the plane of the window and the outer plane of the wall.
- Variable 3: depth the overhang, W_o, which is the distance of the outer edge of the overhang from the plane of the window. For structural reasons, the maximum depth of the overhang was set to 2.00 m.
- Variable 4: distance of the overhang, D_o, which is the distance between the overhang and the highest edge of the window. Its maximum value is a function of how many storeys are above the window. Hence, different limits were chosen for each configuration. Considering that overhangs that are very far from the window would have a negligible influence on shading, the maximum distance was set to

4.00 m (as if the balcony were two storeys above the window). For windows on the highest floor or in the isolated building, the maximum distance was set to 0.85 m, which is the distance between the floor slab and the top edge of the window with the highest W/H. For lower values of W/H the presence of a small attic can be hypothesised.

- Variable 5: overhang extension ratio, $\Delta W/W$, which represents the ratio of the lateral extension of the overhang beyond the vertical sides of the window on the width of the window.

- Variable 6: depth of the fin, W_f, which is the distance of the outer edge of the fin from the plane of the window. For comparison with the overhang, the maximum depth of the fin was set to 2.00 m as well.

- Variable 7: distance of the fin, D_f, which is distance between the fin and the closest lateral edge of the window. For comparison with the overhang, the maximum distance of the fin was set to 4.00 m as well.

- Variable 8: height of the fin, H_f, which is the distance between the base of the window and the highest edge of the fin. Different limits for each configuration were considered.

- Variable 9: position of the fin, p_f, which is a flag variable that indicates whether the fin is placed on the right or left side of the window.

These variables evaluated on six different scenarios according to three different exposures (North, South, East/West) and contexts (isolated and urban).

6.1.1 Objective Function

The shading factor is defined as the ratio of the global solar radiation received on a surface in presence of shading obstacles on the global solar radiation received in their absence. Its average value, with respect to a reference period, is given by:

$$Fs_m = \frac{Fs_{b,m} \cdot H_b + Fs_{d,m} \cdot H_d + H_r}{H_b + H_d + H_r} \tag{6.1}$$

where $Fs_{b,m}$ and $Fs_{d,m}$ are, respectively, the average geometric shading coefficients for direct and diffuse radiation.

The calculation of the shading factor was performed with a model capable of accounting for complex boundary conditions, such as a horizon profile, generic-shaped obstructions and vegetation [127]. Anisotropy of sky was also taken into account but solar radiation reflected from obstructions was evaluated in a simplified way. The monthly shading factor was calculated by assuming its value coincident with the daily shading factor of the average day of the month. For each month, the average day was considered the one with average sun path, corresponding also to the one with average duration of the day.

6.2 Experimentation and discussion

Experimentation carried out is divided into three main frameworks:

- Dataset. For each input design variable, a range of variation that covers most of the recurrent building envelope design solutions was considered and a specific probability density function was taken into account. A significant number of representative cases (about 950) was generated for each configuration (North,South, East/West exposures and isolated/urban context)
- Surrogate Model. Dataset was used to train both Neural Network, and Neural Networks Bagging Ensemble in order to tune an approximated model capable to replace the actual time-consuming simulator. Further details about the surrogate model are discussed in subsection 6.2.1
- Optimisation and post Pareto processing. Multiobjective optimisation is based on NSGA-II and has been carried out on surrogate model previously defined, then the resulting Pareto front has been analysed in order to identify which input design variables are more important (see subsections 6.2.2 and 6.2.3).

Figure 6.2 summarize the process flow of our problem.

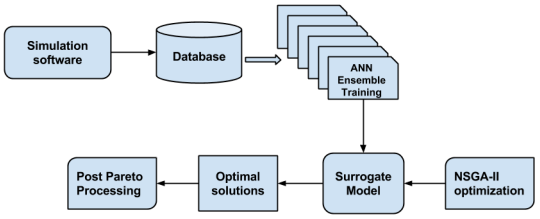

FIGURE 6.2: Process flow

6.2.1 Surrogate Model

As many building design processes, our study involves time consuming simulator computations based on MATLAB. Since population based optimisation algorithms requires from hundreds to thousands evaluation performance, a work around is needed in order to perform optimisation in a reasonable time. Common approaches are reduction in complexity of the design problem [128], neglecting some possible values the discrete variables of the problem may assume, or reducing simulator complexity [129], replacing it with an easier model that simplifies some physical dynamics. A different approach is the reduction of optimisation computational requirements, decreasing population size or generations [130]. Model surrogate approach tries to overcomes some shortcomings related to previous methods (e.g. inaccuracy on modelling some building phenomena, difficult convergence to optimum) by introducing a model that mimics the behaviour of the original one. Such model can be obtained through gray box approaches based on analytical functions and data driven methods or black box models, completely based on data driven methods. In our work we used a black box approach based on Neural Networks model.

In order to setup the tuning of the neural network topology, in particular the number of inputs, a preliminary study of the input variables has been carried on: table 6.2 shows correlation between each variable, and highlights a correlation not significantly high to justify a reduction of the input variables. Therefore, we used a 9 input and 2 output neural network, with a 9 neuron hidden layer. Training was carried on with Levenberg-Marquardt algorithm and stabilisation of sum of squared errors as stopping criteria. Training has been processed on 80% of the learning dataset.Figure 6.1 shows a comparison between the output obtained from the neural network model and the target output.

Successively, we used BAGGING technique for improving generalisation of the network. In our experimentation we used a bagging factor of 0.75, which means that 3/4 of the training data are recombined, an ensemble of 10 neural networks is used.

Table 6.3 shows errors obtained with and without ensemble, we can see a significant decrease of error, although deviation is quite high.

TABLE 6.3: RMSE and MAPE on testing prediction of Neural Network with and without Bagging Ensemble

	RMSE	MAPE
NN	$4.70\% \pm 1.52\%$	$3.26\% \pm 1.34\%$
NN ensemble	$3.41\% \pm 0.63\%$	$2.21\% \pm 0.42\%$

6.2.2 Optimisation

MATLAB environment was used for optimisation phase too and has been carried on with NSGA-II algorithm. The code was slightly modified because we needed to handle both discrete and continuous variables for our problem. Parameters used for the optimisation process on surrogate model are shown in table 6.4. Since input variables are mainly continuous, we preferred an optimisation based on real parameters, instead of binary coded variables. As tournament selection criteria, dominance and crowding distance have been taken into account: firstly non dominated solution is compared in order to establish strongest individual, between two individuals with same rank, crowding distance establish the best one. Simulated Binary Crossover (SBX) applies crossover principle of genetic combination of the parents to the offsprings, η_c parameter represent the crossover spreading, establishing how much offspring individuals can differ from the parents. According to spreading, β_{q_i} parameter is evaluated.

$$\beta_{q_i} = \begin{cases} (2u_i)^{\frac{1}{\eta_c+1}} & \text{if } u_i \leq 0.5 \\ \left(\frac{1}{2(1-u_i)}\right)^{\frac{1}{\eta_c+1}} & \text{otherwise} \end{cases} \tag{6.2}$$

Offspring solutions are assigned according to (6.3) and (6.4)

$$x_i^{(1,t+1)} = 0.5\left[(1+\beta_{q_i})x_i^{(1,t)} + (1-\beta_{q_i})x_i^{(2,t)}\right] \tag{6.3}$$

$$x_i^{(2,t+1)} = 0.5\left[(1-\beta_{q_i})x_i^{(1,t)} + (1+\beta_{q_i})x_i^{(2,t)}\right] \tag{6.4}$$

Polynomial mutation applies a random small change to offspring solutions according to a polynomial probability distribution, which depends on η_m parameter. Mutation coefficient δ_i is calculated through (6.5)

$$\delta_i = \begin{cases} (2u_i)^{\frac{1}{(\eta_m+1)}} - 1 & if \quad u_i < 0.5 \\ 1 - [2(1-u_i)]^{\frac{1}{(\eta_m+1)}} & otherwise \end{cases} \tag{6.5}$$

Mutated solution value given by (6.6)

$$y_i^{(1,t+1)} = x_i^{(1,t+1)} + (x_i^{(U)} - x_i^{(L)})\delta_i \tag{6.6}$$

TABLE 6.4: NSGA-II Parameters

Parameter	Value
Optimisation Type	Real Parameters
Population Size	30
Generations	20
Selection	Tournament
Crossover	SBX
Crossover factor	0.8
Mutation	Polynomial Mutation

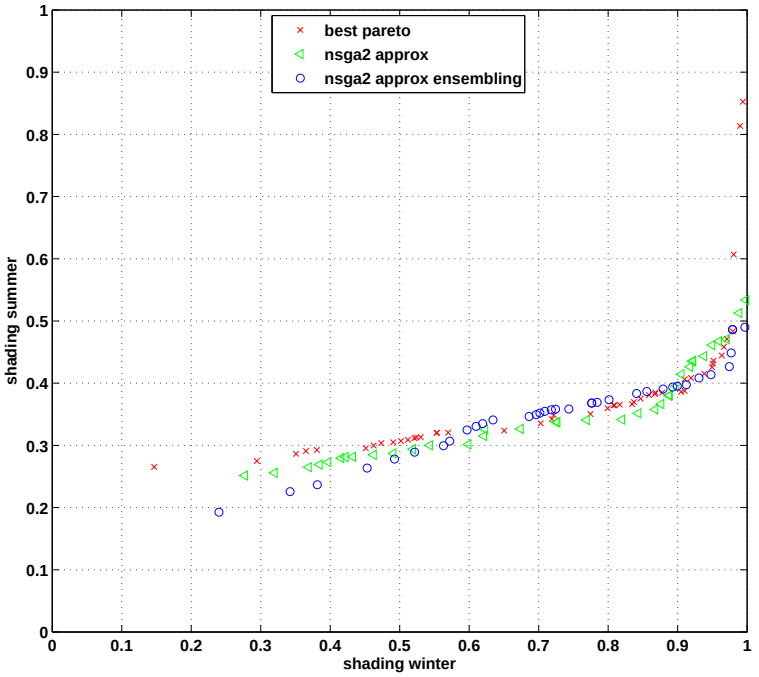

FIGURE 6.3: Pareto comparison

Figure 6.3 shows a comparison between Pareto front of original dataset, obtained applying non dominated sorting on every solution of the dataset and Pareto fronts obtained applying NSGA-II multiobjective optimisation on NNs and ensemble NNs surrogate models. Objective functions taken into account are maximisation of shading factor during winter (January) and minimisation of shading factor in summer (July). The basic idea is to demonstrate that the dataset realized is representative of the research space even with a limited number of samples (950): from a qualitative analysis we can assert that Pareto fronts obtained through models follow the same trend of the original one.

6.2.3 Pareto Fronts discussion

Figures 6.4, 6.5 and 6.6 show Pareto fronts of shading factor in January and July of three representative locations of different altitudes (Madrid, Brussels and Helsinki). Fronts shown represents the optimal solutions set which maximize shading factor in January and minimize in July. Two fronts are compared for each subfigure, *best pareto*, obtained applying non dominated sorting on the whole dataset and taking first rank solutions, and *approximated pareto*, obtained applying NSGA-II multiobjective optimisation on approximated model of the original dataset. For each location, six pareto fronts have been evaluated: three different expositions (North, South, East/West) in both isolated and urban contexts. It is interesting that pareto fronts in isolated context (1-3) show a very wide spreading of solutions , while in urban context fronts are limited to few values of objective functions. In particular we can see that in Madrid, for south and east expositions, shading factor of both summer and winter assumes a wide range of the all possible values, so the choice of design variables can drive the performance of the shading to a wide range of possible scenarios, in a limited way this happens also for north exposure. It is worth to note that as not as expected, the minimum shading factor for north exposure is higher than other exposures. This happens because shading factor index (6.1) is evaluated by the direct and diffuse radiation contributions and since north exposure implies very low direct radiation contribution, the total shading factor results lesser than other exposures. In urban context the variation range of objective functions highly decrease, mainly because of the presence of other buildings covering solar radiation. In fact, particularly in Helsinki and Brussels, shading factor during winter for south exposure is very limited (from 0 to 0.1), for east exposure from 0.1 to 0.3 and for north exposure from 0.2 to about 0.45. Summer shading also significantly

decreases, both in Helsinki and Madrid, in particular for north exposure. Since the variance of shading factors is very low, in such scenarios the choice of optimal design variables has less impact on the priority between conflicting objectives. Moreover a very low maximum shading factor during winter suggests to support solutions maximizing winter shading. To sum up, a qualitative analysis of Pareto fronts shows that the decision making phase is more important in isolated contexts compared to urban context, hence, during project phase, the choice of design variables is crucial. Moreover, in many urban contexts, solutions maximizing winter shading factor are recommended in order to exploit as maximum as possible solar radiation and then avoiding radiation surplus during summer through shielding.

6.2.4 Design variables importance

Figures 6.7, 6.8 and 6.9 show the normalized values that optimal design variables (belonging to optimal pareto front) assume. In order to evaluate the variance range of the variables, a box plot has been carried out. For each variable, median value, first and third quartile are represented (q_1 and q_3), upper whisker is given by $q_3 + w(q_3 - q_1)$ while lower by $q_1 - w(q_3 - q_1)$. In our case study, whiskers parameter was set to $w = 1.5$. Outliers are shown as red crosses and lay over the whiskers boundaries. The study has been carried out both on 9-input problem, which includes the discrete variable fin position and on 8-input problem, where two fins are placed, hence positioning of the fin is not a variable in such case. We neglected the 9-input graph as we did not considered meaningful showing discrete variables in such discussion, because in most cases it resulted in a box plot covering the whole range.

The main idea is to identify which variable is more important to be taken into account during project phase, analyzing the variance such variable assumes over the optimal solutions pareto front. A small box plot means the value for that variables does not change very much from the median over the front, hence, such value is a strict requirement during project design phase. In general, overhang design has more influence respect of fin: as we can see, in most cases overhang depth (W_o), overhang distance (D_o) and overhang extension ratio (DW) box plots are very small, while fin height H_f and fin distance D_f have greater variance, fin depth W_f is an exception, since its variance is often low. It is worth to note that also reveal depth plays an important role (s) in Helsinki and slightly

in Brussels, in particular for East/West exposures, while in Madrid is not influential at all. The behaviour in Madrid, Brussels and Helsinki in urban context and north exposition is different: all variables box plots tend to be wider, and even if overhang depth still remain dominant, it has not as much influence as on other exposures.

6.3 Conclusions

In this work we firstly set up a dataset based on a simulator through we evaluated the shading factor corresponding to a set of input design variables describing the fenestration configuration. The variation of the inputs values to be sent to the simulation has been carried on according to a uniform distribution. Dataset has been used in order to train surrogate model, which was based at first place on a NN and then improved into an Bootstrap AGGregatING (BAGGING) ensemble of NNs, the improvement achieved is noticeable. The optimisation phase has been processed on the surrogate model and the Pareto front obtained is really close to the "real" one as we expected. Then we investigated Pareto fronts of every configuration through box plot of the design variables belonging to Pareto front. Such analysis provides a qualitative overview on the variance of the input variables, indicating which are required to be set to a limited set of values and, on the other hand, ones can assume a wide range of values. Turn out that in most cases, overhang features are more critical than fin ones, in particular overhang depth and distance. Hence, they have to be carefully considered during design phase.

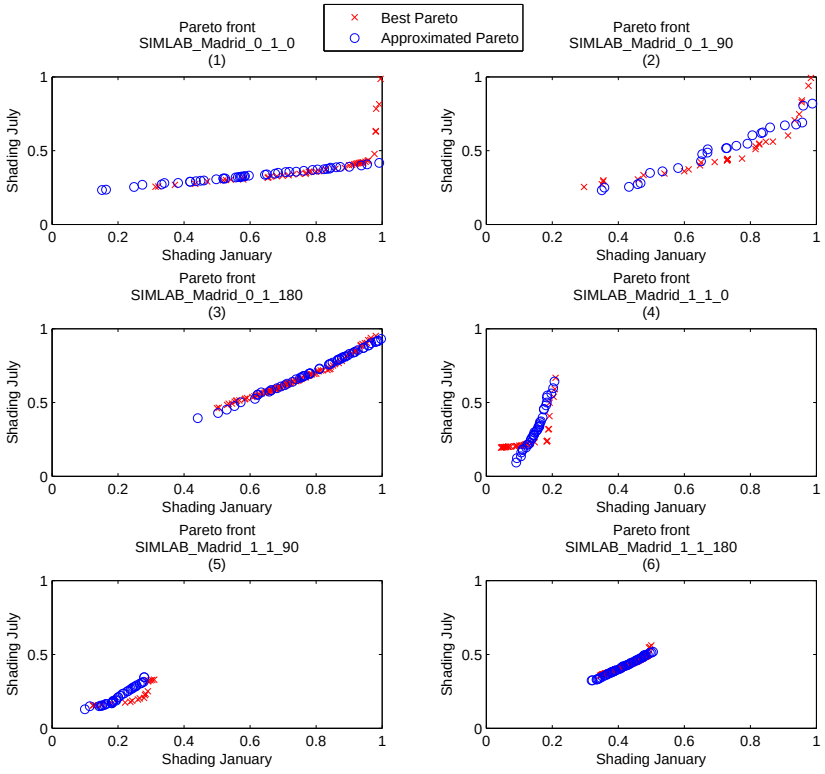

FIGURE 6.4: Pareto fronts plots in Madrid. Isolated context at different expositions: South(1), East/West(2), North(3) and urban context South(4), East/West(5), North(6).

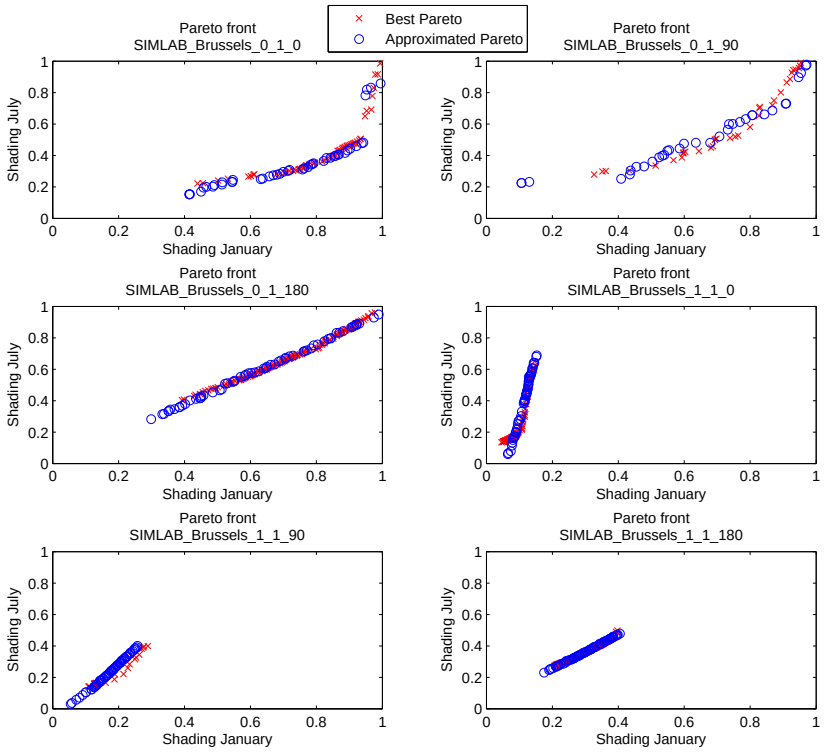

FIGURE 6.5: Pareto fronts plots in Brussels. Isolated context at different expositions: South(1), East/West(2), North(3) and urban context South(4), East/West(5), North(6).

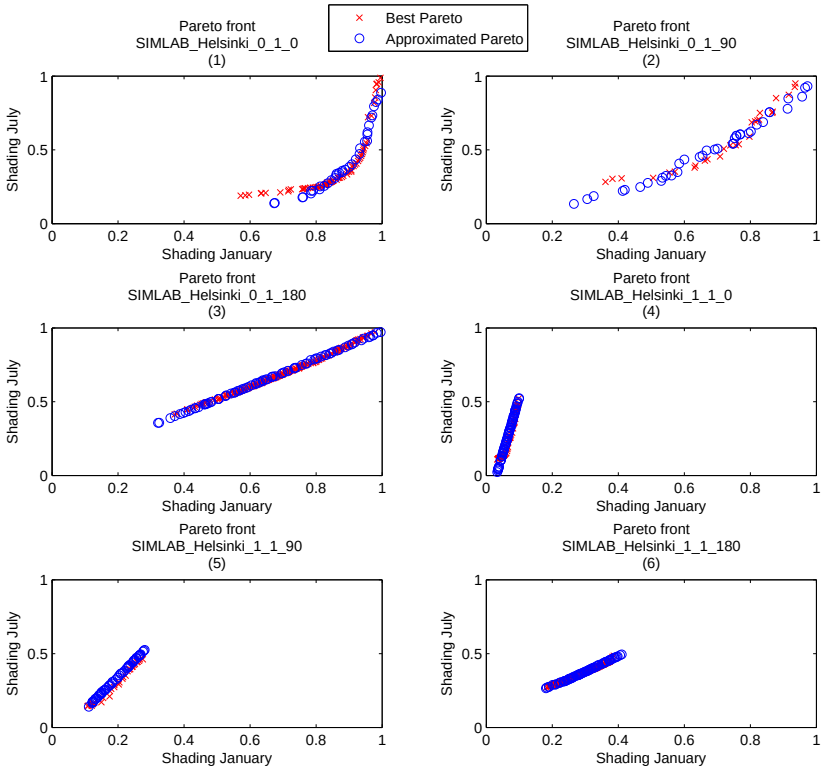

FIGURE 6.6: Pareto fronts plots in Helsinki. Isolated context at different expositions: South(1), East/West(2), North(3) and urban context South(4), East/West(5), North(6).

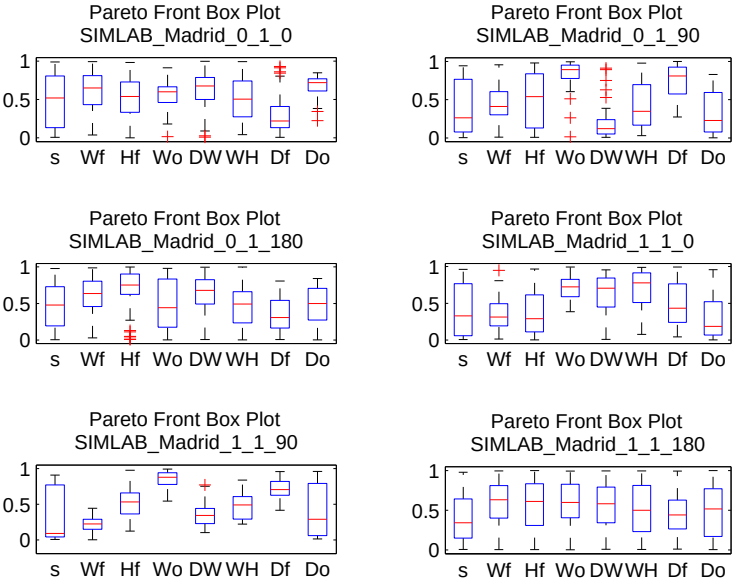

FIGURE 6.7: Madrid Box Plot. Isolated context at different expositions: South(1), East/West(2), North(3) and urban context South(4), East/West(5), North(6).

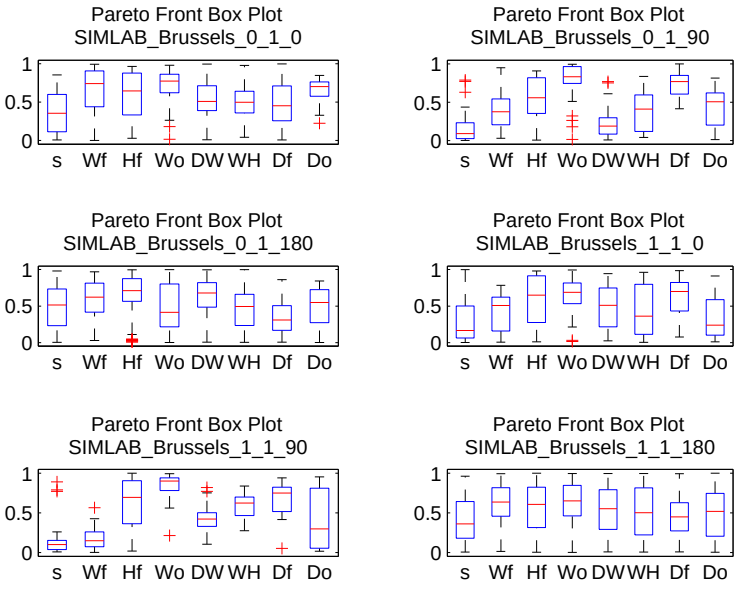

FIGURE 6.8: Brussels Box Plot. Isolated context at different expositions: South(1), East/West(2), North(3) and urban context South(4), East/West(5), North(6).

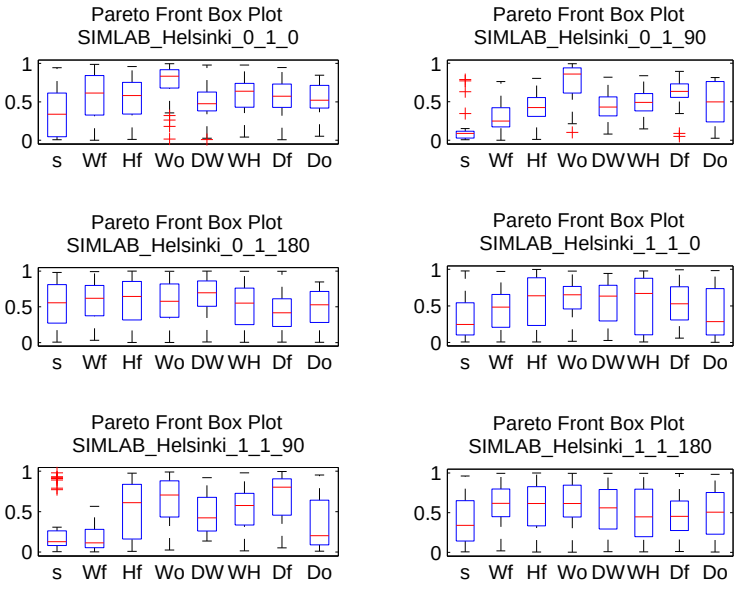

FIGURE 6.9: Helsinki Box Plot. Isolated context at different expositions: South(1), East/West(2), North(3) and urban context South(4), East/West(5), North(6).

Chapter 7

Urban traffic flow forecasting through statistical and neural network bagging ensemble hybrid modeling

7.1 Introduction

Transportation is a wide human-oriented field with diverse and challenging problems waiting to be solved. Characteristics and performances of transport systems, services, costs, infrastructures, vehicles and control systems are usually defined on the basis of quantitative evaluation of their main effects. Most of the transport decisions take place under imprecision, uncertainty and partial truth. Some objectives and constraints are often difficult to be measured by crisp values. Traditional analytical techniques were found to be not-effective when dealing with problems in which the dependencies between variables were too complex or ill-defined. Moreover, hard computing models cannot deal effectively with the transport decision-makers ambiguities and uncertainties. In order to come up with solutions to some of these problems, over the last decade there has been much interest in soft computing applications of traffic and transport systems, leading to some successful implementations [131]. The use of soft computing methodologies for modelling and analysing traffic and transport systems is of particular interest

to researchers and practitioners due to their ability to handle quantitative and qualitative measures, and to efficiently solve complex problems which involve imprecision, uncertainty and partial truth. Soft computing can be used to bridge modelling gaps of normative and descriptive decision models in traffic and transport research. Transport problems can be classified into four main areas : traffic control and management, transport planning and management, logistics, design and construction of transport facilities. The first category includes traffic flow forecasting which is the topic tackled in this work. This issue has been faced by the soft computing community since the nineties [132–138] up today [139–141] with ANN. As example, among the most recent work [140] focuses on traffic flow forecasting approach based on PSO with Wavelet Network Model (WNM). Pamula et al. [141] reviews neural networks applications in urban traffic management systems and presents a method of traffic flow prediction based on neural networks. Bucur et al. [139] proposes the use of a self-adaptive fuzzy neural network for traffic prediction suggesting an architecture which tracks probability distribution drifts due to weather conditions, season, or other factors. All the mentioned applications have one feature in common: they use one single global model in order to perform the prediction. Therefore, the main novelty of the proposed work is to combine different heterogeneous models in order to get a meta-model capable of providing predictions more accurate than the best of the constituent models. This work is an extension of previous work [142, 143], where a basic neural networks ensemble and a simple statistical model have been used, introducing BAGGING ensembling model. Results shown highlight a remarkable decrease of error through the BAGGING learning phase.

7.2 Methods

7.2.1 Basic model

In order to perform a meaningful comparison for the forecasting, a basic model should be introduced in order to quantify the improvement given by more intelligent and complex forecasting techniques. For seasonal data a basic model might be defined as:

$$x_t = x_{t-s} \tag{7.1}$$

with S the appropriate seasonality period. This model gives a prediction at time t presenting the value observed exactly a period of S steps before. For this work we put the value of $S = 1$ which corresponds to the previous hour. It means that to predict the flow rate of the following hour it is used the current flow measure.

7.2.2 Statistical

One the simplest and most widely used models when dealing with regular time series (as urban traffic flows) is to build an average weekly distribution of the traffic flow sampled hourly. Thus, from the data we compute for each day the average flow rate hour by hour in such a way that we get an average distribution made of $24 \cdot 7 = 168$ points.

7.2.3 Neural Network Ensembling

Models ensemble is a technique where many prediction models cooperate on the same task. The aggregation of multiple prediction of the same variable may lead to better results and generalization than using a single model prediction. In order to increase generalization capability, the model learning phase is crucial. The goal is obtain better predictive performance than could be obtained from any of the constituent models. In the last years several ensembling methods have been carried out [144–146]. The first one, also known as Basic Ensemble Method (BEM), is the simplest way to combine M neural networks as an arithmetic mean of their outputs. This method can improve the global performance [125, 147] although it does not takes into account that some models can be more accurate than others. This method has the advantage to be very easy to apply. A direct BEM extension is the Generalised Ensemble Method (GEM) in which the outputs of the single models are combined in a weighted average where the weights have to be properly set, sometimes after an expensive tuning process. Bagging (Bootstrap AGGregatING) [126] technique improves generalisation: for each learner replaces part of training data set with a random combination of training data itself. Thus each dataset may contain duplicated entries of the same sample or not at all. Improvement occurs especially when small changes in dataset may lead to a large changes in prediction. Adaboosting [148] introduces weights on the training points.

7.2.4 Hybrid model

Hybrid models are an extension of the ensembling approach in the sense that the final goal is to combine different models in such a way that the accuracy of the composition is higher than the best of the single models. The difference is that the combination is performed among highly heterogeneous models, that is models generated by different methods with different properties and thus the composition among them is a complex rule taking into account the peculiarities of the models and/or of the problem itself. Therefore, in this work we propose a novel hybrid model which combines an ANN ensemble with the statistical model. The composition rule is the following : *"IF the statistical model has a high error (meaning that for some reason we are out of a normal situation) THEN use the neural model ELSE use the statistical one"*. This criterion is based on the absolute error of the statistical model, thus the composition rule turns into

$$|x^t - y^t| > \epsilon \qquad \Rightarrow \qquad y^{t+1} = y_n^{t+1} \tag{7.2}$$

$$|x^t - y^t| \leq \epsilon \qquad \Rightarrow \qquad y^{t+1} = y_s^{t+1} \tag{7.3}$$

Where y^{t+1} is the outcome (one hour prediction) after the composition rule, y_n^{t+1} is the prediction of the neural ensemble, y_s^t is the current outcome of the statistical model and y_s^{t+1} is its prediction. This basically means that if we are in normal statistical conditions (where the statistical model makes a small error) then use as prediction model the statistical one (which is very accurate in this condition), else (when out of normal statistical situations) take the neural ensembling estimation.

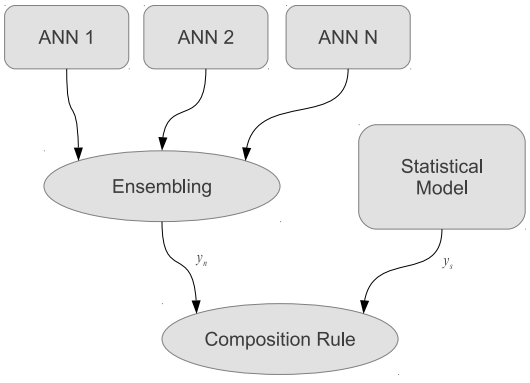

FIGURE 7.1: Proposed hybrid model approach

7.3 Experimentation

In this paragraph we test and compare the methods presented in the previous section. The test case has concerned the short term traffic flow rate of three different streets, shown in Table 7.1, located in the town of Terni (about 90km north of Rome). The data set is made of 3 months (13 weeks) of measurement corresponding to 2184 hourly samples.

TABLE 7.1: Street parameters

	Maximum traffic flow rate
Street 1	600
Street 2	800
Street 3	950

The data set has been partitioned into training/testing and validation made respectively of 10 and 3 weeks each. We firstly present result obtained using hybrid model based on Neural Network Basic Ensemble model and statistic model and we show an improvement on the forecasting, then we replace Basic Ensemble Model with a Bagging based one. Results show a further improvement on the forecasting. Performance evaluation of the models is based on MAPE (7.4)

$$e = \frac{1}{n} \sum_{i=1}^{N} \frac{|x_i - y_i|}{M - m} \tag{7.4}$$

Where x is the target value to be predicted, y is the output model, M is the real maximum value and m is the minimum.

7.3.1 Neural Network setup

The ANN are feed-forward Multi Layer Perceptron (MLP) with 10 hidden neurons and one output (the one hour flow forecast) with sigmoid as activation function for all the neurons. The number of inputs N has been chosen with a preliminary analysis by calculating the validation prediction error after ensembling for different values of N as shown in Table 7.2.

TABLE 7.2: History length selection

N (hours)	Street 1	Street 2	Street 3
3	5.72	6.88	5.81
5	3.90	5.07	3.99
8	3.29	3.43	3.02
10	3.54	4.12	3.74

By this analysis it turned out the optimal number of input neurons (namely the length of the history window) to be eight. Training has been performed through the Back-Propagation algorithm with adaptive learning rate and momentum stopping after 10^8 iterations and a save best strategy, which save the ANN model coefficients and weights when the error is lesser than the one in previous iterations. The reported result are averaged over 10 different runs and the ensemble is therefore made by the same 10 models.

Afterwards, it has been tuned parameter ϵ of the hybrid model. Table 7.3 shows error obtained with the hybrid model composed by statistical and BEM models, ϵ value is the threshold expressed in number of vehicles.

TABLE 7.3: Hybrid model parameter ϵ tuning. Errors percentage of hybrid model at different values of ϵ parameter.

	$\epsilon = 10$	$\epsilon = 20$	$\epsilon = 30$	$\epsilon = 40$	$\epsilon = 50$	$\epsilon = 60$
Street 1	2.98	2.83	2.81	2.80	2.88	2.99
Street 2	2.85	2.69	2.65	2.66	2.68	2.75
Street 3	3.25	3.13	3.08	3.04	3.03	3.04

7.3.2 Bagging ensemble setup

Bagging factor parameter determines the percentage of the original dataset that is going to be replaced by a recombination. Therefore we carried out a tuning of the parameter, evaluating mean ensemble error for different bagging factors. Table 7.4 shows that increasing bagging factor implies an almost negligible improvement of the performances. In our tests we used bagging factor 1, that is a recombination of the whole learning dataset.

TABLE 7.4: Bagging factor parameter tuning. Results are averaged over 10 runs with different bagging factors.

bf	0.75	0.8	0.85	0.9	0.95	1
Street 1	3.56 ± 0.11	3.41 ± 0.14	3.39 ± 0.17	3.21 ± 0.17	3.12 ± 0.14	3.11 ± 0.20
Street 2	4.06 ± 0.15	4.03 ± 0.21	3.87 ± 0.17	3.73 ± 0.19	3.65 ± 0.18	3.52 ± 0.21
Street 3	3.14 ± 0.14	2.98 ± 0.15	2.94 ± 0.19	2.86 ± 0.11	2.76 ± 0.13	2.69 ± 0.11

7.3.3 Results

Experimentations carried on shows a comparison of the performance of the models described. Basic model method simply forecast next hour traffic flow according to the previous measured one, so $x_{t+1} = x_t$. Statistic model build a weekly profile of the traffic flow, so in our case the profile is an average over the 10 weeks of the hourly traffic flow. The result is a model of 168 points representing the average profile of 24 hours for 7 days. Since such models do not involve stochastic processes standard deviation is not expressed. Artificial Neural Networks result is the averaged error over 10 runs. BEM is the Basic Ensemble Method, built averaging the output of the Neural Networks previously evaluated. Since BEM error is evaluated on the averaged output also in this case standard deviation is not expressed. HBEM is the hybrid statistic and neural network ensemble based model, in our tests we used $\epsilon = 40$ that means that if the error of the statistical models exceeds ϵ parameter value, is used ensemble model, otherwise statistical one. Bagging ensemble results are evaluated over 10 runs with bagging factor parameter set to 1. HBAG is the result of hybrid statistic and bagging ensemble based model. In order to be comparable with HBEM, bagging ensemble output is averaged over 10 runs, then we used the same logic: if statistical error exceeds ϵ parameter, bagging ensemble model is used. Table 7.5 shows that hybrid model with bagging outperforms previous ones.

Figures 7.2, 7.3, 7.4 show graphical comparison of statistical, BEM and Bagging models and highlight that the use of bagging ensemble outperforms previous techniques.

TABLE 7.5: Comparison of models percentage error. Basic is the 1-step forward model, Stat is the weekly average profile, ANN is Artificial Neural Networks model, BEM is Basic Ensemble Method obtained averaging each neural network output, HBEM is the hybrid statistical and BEM model, BEG is the bagging ensemble model and finally HBAG is the hybrid statistical and Bagging ensemble model

	Basic	Stat	ANN	BEM	HBEM	BAG	HBAG
Street 1	8.92	5.90	4.93 ± 0.25	4.58	3.29	3.01 ± 0.11	2.42
Street 2	9.99	7.14	5.22 ± 0.31	4.59	4.15	3.52 ± 0.21	3.01
Street 3	7.66	5.56	3.70 ± 0.28	3.71	2.93	2.69 ± 0.11	2.30

FIGURE 7.2: Street 1 models comparison

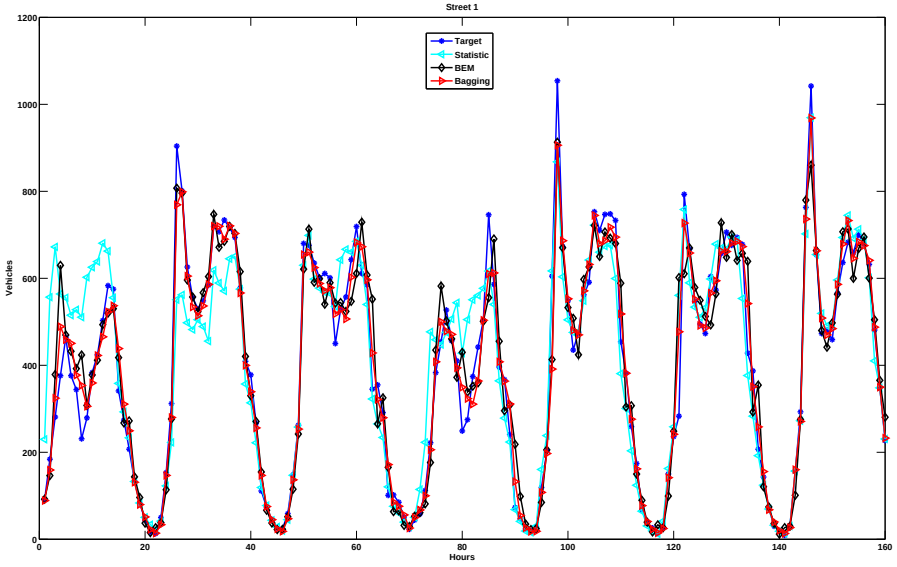

Figure 7.5 shows comparison between the two hybrid models on the 3 streets: target is followed slighly better by the hybrid statistical and bagging model.

FIGURE 7.3: Street 2 models comparison

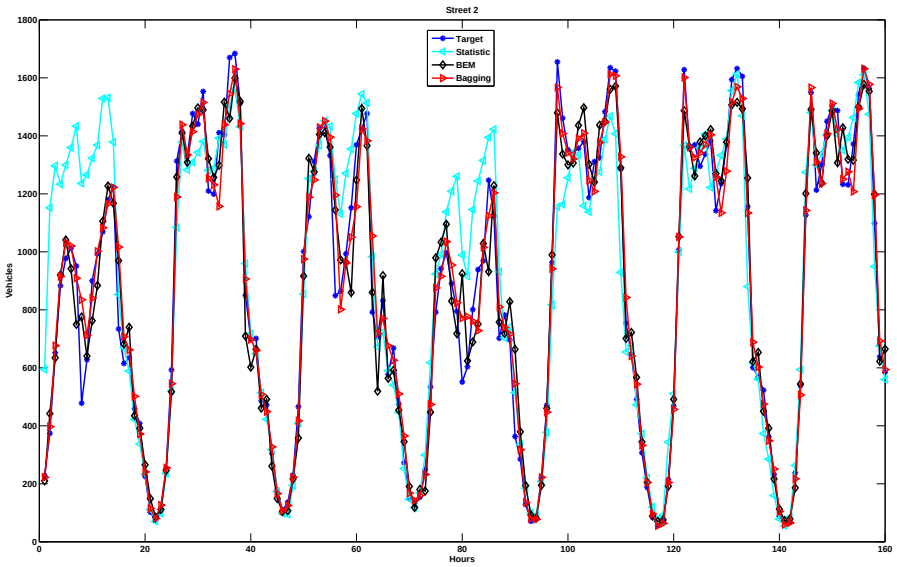

FIGURE 7.4: Street 3 models comparison

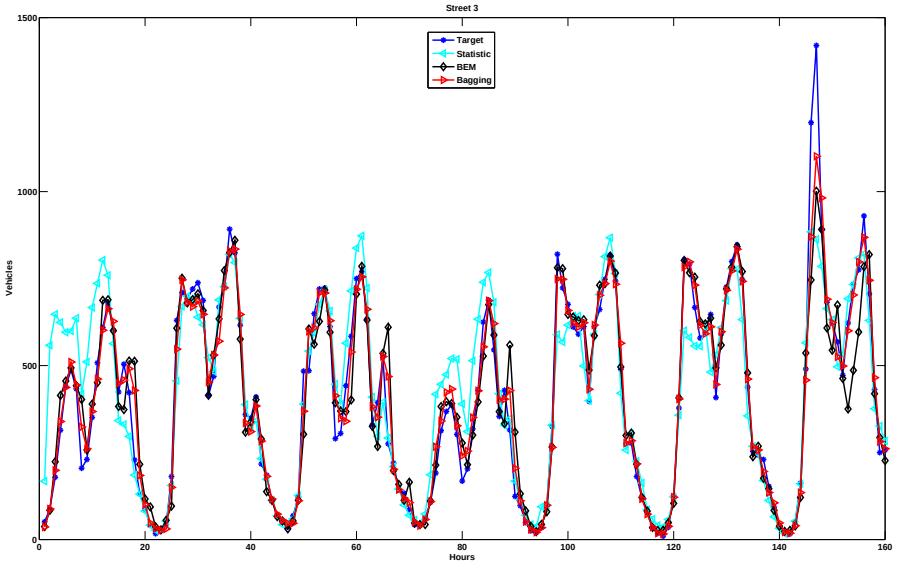

7.4 Conclusions

In this chapter we showed an hybrid modelling approach which combines ANN and a simple statistical approach in order to provide a one hour forecast of urban traffic flow rates. Experimentation has been carried out on three different classes of real streets and results showed that the proposed approach clearly outperforms the best of the methods

FIGURE 7.5: Comparison of the statistical and BEM hybrid model with statistical and Bagging hybrid model on the 3 streets case study.

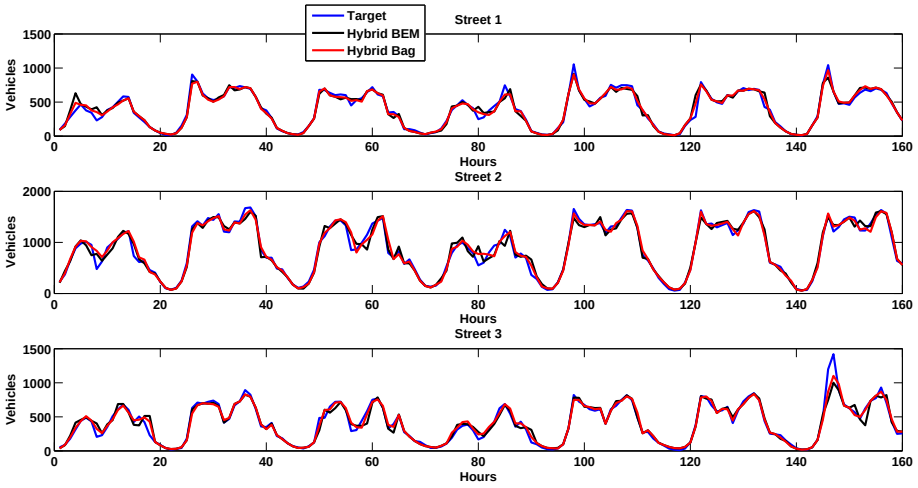

it puts together achieving a prediction error lower than 3%. The reason for that is that the neural ensembling model is capable to provide more reliable estimations when out of standard conditions because it considers the real traffic dynamics. The accuracy of the proposed hybrid modelling approach is such that it can be applied for intelligent monitoring, diagnostic systems and optimal control.

Conclusions and future directions

This dissertation recap activities carried out during my Ph.D. with my research group, mainly focused on application of soft computing based techniques for energy saving issues, following the Smart Cities paradigm. Applications involving Smart Cities are really up-to-date and many new ideas are arising. Thus, it is challenging and at the same time pleasant tackle such problems.

The work is mainly focused on buildings as they are potentially one the best source of improvement from efficiency and innovation points of view. An overview of building control methodologies has been done and soft computing techniques resulted reasonably promising, as they provide a faster tuning and a lesser knowledge of the modelled systems. Even hard computing based techniques have been largely applied, MPC control particularly fits in building control problems, especially under 24 hours granularity.

Building diagnostics framework proposed has been applied to an actual building inside R.C. Casaccia, applying statistical methodologies for preprocessing and Fuzzy Logic for data fusion on Situations and Causes levels. Despite its straightforward applicability, we believe it can be applied also in a scaled level, such as building networks. Of course, other data fusion methodologies can be considered and tested, as well as the PSC tables can be further extended. Moreover, a significant set of diagnostics processes can be implemented and applied on the same F40 test case, in order to obtain a robust tool that can be used on a commercial level. As for the diagnostics framework, ICT platform too can be improved: while currently its main purpose is to passively support diagnostics and optimisation processes, STP could provide several solutions for simplifying tuning of such processes and offering further useful user friendly services, such as mobile notifications, captivating user interface and so on.

Multiobjectve optimisation was based on soft computing too, in particular, Population based algorithms, respect of gradient-based algorithms are way more suitable in multiobjective problems, in particular, we tried to obtain optimal configuration of F40 building for best thermal consumptions savings without affecting comfort. Our approach was based on the tuning of supplied water temperature in the thermal plant and local thermostats of the rooms. Results obtained through simulators showed a promising potential saving both on seasonal approach (keeping a fixed setpoint for three months) and daily approach (changing setpoints every day). We believe a smaller time window interval should be investigated too, as some fast dynamics such as solar radiation cannot be managed on a daily basis approach. Grey Box modeling was based on Stochastic Differential Equations describing a physical lumped model of F40 building, the complexity of the model has been progressively increased and the error obtained on thermal and internal temperature forecasting is acceptable.

Multiobjective optimisation has been used also for fenestration design optimisation, aiming to find out design variable more worth to be taken into account while planning shading devices installation. Such analysis has been made through an accurate investigation of Pareto fronts obtained optimising shading devices features such that shading factor is maximised during winter and minimised during summer on three representative cities (Madrid, Brussels, Helsinki). Results shown substantial differences depending to contexts considered (urban or isolated) and also depending on latitude level. Especially for isolated contexts, it is important to take in account the overhang rather than fin as it has a huge impact on Pareto front optimal solutions.

Final work proposed regards a different application field such as public lighting, but involved as well on Smart Cities paradigm. Moreover, techniques used were almost the same, hence it is worth to be discussed. We proposed an hybrid statistical and Neural Network Ensemble model for forecasting traffic flow. Such model provided a significant improvement on the performance, reaching a 3% error level on the test case taken into account. Such model can be used as a support for active demand approach on public lighting systems, such that energy provided can be adapted according to forecasted traffic flow level.

Publications

- Journal
  - S. Pizzuti, M. Annunziato, F. Moretti. Smart Street Lighting management. Journal of Energy Efficiency, Volume 6, Issue 3 (2013), Page 607-616.
  - F. Moretti S. Pizzuti, M. Annunziato, S. Panzieri. Urban traffic flow forecasting through statistical and neural network bagging ensemble hybrid modeling. Neurocomputing 2014, SOCO Special Issue (to appear)
  - F. Lauro, F. Moretti, S. Pizzuti, A. Capozzoli, I. Khan, S. Panzieri. Building fan coil electric consumption analysis with fuzzy approaches for fault detection and diagnosis. Energy Procedia.
- Conference Proceedings
  - F. Moretti, S. Pizzuti, M. Annunziato, S. Panzieri. Advanced street lighting control. The Second International Conference on Smart Systems, Devices and Technologies, SMART 2013, June 23 - 28, 2013 - Rome, Italy.
  - M. Annunziato, F. Moretti, S. Pizzuti. Urban Traffic Flow Forecasting using Neural-Static Hybrid Modeling. Soft Cocmputing Models in Industrial and Environmental Applications, vol. 188, pp. 183-190. Springer, Heidelberg (2013)
  - F. Marino, A. Capozzoli, M. Grossoni, F. Lauro, F. Leccese, F. Moretti, S. Panzieri, S. Pizzuti. Indoor lighting fault detection and diagnosis using a data fusion approach. Energy Quest 2014, Energy Production and Management in the 21st Century - The Quest for Sustainable Energy, 23 - 25 April 2014, Ekaterinburg, Russia.

  - M. Macas, F. Moretti, F. Lauro, S. Pizzuti, M. Annunziato, A. Fonti, ... & A. Giantomassi (2014). Importance of Feature Selection for Recurrent Neural Network Based Forecasting of Building Thermal Comfort. In Adaptive and Intelligent Systems (pp. 11-19). Springer International Publishing.
  - M. Macas, F. Moretti, F. Lauro, S. Pizzuti, M. Annunziato, A. Fonti, ... & A. Giantomassi (2014, January). Sensitivity based feature selection for recurrent neural network applied to forecasting of heating gas consumption. In International Joint Conference SOCO14-CISIS'14-ICEUTE'14 (pp. 259-268). Springer International Publishing.

- Technical Reports

  - M. Annunziato, G. Comodi, F. Lauro, C. Meloni, F. Moretti, S. Pizzuti, S. Romano. "Sviluppo di una sperimentazione dimostrativa di "Smart Village" e metodi di progettazione" (Italian).
  - S. Panzieri, F. Moretti, S. Pizzuti, P. Cicolin. "Realizzazione di una piattaforma integrata per il data fusion di segnali provenienti da sistemi sensoriali per applicazioni di smart city integrate nella rete della pubblica illuminazione" (Italian).
  - F. Moretti, S. Panzieri. Sviluppo di algoritmi per la gestione ottimale di edifici: applicazione su un caso pilota. Technical report for "Ricerca di Sistema Elettrico" Project (Italian).

Bibliography

[1] Lotfi A Zadeh. Fuzzy sets. *Information and control*, 8(3):338–353, 1965.

[2] Metin Akay. Noninvasive diagnosis of coronary artery disease using a neural network algorithm. *Biological cybernetics*, 67(4):361–367, 1992.

[3] L Zadeh. A critical view of our research in automatic control. *Automatic Control, IRE Transactions on*, 7(3):74–75, 1962.

[4] Lotfi A Zadeh. *Possibility theory and soft data analysis*. World Scientific Publishing Co., Inc., 1996.

[5] F Lauro, F Moretti, A Capozzoli, I Khan, S Pizzuti, M Macas, and S Panzieri. Building fan coil electric consumption analysis with fuzzy approaches for fault detection and diagnosis. *Energy Procedia*, 62:411–420, 2014.

[6] Alessandra De Paola, Marco Ortolani, Giuseppe Lo Re, Giuseppe Anastasi, and Sajal K Das. Intelligent management systems for energy efficiency in buildings: A survey. *ACM Computing Surveys (CSUR)*, 47(1):13, 2014.

[7] Enel smart meter. http://eneldistribuzione.enel.it/it-IT/enel_info_piu_sezione.

[8] Miscrosoft hohm. http://www.microsoft.com/environment.

[9] berkeley dashboard. https://us.pulseenergy.com/UniCalBerkeley/dashboard.

[10] Xiaofan Jiang, Stephen Dawson-Haggerty, Prabal Dutta, and David Culler. Design and implementation of a high-fidelity ac metering network. In *Information Processing in Sensor Networks, 2009. IPSN 2009. International Conference on*, pages 253–264. IEEE, 2009.

[11] Xiaofan Jiang, Minh Van Ly, Jay Taneja, Prabal Dutta, and David Culler. Experiences with a high-fidelity wireless building energy auditing network. In *Proceedings of the 7th ACM Conference on Embedded Networked Sensor Systems*, pages 113–126. ACM, 2009.

[12] International Energy Agency. *Cool appliances: policy strategies for energy-efficient homes*. OECD Publishing, 2003.

[13] Francesco Corucci, Giuseppe Anastasi, and Francesco Marcelloni. A wsn-based testbed for energy efficiency in buildings. In *Computers and Communications (ISCC), 2011 IEEE Symposium on*, pages 990–993. IEEE, 2011.

[14] AIM Consortium et al. A novel architecture for modelling, virtualising and managing the energy consumption of household appliances-aim, 2008.

[15] Hossein Mirinejad, Seyed Hossein Sadati, Maryam Ghasemian, and Hamid Torab. Control techniques in heating, ventilating and air conditioning systems. *Journal of computer science*, 4(9):777, 2008.

[16] Guang-Yu Jin, Pek-Yew Tan, Xu-Dong Ding, and Tien-Ming Koh. Cooling coil unit dynamic control of in hvac system. In *Industrial Electronics and Applications (ICIEA), 2011 6th IEEE Conference on*, pages 942–947. IEEE, 2011.

[17] I Jetté, M Zaheer-Uddin, and P Fazio. Pi-control of dual duct systems: manual tuning and control loop interaction. *Energy conversion and management*, 39(14): 1471–1482, 1998.

[18] Zhang Jun and Zhang Kanyu. A particle swarm optimization approach for optimal design of pid controller for temperature control in hvac. In *Measuring Technology and Mechatronics Automation (ICMTMA), 2011 Third International Conference on*, volume 1, pages 230–233. IEEE, 2011.

[19] Manohar R Kulkarni and Feng Hong. Energy optimal control of a residential space-conditioning system based on sensible heat transfer modeling. *Building and Environment*, 39(1):31–38, 2004.

[20] AK Pal and RK Mudi. Self-tuning fuzzy pi controller and its application to hvac systems. *International journal of computational cognition*, 6(1):25–30, 2008.

[21] Min Xu, Shaoyuan Li, and Wenjian Cai. Practical receding-horizon optimization control of the air handling unit in hvac systems. *Industrial & engineering chemistry research*, 44(8):2848–2855, 2005.

[22] Dongwon Lim, Bryan P Rasmussen, and Darbha Swaroop. Selecting pid control gains for nonlinear hvac&r systems. *HVAC&R Research*, 15(6):991–1019, 2009.

[23] Gopal P Maheshwari, Hanay Al-Taqi, Rajinder K Suri, et al. Programmable thermostat for energy saving. *Energy and buildings*, 33(7):667–672, 2001.

[24] Anastasios I Dounis and Christos Caraiscos. Advanced control systems engineering for energy and comfort management in a building environment - a review. *Renewable and Sustainable Energy Reviews*, 13(6):1246–1261, 2009.

[25] Karl J Åström and Björn Wittenmark. *Adaptive control*. Courier Corporation, 2013.

[26] John T Wen, Sandipan Mishra, Sumit Mukherjee, Nicholas Tantisujjatham, and Matt Minakais. Building temperature control with adaptive feedforward. In *Decision and Control (CDC), 2013 IEEE 52nd Annual Conference on*, pages 4827–4832. IEEE, 2013.

[27] Jose Luis Torres and Marcelo Luis Martin. Adaptive control of thermal comfort using neural networks. In *Argentine Symposium on Computing Technology*, 2008.

[28] Sumera I Chaudhry and Manohar Das. Adaptive control of indoor temperature in a building. In *Electro/Information Technology (EIT), 2012 IEEE International Conference on*, pages 1–6. IEEE, 2012.

[29] Lv Hongli, Duan Peiyong, Yao Qingmei, Li Hui, and Yang Xiuwen. A novel adaptive energy-efficient controller for the hvac systems. In *Control and Decision Conference (CCDC), 2012 24th Chinese*, pages 1402–1406. IEEE, 2012.

[30] Thananchai Leephakpreeda. Implementation of adaptive indoor comfort temperature control via embedded system for air-conditioning unit. *Journal of mechanical science and technology*, 26(1):259–268, 2012.

[31] M Zaheer-Uddin. Optimal, sub-optimal and adaptive control methods for the design of temperature controllers for intelligent buildings. *Building and Environment*, 28(3):311–322, 1993.

[32] Gregor P Henze, Clemens Felsmann, and Gottfried Knabe. Evaluation of optimal control for active and passive building thermal storage. *International Journal of Thermal Sciences*, 43(2):173–183, 2004.

[33] Erik M Greensfelder, Gregor P Henze, and Clemens Felsmann. An investigation of optimal control of passive building thermal storage with real time pricing. *Journal of Building Performance Simulation*, 4(2):91–104, 2011.

[34] Bing Dong. Non-linear optimal controller design for building hvac systems. In *Control Applications (CCA), 2010 IEEE International Conference on*, pages 210–215. IEEE, 2010.

[35] Junya Nishiguchi, Tomohiro Konda, and Ryota Dazai. Data-driven optimal control for building energy conservation. In *SICE Annual Conference 2010, Proceedings of*, pages 116–120. IEEE, 2010.

[36] M Mossolly, K Ghali, and N Ghaddar. Optimal control strategy for a multi-zone air conditioning system using a genetic algorithm. *Energy*, 34(1):58–66, 2009.

[37] Yongmin Yan, Jin Zhou, Yaolin Lin, Wei Yang, Ping Wang, and Guoqiang Zhang. Adaptive optimal control model for building cooling and heating sources. *Energy and Buildings*, 40(8):1394–1401, 2008.

[38] Jian Sun and Agami Reddy. Optimal control of building hvac&r systems using complete simulation-based sequential quadratic programming (csb-sqp). *Building and environment*, 40(5):657–669, 2005.

[39] Sze-Tsen Hu. *Elements of general topology*. Holden-Day San Francisco, 1964.

[40] Paul Werbos. Beyond regression: New tools for prediction and analysis in the behavioral sciences. 1974.

[41] Alan Lapedes and Robert Farber. Nonlinear signal processing using neural networks: Prediction and system modelling. Technical report, 1987.

[42] Jian Liang and Ruxu Du. Thermal comfort control based on neural network for hvac application. In *Control Applications, 2005. CCA 2005. Proceedings of 2005 IEEE Conference on*, pages 819–824. IEEE, 2005.

[43] Abdullatif E Ben-Nakhi and Mohamed A Mahmoud. Energy conservation in buildings through efficient a/c control using neural networks. *Applied Energy*, 73(1): 5–23, 2002.

[44] Gregor P Henze and Richard E Hindman. Control of air-cooled chiller condenser fans using clustering neural networks. *TRANSACTIONS-AMERICAN SOCIETY OF HEATING REFRIGERATING AND AIR CONDITIONING ENGINEERS*, 108(2):232–244, 2002.

[45] Ying Zhang and Qijun Chen. Prediction of building energy consumption based on pso-rbf neural network. In *System Science and Engineering (ICSSE), 2014 IEEE International Conference on*, pages 60–63. IEEE, 2014.

[46] EWM Lee, IWH Fung, VWY Tam, and M Arashpour. A fully autonomous kernel-based online learning neural network model and its application to building cooling load prediction. *Soft Computing*, 18(10):1999–2014, 2014.

[47] AP Melo, Daniel Cóstola, Roberto Lamberts, and JLM Hensen. Development of surrogate models using artificial neural network for building shell energy labelling. *Energy Policy*, 69:457–466, 2014.

[48] Ehsan Asadi, Manuel Gameiro da Silva, Carlos Henggeler Antunes, Luís Dias, and Leon Glicksman. Multi-objective optimization for building retrofit: A model using genetic algorithm and artificial neural network and an application. *Energy and Buildings*, 81:444–456, 2014.

[49] Martin Macas, Fiorella Lauro, Fabio Moretti, Stefano Pizzuti, Mauro Annunziato, Alessandro Fonti, Gabriele Comodi, and Andrea Giantomassi. Sensitivity based feature selection for recurrent neural network applied to forecasting of heating gas consumption. In *International Joint Conference SOCO-14*, pages 259–268. Springer, 2014.

[50] Rafael Mena Yedra, Francisco Rodríguez Díaz, María del Mar Castilla Nieto, and Manuel R Arahal. A neural network model for energy consumption prediction of ciesol bioclimatic building. In *International Joint Conference SOCO-13*, pages 51–60. Springer, 2014.

[51] Subodh Paudel, Mohamed Elmtiri, Wil L Kling, Olivier Le Corre, and Bruno Lacarriere. Pseudo dynamic transitional modeling of building heating energy demand using artificial neural network. *Energy and Buildings*, 70:81–93, 2014.

[52] Raad Z Homod, Khairul Salleh Mohamed Sahari, Haider AF Almurib, and Farrukh Hafiz Nagi. Gradient auto-tuned takagi–sugeno fuzzy forward control of a hvac system using predicted mean vote index. *Energy and Buildings*, 49:254–267, 2012.

[53] MM Gouda, Sean Danaher, and CP Underwood. Thermal comfort based fuzzy logic controller. *Building services engineering research and technology*, 22(4):237–253, 2001.

[54] Zhen Yu and Arthur Dexter. Hierarchical fuzzy control of low-energy building systems. *Solar Energy*, 84(4):538–548, 2010.

[55] Antoine Guillemin and Nicolas Morel. An innovative lighting controller integrated in a self-adaptive building control system. *Energy and Buildings*, 33(5):477–487, 2001.

[56] Mahroo Eftekhari, Ljiljana Marjanovic, and Plamen Angelov. Design and performance of a rule-based controller in a naturally ventilated room. *Computers in Industry*, 51(3):299–326, 2003.

[57] Energy Information Administration (US). *Annual Energy Review 2011*. Government Printing Office, 2012.

[58] Jens Laustsen. Energy efficiency requirements in building codes, energy efficiency policies for new buildings. *International Energy Agency (IEA)*, pages 477–488, 2008.

[59] Energy Efficiency. Buildings energy data book. *US Department of Energy. http://buildingsdatabook. eere. energy. gov/. John Dieckmann is a director and Alissa Cooperman is a technologist in the Mechanical Systems Group of TIAX, Cambridge, Mass. James Brodrick, Ph. D., is a project manager with the Building Technologies Program, US Department of Energy, Washington, DC*, 2009.

[60] David L Hall and James Llinas. An introduction to multisensor data fusion. *Proceedings of the IEEE*, 85(1):6–23, 1997.

[61] David Lee Hall and Sonya AH McMullen. *Mathematical techniques in multisensor data fusion*. Artech House, 2004.

[62] Lawrence A Klein. Sensor and data fusion concepts and applications. Society of Photo-Optical Instrumentation Engineers (SPIE), 1993.

[63] Edward Waltz, James Llinas, et al. *Multisensor data fusion*, volume 685. Artech house Boston, 1990.

[64] DL Hall, RJ Linn, and J Llinas. A survey of data fusion systems. In *Proc. SPIE Conf. on data structure and target classification*, volume 1470, pages 13–36, 1991.

[65] Mark Maybury. Detecting malicious insiders in military networks. Technical report, DTIC Document, 2006.

[66] Yaakov Bar-Shalom, Peter K Willett, and Xin Tian. Tracking and data fusion. *A Handbook of Algorithms. Yaakov Bar-Shalom*, 2011.

[67] A Shahi, CT Haas, and JS West. Automated construction activity assessment using workflow-based data fusion. *Gerontechnology*, 11(2):333, 2012.

[68] Annett Chilian, Heiko Hirschmuller, and Martin Gorner. Multisensor data fusion for robust pose estimation of a six-legged walking robot. In *Intelligent Robots and Systems (IROS), 2011 IEEE/RSJ International Conference on*, pages 2497–2504. IEEE, 2011.

[69] Dragos Datcu and Leon JM Rothkrantz. Semantic audio-visual data fusion for automatic emotion recognition. *Emotion Recognition: A Pattern Analysis Approach*, page 411, 2014.

[70] Jie Chen, Kian Hsiang Low, Colin Keng-Yan Tan, Ali Oran, Patrick Jaillet, John M Dolan, and Gaurav S Sukhatme. Decentralized data fusion and active sensing with mobile sensors for modeling and predicting spatiotemporal traffic phenomena. *arXiv preprint arXiv:1206.6230*, 2012.

[71] Trevor F Keenan, Eric Davidson, Antje M Moffat, William Munger, and Andrew D Richardson. Using model-data fusion to interpret past trends, and quantify uncertainties in future projections, of terrestrial ecosystem carbon cycling. *Global Change Biology*, 18(8):2555–2569, 2012.

[72] Marc L Kessler. Image registration and data fusion in radiation therapy. 2014.

[73] GD Clifford, J Behar, Q Li, and Iead Rezek. Signal quality indices and data fusion for determining clinical acceptability of electrocardiograms. *Physiological measurement*, 33(9):1419, 2012.

[74] Hongliang Ren, Denis Rank, Martin Merdes, Jan Stallkamp, and Peter Kazanzides. Multisensor data fusion in an integrated tracking system for endoscopic surgery. *Information Technology in Biomedicine, IEEE Transactions on*, 16(1):106–111, 2012.

[75] Bahador Khaleghi, Alaa Khamis, Fakhreddine O Karray, and Saiedeh N Razavi. Multisensor data fusion: A review of the state-of-the-art. *Information Fusion*, 14 (1):28–44, 2013.

[76] Arthur P Dempster. A generalization of bayesian inference. *Journal of the Royal Statistical Society. Series B (Methodological)*, pages 205–247, 1968.

[77] Glenn Shafer et al. *A mathematical theory of evidence*, volume 1. Princeton university press Princeton, 1976.

[78] Michio Sugeno and Takahiro Yasukawa. A fuzzy-logic-based approach to qualitative modeling. *IEEE Transactions on fuzzy systems*, 1(1):7–31, 1993.

[79] P Jorge Escamilla-Ambrosio and Neil Mort. Hybrid kalman filter-fuzzy logic adaptive multisensor data fusion architectures. In *Decision and Control, 2003. Proceedings. 42nd IEEE Conference on*, volume 5, pages 5215–5220. IEEE, 2003.

[80] Hongwei Zhu and O Basir. A novel fuzzy evidential reasoning paradigm for data fusion with applications in image processing. *Soft Computing*, 10(12):1169–1180, 2006.

[81] MG McKellar. Failure diagnosis for a household refrigerator. *Master's thesis, School of Mechanical Engineering, Purdue University, West Lafayette, Indiana*, 1987.

[82] LA Stallard. Model based expert system for failure detection and identification of household refrigerators. *Master's thesis, School of Mechanical Engineering, Purdue University, West Lafayette, Indiana*, 1989.

[83] G Palshikar et al. Simple algorithms for peak detection in time-series. In *Proc. 1st Int. Conf. Advanced Data Analysis, Business Analytics and Intelligence*, 2009.

[84] Martin Ester, Hans-Peter Kriegel, Jörg Sander, and Xiaowei Xu. A density-based algorithm for discovering clusters in large spatial databases with noise. In *Kdd*, volume 96, pages 226–231, 1996.

[85] George EP Box. Evolutionary operation: A method for increasing industrial productivity. *Applied Statistics*, pages 81–101, 1957.

[86] Yacov Y Haimes, LS Ladson, and David A Wismer. Bicriterion formulation of problems of integrated system identification and system optimization, 1971.

[87] J David Schaffer. Multiple objective optimization with vector evaluated genetic algorithms. In *Proceedings of the 1st International Conference on Genetic Algorithms, Pittsburgh, PA, USA, July 1985*, pages 93–100, 1985.

[88] Carlos M Fonseca, Peter J Fleming, et al. Genetic algorithms for multiobjective optimization: Formulation discussion and generalization. In *ICGA*, volume 93, pages 416–423, 1993.

[89] Nidamarthi Srinivas and Kalyanmoy Deb. Muiltiobjective optimization using nondominated sorting in genetic algorithms. *Evolutionary computation*, 2(3):221–248, 1994.

[90] Kalyanmoy Deb, Samir Agrawal, Amrit Pratap, and Tanaka Meyarivan. A fast elitist non-dominated sorting genetic algorithm for multi-objective optimization: Nsga-ii. *Lecture notes in computer science*, 1917:849–858, 2000.

[91] Eckart Zitzler, Lothar Thiele, Eckart Zitzler, Eckart Zitzler, Lothar Thiele, and Lothar Thiele. *An evolutionary algorithm for multiobjective optimization: The strength pareto approach*, volume 43. Citeseer, 1998.

[92] Joshua Knowles and David Corne. The pareto archived evolution strategy: A new baseline algorithm for pareto multiobjective optimisation. In *Evolutionary Computation, 1999. CEC 99. Proceedings of the 1999 Congress on*, volume 1. IEEE, 1999.

[93] Aimin Zhou, Bo-Yang Qu, Hui Li, Shi-Zheng Zhao, Ponnuthurai Nagaratnam Suganthan, and Qingfu Zhang. Multiobjective evolutionary algorithms: A survey of the state of the art. *Swarm and Evolutionary Computation*, 1(1):32–49, 2011.

[94] Kaisa Miettinen. *Nonlinear multiobjective optimization*, volume 12. Springer Science & Business Media, 1999.

[95] David E Goldberg and Jon Richardson. Genetic algorithms with sharing for multimodal function optimization. In *Genetic algorithms and their applications: Proceedings of the Second International Conference on Genetic Algorithms*, pages 41–49. Hillsdale, NJ: Lawrence Erlbaum, 1987.

[96] Eckart Zitzler, Kalyanmoy Deb, and Lothar Thiele. Comparison of multiobjective evolutionary algorithms: Empirical results. *Evolutionary computation*, 8(2):173–195, 2000.

[97] Joshua Knowles and David Corne. On metrics for comparing nondominated sets. In *Evolutionary Computation, 2002. CEC'02. Proceedings of the 2002 Congress on*, volume 1, pages 711–716. IEEE, 2002.

[98] Jason R Schott. Fault tolerant design using single and multicriteria genetic algorithm optimization. Technical report, DTIC Document, 1995.

[99] de MH Wit. Hambase: heat, air and moisture model for building and systems evaluation. 2006.

[100] AWM van Schijndel and JLM Hensen. Integrated heat, air and moisture modeling toolkit in matlab. In *Proc. of 9th International IBPSA Conference*, pages 1107–1111, 2005.

[101] PO Fanger. Assessment of man's thermal comfort in practice. *British journal of industrial medicine*, 30(4):313–324, 1973.

[102] Niels Rode Kristensen, Henrik Madsen, and Sten Bay Jørgensen. Parameter estimation in stochastic grey-box models. *Automatica*, 40(2):225–237, 2004.

[103] Rune Juhl, Niels Rode Kristensen, Peder Bacher, Jan Kloppenborg, and Henrik Madsen. Grey-box modeling of the heat dynamics of a building with ctsm-r. 2013.

[104] Rune Juhl, Niels Rode Kristensen, Peder Bacher, Jan Kloppenborg, and Henrik Madsen. Ctsm-r user guide. *Technical University of Denmark*, 2, 2013.

[105] Gouri Datta. Effect of fixed horizontal louver shading devices on thermal perfomance of building by trnsys simulation. *Renewable Energy*, 23(3):497–507, 2001.

[106] Anthony D Radford and John S Gero. *Design by optimization in architecture, building, and construction*. John Wiley & Sons, Inc., 1987.

[107] W Huang and HN Lam. Using genetic algorithms to optimize controller parameters for hvac systems. *Energy and Buildings*, 26(3):277–282, 1997.

[108] Jean-Marie Hauglustaine and Sleiman Azar. Interactive tool aiding to optimise the building envelope during the sketch design. In *Proceedings of the Seventh International IBPSA Conference. IBPSA*, pages 387–94, 2001.

[109] Jonathan A Wright, Heather A Loosemore, and Raziyeh Farmani. Optimization of building thermal design and control by multi-criterion genetic algorithm. *Energy and Buildings*, 34(9):959–972, 2002.

[110] Björn Rolfsman. Co2 emission consequences of energy measures in buildings. *Building and Environment*, 37(12):1421–1430, 2002.

[111] Weimin Wang, Radu Zmeureanu, and Hugues Rivard. Applying multi-objective genetic algorithms in green building design optimization. *Building and Environment*, 40(11):1512–1525, 2005.

[112] Ala Hasan, Mika Vuolle, and Kai Sirén. Minimisation of life cycle cost of a detached house using combined simulation and optimisation. *Building and Environment*, 43 (12):2022–2034, 2008.

[113] Houcem Eddine Mechri, Alfonso Capozzoli, and Vincenzo Corrado. Use of the anova approach for sensitive building energy design. *Applied Energy*, 87(10):3073–3083, 2010.

[114] Athanassios Tzempelikos and Andreas K Athienitis. The impact of shading design and control on building cooling and lighting demand. *Solar Energy*, 81(3):369–382, 2007.

[115] Christelle Franzetti, Gilles Fraisse, and Gilbert Achard. Influence of the coupling between daylight and artificial lighting on thermal loads in office buildings. *Energy and Buildings*, 36(2):117–126, 2004.

[116] Ming-Chin Ho, Che-Ming Chiang, Po-Cheng Chou, Kuei-Feng Chang, and Chia-Yen Lee. Optimal sun-shading design for enhanced daylight illumination of subtropical classrooms. *Energy and buildings*, 40(10):1844–1855, 2008.

[117] Danny HW Li, SL Wong, CL Tsang, and Gary HW Cheung. A study of the daylighting performance and energy use in heavily obstructed residential buildings via computer simulation techniques. *Energy and Buildings*, 38(11):1343–1348, 2006.

[118] Marco Manzan and Francesco Pinto. Genetic optimization of external shading devices. In *Proceedings of 11th international IBPSA conference, Glasgow, Scotland*, pages 27–30, 2009.

[119] M Manzan. Genetic optimization of external fixed shading devices. *Energy and Buildings*, 2014.

[120] Michael Wetter and Jonathan Wright. A comparison of deterministic and probabilistic optimization algorithms for nonsmooth simulation-based optimization. *Building and Environment*, 39(8):989–999, 2004.

[121] Fani Boukouvala and Marianthi G Ierapetritou. Surrogate-based optimization of expensive flowsheet modeling for continuous pharmaceutical manufacturing. *Journal of Pharmaceutical Innovation*, 8(2):131–145, 2013.

[122] Xiqun Michael Chen, Lei Zhang, Xiang He, Chenfeng Xiong, and Zhiheng Li. Surrogate-based optimization of expensive-to-evaluate objective for optimal highway toll charges in transportation network. *Computer-Aided Civil and Infrastructure Engineering*, 2013.

[123] S Vakili and MS Gadala. Low cost surrogate model based evolutionary optimization solvers for inverse heat conduction problem. *International Journal of Heat and Mass Transfer*, 56(1):263–273, 2013.

[124] Laurent Magnier and Fariborz Haghighat. Multiobjective optimization of building design using trnsys simulations, genetic algorithm, and artificial neural network. *Building and Environment*, 45(3):739–746, 2010.

[125] Michael P Perrone and Leon N Cooper. When networks disagree: Ensemble methods for hybrid neural networks. Technical report, DTIC Document, 1992.

[126] Leo Breiman. Bagging predictors. *Machine learning*, 24(2):123–140, 1996.

[127] Ylenia Cascone, Vincenzo Corrado, and Valentina Serra. Calculation procedure of the shading factor under complex boundary conditions. *Solar Energy*, 85(10): 2524–2539, 2011.

[128] Mohamed Hamdy, Ala Hasan, and Kai Siren. Applying a multi-objective optimization approach for design of low-emission cost-effective dwellings. *Building and environment*, 46(1):109–123, 2011.

[129] K Peippo, PD Lund, and E Vartiainen. Multivariate optimization of design trade-offs for solar low energy buildings. *Energy and Buildings*, 29(2):189–205, 1999.

[130] Luisa Gama Caldas and Leslie K Norford. A design optimization tool based on a genetic algorithm. *Automation in construction*, 11(2):173–184, 2002.

[131] Erel Avineri. Soft computing applications in traffic and transport systems: a review. In *Soft computing: methodologies and applications*, pages 17–25. Springer, 2005.

[132] D Canca, J Larrañeta, S Lozano, and L Onieva. Traffic intensity forecast in urban networks using a multilayer perceptron. In *Joint International Meeting EURO XV-INFORMS XXXIV. Barcelona, Spain*, 1997.

[133] Mark S Dougherty and Mark R Cobbett. Short-term inter-urban traffic forecasts using neural networks. *International journal of forecasting*, 13(1):21–31, 1997.

[134] Sherif Ishak, Prashanth Kotha, and Ciprian Alecsandru. Optimization of dynamic neural network performance for short-term traffic prediction. *Transportation Research Record: Journal of the Transportation Research Board*, 1836(1):45–56, 2003.

[135] Dongjoo Park, Laurence R Rilett, and Gunhee Han. Spectral basis neural networks for real-time travel time forecasting. *Journal of Transportation Engineering*, 125 (6):515–523, 1999.

[136] Cynthia Taylor and Deirdre Meldrum. Freeway traffic data prediction using neural networks. In *Vehicle Navigation and Information Systems Conference, 1995.*

Proceedings. In conjunction with the Pacific Rim TransTech Conference. 6th International VNIS.'A Ride into the Future', pages 225–230. IEEE, 1995.

[137] J WC van Lint, SP Hoogendoorn, and Henk J van Zuylen. Freeway travel time prediction with state-space neural networks: modeling state-space dynamics with recurrent neural networks. *Transportation Research Record: Journal of the Transportation Research Board*, 1811(1):30–39, 2002.

[138] Weizhong Zheng, Der-Horng Lee, and Qixin Shi. Short-term freeway traffic flow prediction: Bayesian combined neural network approach. *Journal of transportation engineering*, 132(2):114–121, 2006.

[139] L Bucur, A Florea, and BS Petrescu. An adaptive fuzzy neural network for traffic prediction. In *Control & Automation (MED), 2010 18th Mediterranean Conference on*, pages 1092–1096. IEEE, 2010.

[140] Snehal Jawanjal and Preeti Bajaj. A design approach to traffic flow forecasting with soft computing tools. In *Emerging Trends in Engineering and Technology (ICETET), 2010 3rd International Conference on*, pages 81–84. IEEE, 2010.

[141] Teresa Pamuła. Road traffic parameters prediction in urban traffic management systems using neural networks. *Transport Problems*, 6(3):123–129, 2011.

[142] Mauro Annunziato, Fabio Moretti, and Stefano Pizzuti. Urban traffic flow forecasting using neural-statistic hybrid modeling. In *Soft Computing Models in Industrial and Environmental Applications*, pages 183–190. Springer, 2013.

[143] S Pizzuti, M Annunziato, and F Moretti. Smart street lighting management. *Energy Efficiency*, 6(3):607–616, 2013.

[144] Amanda JC Sharkey. Combining predictors. In *Combining artificial neural nets*, pages 31–50. Springer, 1999.

[145] Anders Krogh, Jesper Vedelsby, et al. Neural network ensembles, cross validation, and active learning. *Advances in neural information processing systems*, pages 231–238, 1995.

[146] Yong Liu and Xin Yao. Ensemble learning via negative correlation. *Neural Networks*, 12(10):1399–1404, 1999.

[147] Christopher M Bishop et al. Neural networks for pattern recognition. 1995.

[148] Yoav Freund, Robert E Schapire, et al. Experiments with a new boosting algorithm. In *ICML*, volume 96, pages 148–156, 1996.